CHAPTER 12

LOCALIZED PROTON MAGNETIC RESONANCE SPECTROSCOPY OF BRAIN DISORDERS IN CHILDHOOD

JENS FRAHM and FOLKER HANEFELD

SUMMARY

Localized proton magnetic resonance spectroscopy is used to study cerebral metabolic disorders in children. The development of single-voxel techniques allows quantitative calculation of the absolute concentrations in different regions of the brain of metabolites that are readily observed in ^{1}H spectra. These include *N*-acetylaspartate (NAA), lactate, amino acids, inositols, choline-containing compounds, and total creatine. The studies are illustrated by the results on numerous childhood disorders: the leukodystrophies, other white-matter diseases,gray-matter diseases, mitochondrial diseases, and miscellaneous deficiency disorders.

JENS FRAHM • Biomedical NMR Research, Inc., at the Max-Planck-Institute for Biophysical Chemistry, D-37070 Göttingen, Germany. FOLKER HANEFELD • Department of Neuropediatrics, University of Göttingen. D-37075 Göttingen, Germany.

Magnetic Resonance Spectroscopy and Imaging in Neurochemistry, Volume 8 of *Advances in Neurochemistry*, edited by Bachelard, Plenum Press, New York, 1997.

1. INTRODUCTION

Beyond structural and functional investigations of the central nervous system by X-ray computed tomography and positron-emission tomography, advances in magnetic resonance have opened new and truly noninvasive avenues into the functioning human brain. In particular, state-of-the-art magnetic resonance imaging (MRI) provides access to high-resolution anatomy and brain function, while magnetic resonance spectroscopy (MRS) offers unique insights into cerebral metabolism.

The primary aim of this chapter is to demonstrate the usefulness and potential of localized ^{1}H MRS and its application to brain disorders in childhood. To emphasize practical access to *in vivo* neurochemistry, Section 2 describes a simple and robust single-voxel technique that facilitates transformation of spectral data into neurochemical quantities such as absolute metabolite concentrations. Pertinent applications in the field of neuropediatrics are presented in Sections 3–9 and underline the remarkable progress during recent years. Major achievements are illustrated by selected examples from our experience with more than 400 MRS examinations of over 300 children (Table 1).

The focus of this chapter is on neurometabolic, neurodegenerative, and neuroinflammatory disorders. Although this selection is driven by our personal interest, it also reflects preliminary observations that ^{1}H MRS seems to give less information in cases of unclassified mental retardation, psychosis, generalized epilepsies, and other conditions without definite biochemical or structural abnormalities.

A comprehensive coverage of *in vivo* MRS or even ^{1}H MRS of the brain is beyond the scope of this chapter. The use of MRS for the understanding of disease has been discussed in a large number of articles, e.g., by Bottomley *et al.* (1985), Radda (1986), Prichard and Shulman (1986), Frahm *et al.* (1989), Howe *et al.* (1993), and Kemp and Radda (1994). Applications to brain disorders in childhood have been described by Grodd *et al.* (1991), van der Knaap *et al.* (1992), Tzika *et al.* (1993a, b), and Ross and Michaelis (1994). The clinical, genetic, biochemical, and radiological characteristics of neurological disorders in childhood have been summarized by Aicardi (1992) and Barkovich (1995).

2. LOCALIZED PROTON MAGNETIC RESONANCE SPECTROSCOPY

The purpose of this section is to outline the methodology used for quantitative localized ^{1}H MRS and its application to the study of brain disorders in childhood. A discussion of basic localization strategies is followed by a description of the stimulated-echo acquisition mode (STEAM) technique. Experimental

TABLE 1. Brain Disorders in Childhood Studied by Localized ^1H MRS

Classification	Disease/syndrome	Number of patients
Leukodystrophies		
Known origin	Metachromatic leukodystrophy	8
	Globoid cell leukodystrophy	2
	Pelizaeus–Merzbacher disease	4
	Canavan's disease	1
	Adrenoleukodystrophy	26
Unknown origin	Alexander's disease	2
	Congenital muscular dystrophy plus leukodystrophy	6
	Myelinopathia centralis diffusa	6
	Cystic leukoencephalopathy	3
	Unclassified leukodystrophies	26
Other white-matter disorders	L-2-Hydroxyglutaric aciduria	1
	Succinate dehydrogenase deficiency	1
	Multiple sclerosis	24
Gangliosidoses	G_{M_2} gangliosidosis	1
	Neuronal ceroid lipofuscinosis	7
Mitochondrial disorders	Leigh syndrome	15
	Mitochondrial encephalopathy, lactic acidosis, and stroke-like episodes (MELAS)	1
	Myoclonic epilepsy with ragged red fibers (MERRF)	2
	Kearns–Sayre Syndrome	3
	Others	17
Mucopolysaccharidoses	Type VI	1
Other lysosomal disorders	Niemann–Pick type C	1
	Mannosidosis	1
Peroxisomal disorders	Cerebro-hepato-renal syndrome	3
Amino aciduria	Nonketotic hyperglycinemia	5
	Phenylketonuria	4
	Isovaleric acidemia	1
Purine/pyrimidine disorders	Lesh–Nyhan syndrome	2
	Phosphoribosylpyrophosphate synthetase defect	2
Other metabolic disorders	Carbohydrate-deficient glycoprotein syndrome	5
	Creatine deficiency	1
Central nervous system malformations	Hemimegalencephaly	4
	Double cortex	1
	Pachygyria	1
Heredodegenerative disorders	Huntington chorea	2
	Olivopontocerebellar atrophy	1
Miscellaneous disorders	Rett syndrome	21
	Hyperekplexia	2
	Anorexia nervosa	13
	Hallervorden–Spatz disease	2
	Epilepsy	9
	Brain tumors	9
	Extrapyramidal disorders	8
	Cerebrovascular disorders	2
	Unclassified diseases	64

conditions are presented that allow quantification of the concentrations of metabolites identified in ^{1}H STEAM spectra of human brain. Regional variability, age dependencies, and other physiological influences are briefly discussed prior to a description of the requirements for a typical patient examination.

2.1. Single-Voxel Spectroscopy: A Rationale

Meaningful insights into the chemistry of the intact human brain require spatial discrimination of MRS responses. Two different concepts have been proposed that either emphasize spatial (imaging) or biochemical resolution (spectroscopy). *Chemical shift imaging* techniques employ one to three gradient pulses to encode spatial information along respective gradient axes into the phase of a time-domain signal from the entire object. This signal is acquired in the absence of a magnetic field gradient and thus carries the chemical shift information. Multidimensional image reconstruction then leads to metabolite maps that represent the spatial intensity distributions of individual metabolite resonances at selected chemical shift frequencies. Alternatively, *single-voxel spectroscopy* techniques attempt to restrict the radio-frequency (RF) excitation to a predefined volume of interest (VOI). They acquire the uncompromised though spatially localized frequency spectrum directly as a time-domain signal from the VOI, and, therefore no further processing is required except for one-dimensional Fourier transformation.

To complement high-resolution morphological information from MRI with detailed neurochemical information from MRS, it seems advisable to employ localized single-voxel spectra, which, in general, reveal a much more detailed and quantifiable metabolic picture of selected foci than metabolite maps. More specifically, the advantages of the single-voxel approach are due to the excellent spectral resolution and water suppression that are achievable by optimizing the magnetic field homogeneity over only a small VOI of 1–18 ml. Moreover, the relatively short measurement times of 1–10 min are clearly beneficial for a reliable quantification of metabolite concentrations as they allow the use of long repetition times (TR). For example, selection of TR $\geq$ 6000 msec ensures full relaxation of proton spin systems between successive RF excitations and thus avoids the need for corrections due to T_1 saturation when transforming resonance areas into metabolite concentrations. This is of particular importance for studies of disease states of the brain because potential changes in T_1 relaxation are usually unknown.

In general, of course, the choice of a technique should only depend on the question to be answered. While details about localization techniques are necessary to properly apply such methods and to facilitate the evaluation and interpretation of the resulting data, MRS findings in metabolic research and medical decision making must be independent of the technique chosen. The best way to

accomplish this goal is to convert *relative* spectral findings, often expressed as peak heights or area ratios, into *absolute* spectral quantities, i.e., absolute resonance areas, and to convert these values into metabolite concentrations by calibrating *in vivo* resonance areas with those of model metabolite solutions.

2.2. Localization Using Stimulated Echoes

In accordance with the aforementioned considerations, most investigations have been performed using fully relaxed single-voxel ^1H MRS. The two techniques that may be employed for single-shot gradient localization are PRESS (Bottomley, 1984, 1987; Ordidge *et al.*, 1985) and STEAM sequences (Frahm *et al.*, 1984, 1987). In the work described here, we have exclusively used STEAM sequences because this technique provides optimum conditions for MRS acquisition at short echo times (TE) that avoid gross corrections for T_2 relaxation and/or spin-coupling modulation. For a comparison of localization strategies, see Frahm and Hänicke (1994, 1996).

In contrast to the double-spin-echo 90°–180°–180° PRESS technique, STEAM localization sequences comprise three frequency-selective 90° RF pulses that are applied in the presence of orthogonal gradients. As shown in Fig. 1, the resulting stimulated-echo (STE) signal (Hahn, 1950) represents magnetizations that originate from a VOI defined by the intersection of three perpendicular sections. During the course of the STEAM sequence, transverse magnetizations excited by the first RF pulse are transformed into longitudinal magnetizations by application of the second pulse. Corresponding components are subject to T_1 relaxation during the middle interval TM. They refocus as a stimulated echo at TE/2 after application of the third pulse. To minimize signal losses due to T_2 relaxation, spin-coupling modulation, and multiple-quantum interferences (Ernst and Hennig, 1991), the echo time TE should be chosen as short as possible. In our studies, the STEAM intervals were TE = 20 msec and TM = 30 msec. Data acquisition covered the second half of the STE signal (1024 msec) with a receiver bandwidth of ±1000 Hz.

Under these conditions, the STEAM sequence is best suited for ^1H MRS, although ^{31}P MRS of human brain at even shorter TE and TM values has been successfully demonstrated (Merboldt *et al.*, 1990). For proton applications, the sequence must be preceded by one to three chemical-shift-selective (CHESS) water suppression pulses plus associated spoiler gradients (Haase *et al.*, 1985). In practice, three successive CHESS pulses of 60 Hz bandwidth (i.e., 0.7 ppm at 2.0 T) attenuate the water proton resonance by about a factor of 1000 while not affecting chemical shifts outside the 4.1–5.3 ppm region of the proton spectrum. Technical details of the water-suppressed STEAM sequence have been described by Frahm *et al.* (1990).

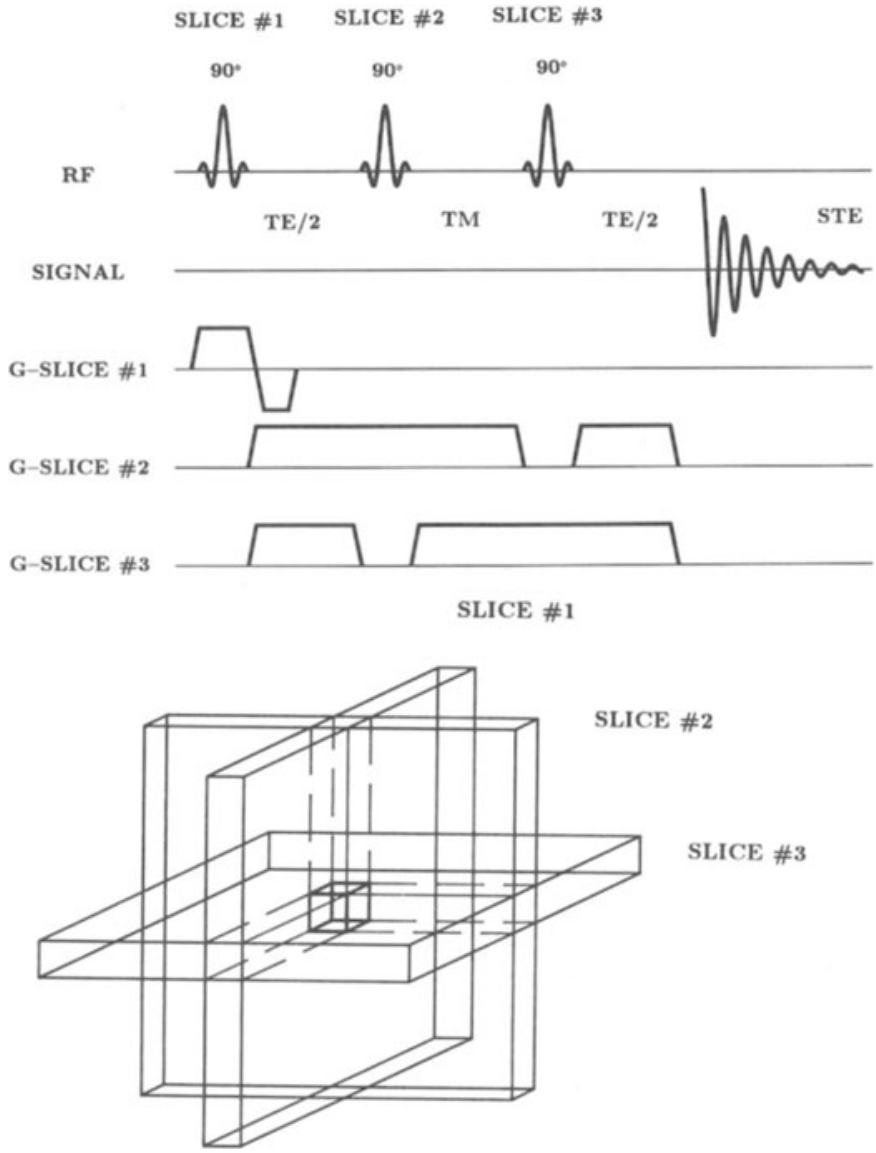

FIGURE 1. Single-voxel spectroscopy using a short-echo-time stimulated-echo acquisition mode (STEAM) localization technique. The STEAM sequence (*top*) defines the volume of interest (VOI) by the intersection of three cross sections (*bottom*) that are excited by frequency-selective 90° radio-frequency (RF) pulses in the presence of orthogonal magnetic field gradients (slices #1 to #3). The stimulated-echo (STE) signal from the selected VOI is attenuated by T_1 relaxation during the middle interval TM and T_2 relaxation during the two echo intervals TE/2.

2.3. Identification of Cerebral Metabolites

Although metabolite concentrations represent the obvious biochemical parameters to be derived from *in vivo* MRS, the accessible information may be extended to rate constants and fluxes provided suitable resonances are detectable and relevant metabolite pools are changing in response to physiological stimuli,

pharmacological treatment, or pathological conditions. In all cases, prerequisites for a reliable interpretation of MRS data are a detailed understanding of the spectra (proton, phosphorus, or carbon-13) and objective methods for spectral evaluation and quantification (Bottomley, 1991).

Figure 2 shows *in vivo* ^{1}H MR spectra of human gray and white matter obtained by fully relaxed (TR = 6000 msec) short-echo-time (TE/TM = 20/30 msec) STEAM spectroscopy. Spectral processing involved zero filling of the original 2K complex time-domain data points to 4K, Gaussian filtering (center zero, half-width 317 msec), Fourier transformation, and zero- and first-order phase correction without spectral baseline manipulation or resolution enhancement. Resonance assignments were guided by biochemical data from biopsies and autopsies (Perry *et al.*, 1971, 1981) and high-resolution high-field ^{1}H MR spectra of perchloric acid extracts from animal (Behar *et al.*, 1983; Arus *et al.*, 1985) and human brain (Petroff *et al.*, 1989; Peeling and Sutherland, 1993). They were confirmed by recording ^{1}H MR spectra of individual metabolites using identical experimental conditions as for *in vivo* human studies (Michaelis *et al.*, 1991; Frahm *et al.*, 1991a; Gyngell *et al.*, 1991; Michaelis *et al.*, 1993a). Such model spectra not only eliminate complications due to spectral overlap and allow assessment of the influence of strong spin–spin coupling at the relatively low field strength of 2.0 T used here but also serve as concentration-calibrated references for a user-independent quantification of absolute concentrations.

So far, the list of major detectable metabolites includes *N*-acetylaspartate (NAA), *N*-acetylaspartylglutamate (NAAG), glutamate (Glu), glutamine (Gln), creatine and phosphocreatine (Cr), choline-containing compounds (Cho), and *myo*-inositol (*myo*-Ins). In addition, the spectra may include resonances from glucose (Glc), lactate (Lac), aspartate (Asp), alanine (Ala), taurine (Tau), *scyllo*-inositol (*scyllo*-Ins), γ-aminobutyrate (GABA), guanidinoacetate (G), and cytosolic protein residues (Kauppinen *et al.*, 1992), although reliable assessments of many of these compounds are only possible for elevated concentrations in disease states of the brain. In the absence of a chemical shift standard, the *in vivo* ^{1}H MR spectra are commonly referenced to the *N*-acetyl resonance of NAA at 2.01 ppm. If NAA is depleted in a brain disorder, then Cr (3.04 ppm), Cho (3.22 ppm), or even Lac (1.33 ppm, center of doublet) may be taken as a reference.

For an understanding of neurochemical and cellular metabolite alterations, it is most important to note that NAA is exclusively located in neurons [see, e.g., the review by Birken and Oldendorf (1989)]. Conversely, the brain osmolyte *myo*-Ins turns out to be glia-specific as it has only been found in perchloric acid extracts of primary glia as well as of C6 and F98 glioma cell lines, but not in neurons (Brand *et al.*, 1993). Thus, taking NAA and *myo*-Ins as markers for neuronal and glial tissue components, respectively, changes in their concentrations reflect metabolic alterations in neuronal and glial pools. In fact, the *irreversible* reduction or loss of NAA observed in diseases ranging from cerebral stroke

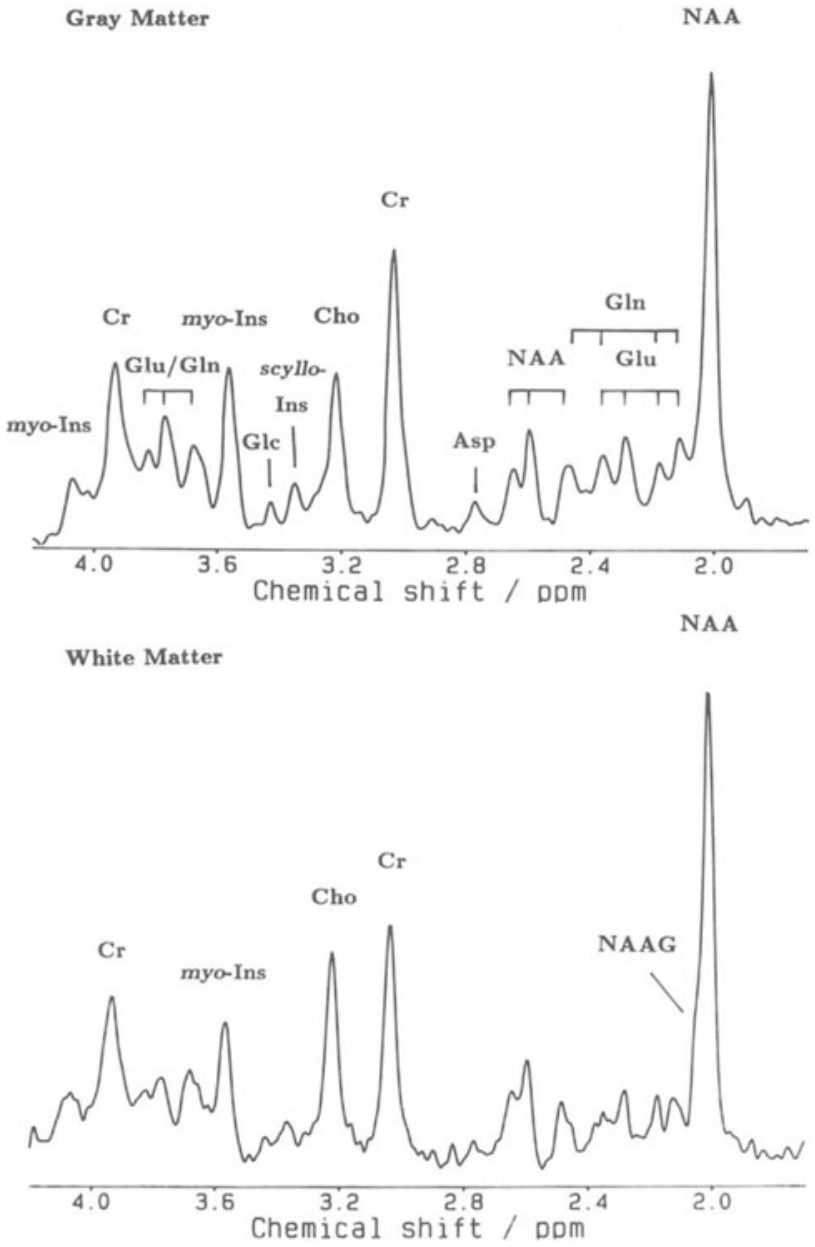

FIGURE 2. Cerebral metabolites detected in fully relaxed (TR = 6000 msec) short-echo-time (TE = 20 msec) ^{1}H MR spectra (STEAM, TM = 30 msec, 64 accumulations) of parietal gray (18 ml) and white matter (12 ml) of a young healthy adult. Spectral assignments include *N*-acetylaspartate (NAA), *N*-acetylaspartylglutamate (NAAG), glutamate (Glu), glutamine (Gln), aspartate (Asp), creatine and phosphocreatine (Cr), choline-containing compounds (Cho), *myo*-inositol (*myo*-Ins), *scyllo*-inositol (*scyllo*-Ins), and glucose (Glc). All spectra in this chapter are scaled in proportion to VOI size and plotted with identical standards.

to brain tumors suggests that spectroscopically detected NAA levels are in direct proportion to the amount of viable neuroaxonal tissue present in the investigated VOI. While putative increases of NAA resulting from regenerative nerve processes should be detectable in principle, occasional reports of *reversible* NAA levels in follow-up MRS studies either were not based on absolute concentrations

or may be explained by tissue replacement of a focal lesion during recovery.

The methyl (3.04 ppm) and methylene (3.93 ppm) resonance signals of creatine and phosphocreatine (PCr) are indistinguishable at the spectral resolution achievable *in vivo*. Thus, the ^1H MRS detected total Cr level is not affected by altered energy demands that are regulated via the creatine kinase reaction and phosphate exchange between PCr and γ-adenosine triphosphate (ATP). An independent evaluation of PCr levels and other aspects of cellular bioenergetics may be obtained by ^{31}P MRS.

The most likely candidates for the Cho signal are phosphorylcholine (PCh), glycerophosphorylcholine (GPC), and choline plasmalogen, while the concentrations of acetylcholine and choline are at least one order of magnitude lower. Proton-decoupled ^{31}P MRS of human brain (Merboldt *et al.*, 1990) as well as more recent findings based on quantitative fitting of proton data with the use of complete metabolite spectra suggests that the predominant contribution to the cerebral Cho level results from GPC (P. J. W. Pouwels, unpublished results).

In normal brain, contamination of the 3.56-ppm resonance from *myo*-Ins by the methylene group of glycine (Gly) at 3.55 ppm is unlikely owing to the low Gly concentration. Pathologically enhanced Gly levels should be distinguishable from *myo*-Ins as the Gly singlet does not contribute to the other resonances of *myo*-Ins, e.g., at 4.06 ppm, if unaffected by water suppression. The contributions from inositol phosphates (secondary messengers) or the head groups of inositolphospholipids (membrane constituents) to the *myo*-Ins spectrum can also be neglected owing to low concentrations, slightly different proton spectra, or partial immobilization.

2.4. Quantification of Cerebral Metabolite Concentrations

Spectral evaluation and quantification of metabolite concentrations is accomplished with use of the fully automated spectral evaluation program LCModel (Provencher, 1993). The approach takes advantage of a nearly model-free constrained regularization method (Provencher, 1982) and incorporates prior knowledge by fitting a library of metabolite reference spectra to the *in vivo* time-domain data. Because RF coil loading and corresponding receiver sensitivity differ for objects of different electrical conductivity (e.g., due to different head sizes), such effects have to be accounted for by correcting resonance areas with the inverse voltage amplitude required for a rectangular 90° reference RF pulse (Hoult and Richards, 1976). The procedure results in absolute metabolite concentrations that are largely independent of instrumental inadequacies and requires only a minimum number of assumptions (e.g., no lineshape and baseline assumptions are necessary). The use of model metabolite solutions may be referred to as an *absolute reference* method (Michaelis *et al.*, 1993b). The alternative choice of an *internal reference* such as water has the potential drawback of uncertain alterations of tissue water content in disease states of the brain. No corrections

TABLE 2. Absolute Tissue Concentrations (Mean ± SD) of Major Cerebral Metabolites in Parietal Gray and White Matter, Basal Ganglia, and Cerebellum of Young Healthy Adults (Mean Age 27 ± 4 Years)

	Concentration (mM)			
Metabolite[a]	Gray matter (n = 60)	White matter (n = 72)	Basal ganglia (n = 11)	Cerebellum (n = 8)
NAA+NAAG	7.7 ± 1.3	8.9 ± 1.3	9.0 ± 1.9	8.8 ± 1.6
NAAG	0.3 ± 0.3	1.3 ± 0.8	0.4 ± 0.5	0.5 ± 0.6
PCr+Cr	5.8 ± 0.9	5.0 ± 0.7	6.1 ± 1.3	7.4 ± 1.5
Cholines	1.0 ± 0.2	1.4 ± 0.3	1.7 ± 0.4	2.1 ± 0.7
myo-Inositol	3.9 ± 0.7	3.2 ± 0.8	3.3 ± 0.7	6.3 ± 3.3
Glutamate	7.3 ± 1.5	5.2 ± 1.2	7.7 ± 2.3	6.2 ± 2.8
Glutamine	3.3 ± 1.2	1.8 ± 0.9	3.9 ± 1.8	2.7 ± 1.7

[a]Abbreviations: NAA, *N*-acetylaspartate; NAAG, *N*-acetylaspartylglutamate; PCr, phosphocreatine; Cr, creatine.

were applied for partial-volume effects with cerebrospinal fluid (CSF). However, in the presence of atrophy, true metabolic alterations may be easily identified by taking ratios of metabolite concentrations.

Table 2 summarizes the concentrations of major metabolites in standardized VOIs of parietal gray and white matter, basal ganglia (including thalamus), and cerebellum (hemispheric center) for young healthy adults. Although gross regional differences are also detectable by visual inspection of the spectra shown in Fig. 3, concentration changes may be obscured by differences in magnetic field homogeneity, i.e., resonance linewidth. It should be noted, however, that all spectra presented in this chapter are scaled in proportion to VOI size and plotted with identical standards.

The quantitative data in Table 2 demonstrate that the combined pool of *N*-acetyl compounds constituted by NAA and NAAG does not vary beyond one standard deviation in the investigated regions. Recently, a more detailed study of metabolite levels within cortical gray matter revealed a gradient of increasing NAA (and decreasing Cho) from frontal and parietal cortex to occipital cortex (Pouwels *et al.,* 1995). A possible explanation involves differences in cellular composition such as increased glial contributions in frontal brain and stronger neuronal populations in occipital brain (visual cortex), but putative links between cortical anatomy, neurochemistry, and brain function remain to be elucidated.

Relatively high levels of NAAG well above detectability (15% of total *N*-acetyl concentration) were only found in white matter. The concentration of Cr increases in the order white matter < gray matter < basal ganglia < cerebellum. It should be noted that, unless otherwise specified, the abbreviations NAA and Cr

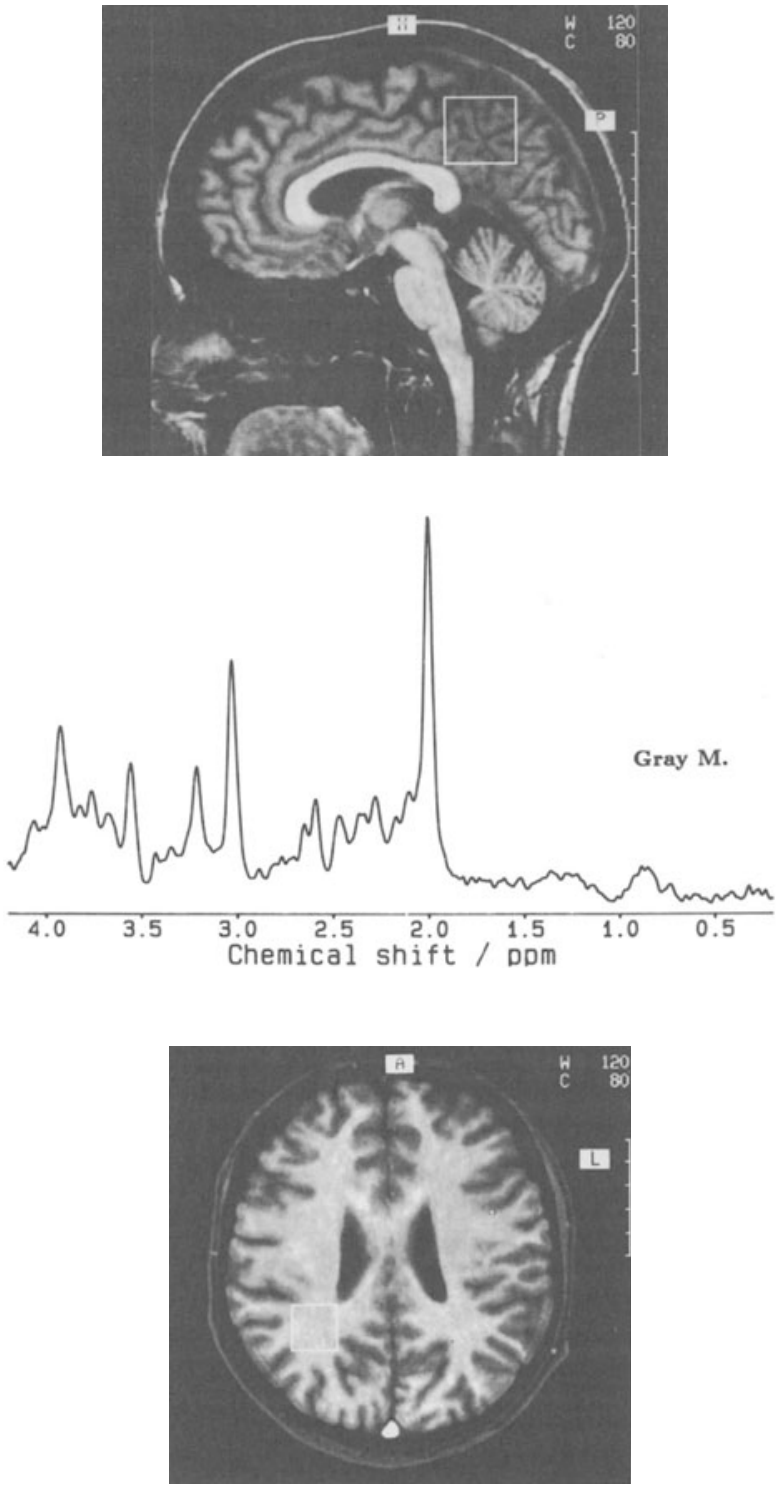

FIGURE 3. Regional variability of the metabolite pattern in the human brain (young adults) as detected by ^1H MRS (STEAM, TR/TE/TM = 6000/20/30 msec, 64 accumulations) of gray matter (18 ml), white matter (12 ml), basal ganglia (8 ml), and cerebellum (8 ml). The VOI locations are indicated on T_1-weighted images (RF spoiled 3-D FLASH, TR/TE = 15/6 msec, 20° flip angle, 4-mm partitions).

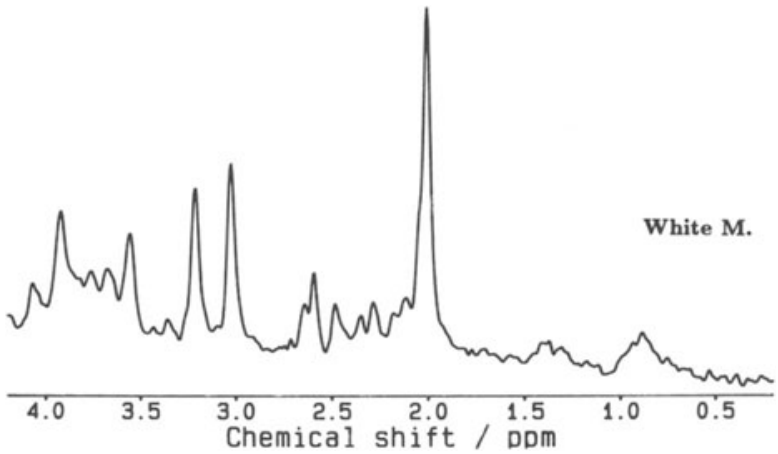

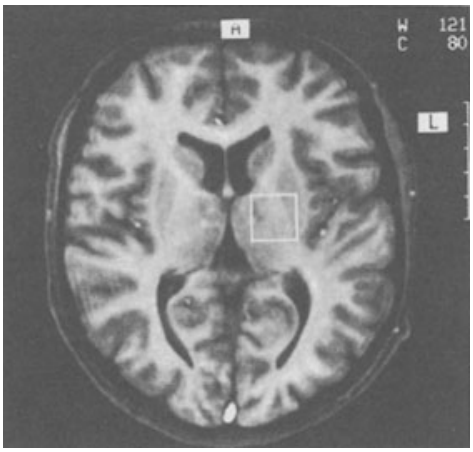

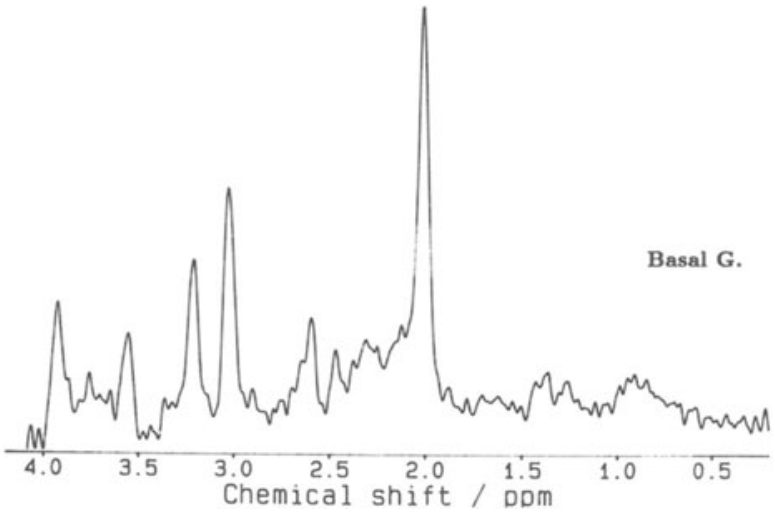

Figure 3. Continued

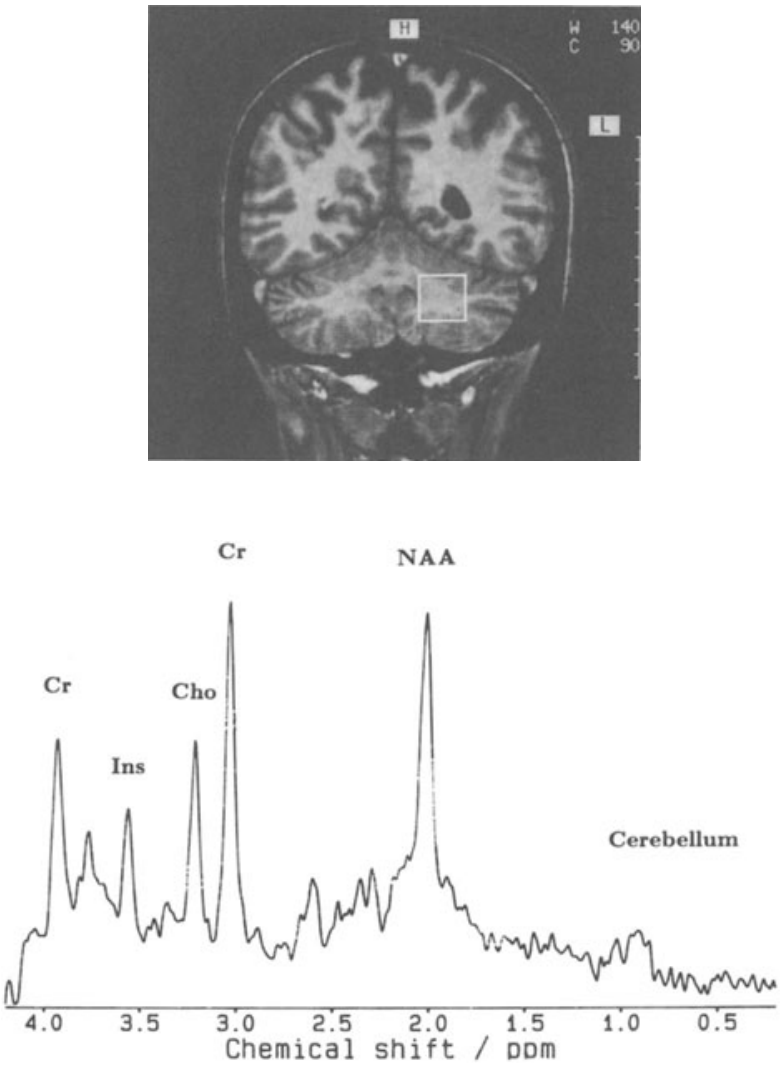

Figure 3. Continued

are used throughout this chapter to denote *total N*-acetyl levels, i.e., NAA and NAAG, and *total* Cr, i.e., Cr and PCr.

Regional Cho levels roughly parallel the degree of tissue myelination and therefore provide a marker of normal and disturbed myelination. Unfortunately, however, elevated Cho concentrations may arise either from enhanced membrane turnover and elevated PCh during cell proliferation (e.g., in early infancy, gliosis, and primary brain tumors) or from the accumulation of breakdown products such as GPC from myelin or other cell membranes (e.g., in leukodystrophies). Related findings apply to the elevation of free *myo*-Ins in various brain disorders including leukodystrophies, Alzheimer's disease (Miller *et al.,* 1993), and gliomas (Frahm *et al.,* 1991b; Bruhn *et al.,* 1992a). As a precursor of phospholipid membrane constituents, *myo*-Ins also is linked to processes involved in the for-

mation and breakdown of myelin or, more generally, in the growth or degeneration of glial cells. Since, at least in early disease stages, such processes are likely to occur simultaneously, ^{1}H MRS observations of altered *myo*-Ins and Cho levels in brain are also compatible with merely a change in the phospholipid composition of myelin and/or other glial cell membranes rather than complete structural disintegration or cellular loss. The latter processes are likely to reflect final stages of disease progression and are expected to yield a global reduction of metabolite concentrations.

A decrease of brain *myo*-Ins levels has been reported in patients with impaired liver function (e.g., liver cirrhosis and hepatic encephalopathy) and high blood ammonia levels by Michaelis *et al.* (1991) and Kreis *et al.* (1990, 1992). The same authors found a concomitant elevation of Gln that was most pronounced in gray matter, where relatively high concentrations of glutamine synthetase in astrocytes produce Gln from brain Glu and blood ammonia.

The range of Lac concentrations in parietal gray matter largely reflects intra- and intersubject variability of physiological states during the MRS examination. Pathologically enhanced concentrations of brain Lac are observed in disorders associated with increased energy demand and/or impaired ability for oxidative phosphorylation. Examples range from acute stroke (Bruhn *et al.,* 1989a) and rapidly growing malignant tumors (Bruhn *et al.,* 1989b; Frahm *et al.,* 1991b; Bruhn *et al.,* 1992a) to mitochondrial myopathies. Similarly, also Glc levels of 0.7 ± 0.4 mM in parietal gray matter reflect variations in physiology and are subject to changes due to a variety of factors ranging from functional to nutritional state. When controlled for plasma Glc levels, preliminary data on long-term diabetics revealed marked differences in brain-to-plasma Glc ratios that may be explained by alternations of Glc transport kinetics across the blood–brain barrier (Bruhn *et al.,* 1991; Kreis and Ross, 1992). Additional metabolite concentrations not included in Table 2 are 2.0 ± 1.0 mM for Tau, 1.8 ± 0.6 mM for Asp, and 1.0 ± 0.6 mM for GABA in parietal gray matter.

Apart from basic function-related differences in cellular composition (and metabolism) of various brain regions, metabolite profiles may be affected by maturation and aging, acute and chronic changes in nutrition (Frahm *et al.,* 1995), functional state (Prichard *et al.,* 1992; Merboldt *et al.,* 1992; Frahm *et al.,* 1996), and medication. Figure 4 illustrates spectral variations in gray and white matter of healthy subjects at the age of 4 months, 2 years, and 12 years. Although current data bases are still insufficient to support a detailed understanding of age-related changes during maturation, and despite the fact that preliminary reports are based on *in vivo* and *in vitro* data acquired under different technical conditions (van der Knaap *et al.,* 1990; Peden *et al.,* 1990; Hüppi *et al.,* 1991, 1995; Kreis *et al.,* 1993; Toft *et al.,* 1994; Hashimoto *et al.,* 1995), some consistent findings have emerged that are in agreement with our own experimental experience:

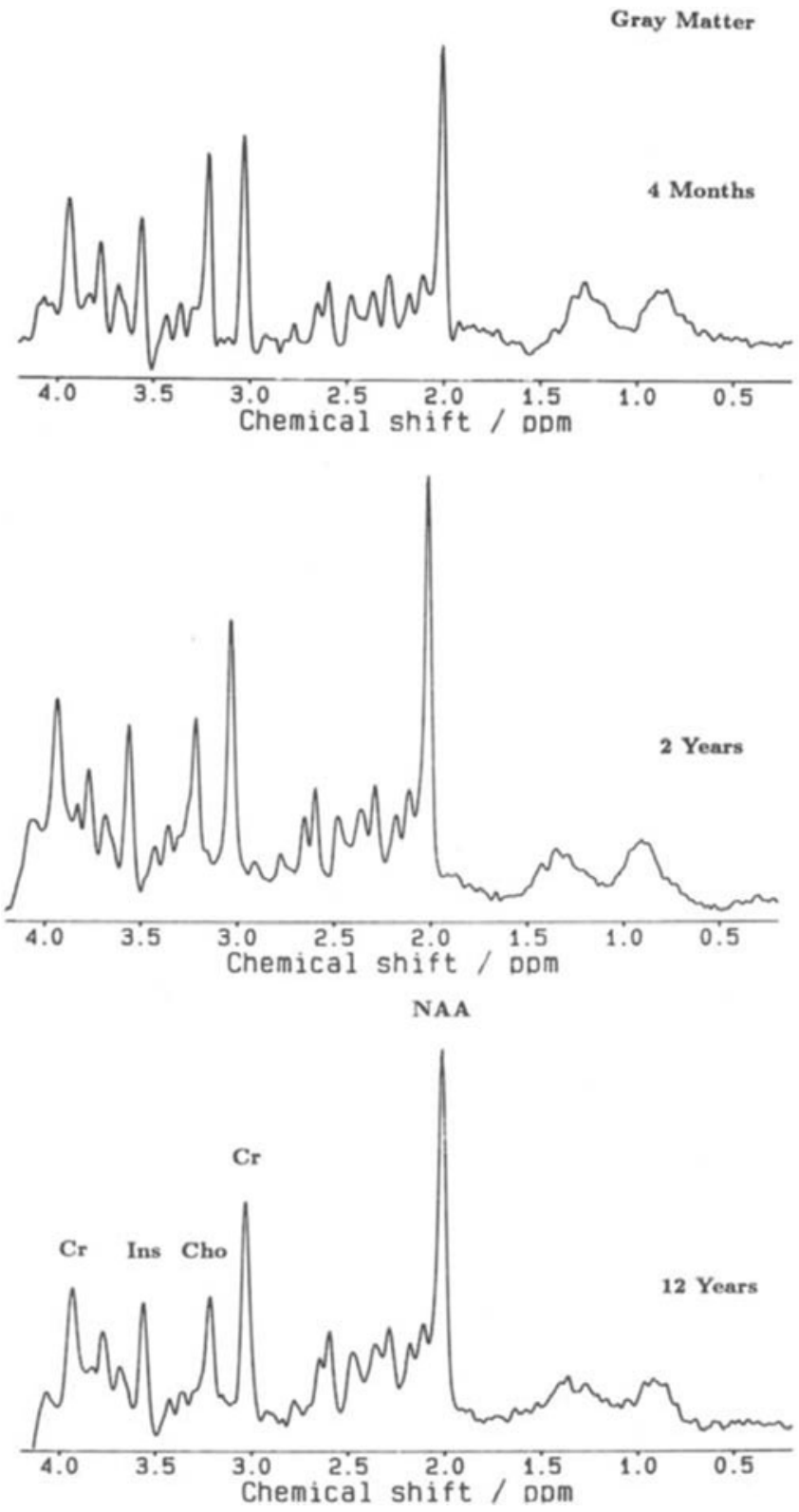

FIGURE 4. Age dependence of the metabolite pattern in the human brain (healthy subjects) as detected by ^1H MRS (STEAM, TR/TE/TM = 3000/20/30 msec, 128 accumulations) of gray (12–18 ml) and white matter (5.1–12 ml) at the age of 4 months (*top*), 2 years (*middle*), and 12 years (*bottom*). It should be noted that true changes in concentration, i.e., resonance area, may not be reflected by corresponding changes in resonance *peak height*, if spectra are measured with different magnetic field homogeneities, i.e., resonance linewidths.

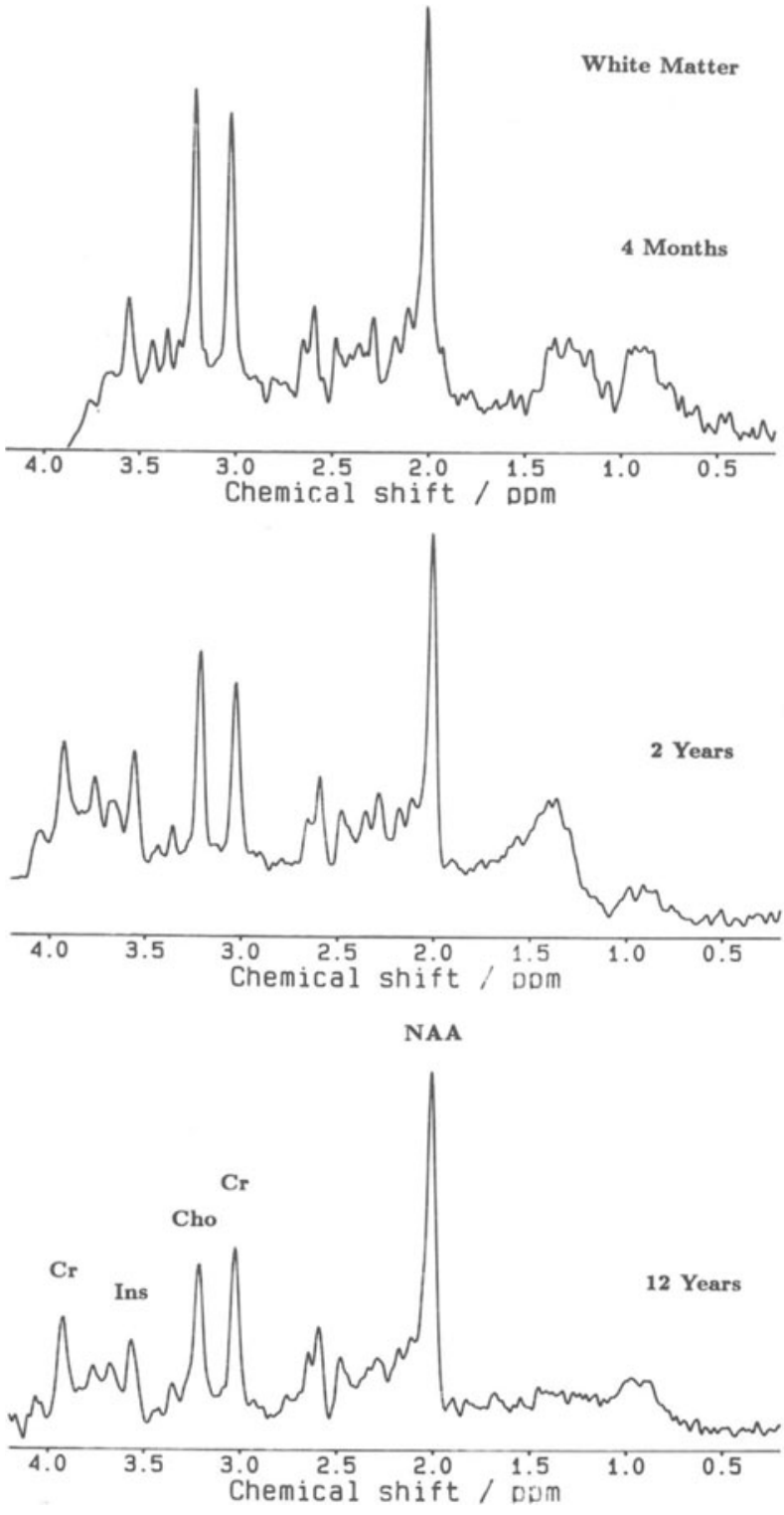

FIGURE 4. Continued

- NAA increases from low values immediately after birth to (almost) adult levels at the age of 3 years, probably in parallel with myelination.
- Cho concentrations decrease over the same time period.
- *myo*-Ins concentrations rapidly fall from very high values after birth to adult levels within the first 3–4 months of life.

All changes occur in both gray and white matter and are also seen in other brain areas, although no systematic investigations are available. For NAA and Cho, normative time courses correlate best with gestational age, while *myo*-Ins decreases with postnatal age (Kreis *et al.,* 1993). The concentration of Cr seems to be fairly stable at the adult level. An interesting observation is the absence of NAAG in white matter of young children. Detectable levels are not reached before adolescence, as indicated by a broadening of the NAA resonance (left shoulder) in the white-matter spectrum of the 12-year-old subject (Fig. 4, bottom right). In agreement with conventional analyses, our data further demonstrate that the concentration of Tau (underlying Glc and *scyllo*-Ins resonances) is elevated in young children in comparison to adult controls.

2.5. Patient Examinations

All MRI and ^1H MRS studies were carried out at 2.0 T (Siemens Magnetom SP4000) using the standard circularly polarized head coil. Examinations of young children of less than about 8 years of age are performed under mild oral sedation using either chloral hydrate or benzodiazepines. Cardiovascular and pulmonory function are monitored throughout the investigation. Since most children sleep during the examination, the combined MRI and MRS study typically lasts 1–1.5 hr and comprises the following:

- T_1-weighted three dimensional (3-D) gradient-echo MRI, eventually complemented by T_2-weighted fast-scan MRI (Frahm *et al.,* 1991c)
- Single-voxel ^1H MRS of parietal gray and white matter and 2–4 additional brain areas reflecting disease-specific requirements

In these studies the measuring time of individual spectra is kept to 6.5 min using 64 accumulations with TR = 6000 msec or 128 accumulations with TR = 3000 msec in some earlier studies. More than 90% of attempted examinations have been successful. Written informed consent is obtained from the parents prior to the examination.

In general, meaningful applications of quantitative ^1H MRS to studies of brain disorders require not only control of data acquisition and evaluation but also careful selection of patients and diseases to avoid unnecessary and costly investigations. In addition to neurological, neurophysiological, and biochemical investigations, conventional computerized tomography (CT) or MRI should precede MRS. Biochemical screening should include the determination of amino

acids, organic acids, ammonia, catecholamines, and lactate in urine, blood, and, if possible, CSF. Such prior information improves MRS examinations by guiding both the selection of VOI locations and the analysis of suspected metabolic/spectroscopic abnormalities.

As far as diseases are concerned, at least three different categories may be identified:

1. *Diseases with abnormal MRI* that lead to focal or generalized lesions in patients with or without clinical symptoms. The main candidates in this category are gray- and white-matter diseases as well as basal ganglia and cerebellar disorders, e.g., leukodystrophies, mitochondrial disorders, infections, epilepsies with structural abnormalities, amino and organic acidopathias, and brain tumors.
2. *Diseases with normal MRI* but distinct neurological and/or biochemical abnormalities. Neurological abnormalities include disturbances of consciousness (acute and chronic encephalopathies), disturbances of muscle tonus (severe hypotonia), movement disorders (extrapyramidal, particularly dystonic syndromes), seizures of suspected metabolic origin, and dementias. Biochemical abnormalities are lactic acidosis, hyperammonemia, and organic and amino acidurias.
3. *Miscellaneous disease conditions,* mainly neurological disorders of unknown origin with normal MRI and unsuspicious biochemistry but suspected metabolic abnormalities (e.g., neurotransmitter disorders).

3. LEUKODYSTROPHIES

Leukodystrophies comprise a group of genetic diseases that affect brain myelin and, in a few disorders, also peripheral myelin. While onset is usually in early childhood, the spectrum ranges from congenital types to adult-onset types. Leukodystrophies represent the classical type of white-matter disorders with motor disturbances, visual loss, and deafness as early symptoms. Associated dysfunction of gray matter such as dementia and seizures is usually secondary and occurs later during the evolution of the disease. Numerous reviews on leukodystrophies cover the molecular biology and genetic basis (Rosenberg *et al.*, 1993) as well as clinical aspects (Aicardi, 1993; Kolodny, 1993) and MRI appearances (Valk and van der Knaap, 1989; Kendall, 1993).

White-matter abnormalities in leukodystrophy are often characterized as demyelination, dysmyelination, and hypomyelination, defined as follows:

- *Demyelination* refers to a breakdown of structurally and biochemically normal myelin (e.g., in multiple sclerosis).

- *Dysmyelination* denotes a breakdown of structurally and biochemically abnormal and/or unstable myelin (e.g., in adrenoleukodystrophy).
- *Hypomyelination* indicates disturbance and delay in the formation of normal myelin (e.g., in Pelizaeus–Merzbacher disease).

Although the clinical course and neuropathology of most leukodystrophies were described almost a century ago, the biochemical and genetic defects were only clarified during the last decades. Despite all diagnostic efforts and progress in modern neuroradiological, biochemical, and genetic methods, a substantial proportion of leukodystrophies in childhood remain unclassified. Even in those cases in which the metabolic defect is known and the gene has been mapped, e.g., in metachromatic and globoid cell leukodystrophy, the pathogenesis of brain abnormalities is still unclear. The following description is based on our experience in more than 100 cases of leukodystrophies including 84 in whom MRS was performed during initial diagnostic procedures and follow-up of the disease.

3.1. Metachromatic Leukodystrophy

Metachromatic leukodystrophy (MLD) was first described by Scholz (1925) as a familial type of diffuse sclerosis. Austin *et al.* (1963) and Mehl and Jatzkewitz (1965) discovered a deficiency of arylsulfatase A that causes a deposition of typical metachromatic material in central and peripheral myelin. The gene has been mapped to chromosome 22 (Polten *et al.*, 1991), and a pseudodeficiency gene was identified. Three clinical forms of MLD can be distinguished according to age of onset: a late infantile, a juvenile, and an adult type. The incidence of MLD is estimated to be 1:40,000. Demyelination as shown on MRI starts most frequently in frontal white matter and capsula interna and is accompanied by peripheral neuropathy in almost all cases. It leads to ataxia, spasticity, and severe motor and mental handicap (Kolodny, 1989).

^1H MRS of cerebral metabolic alterations in MLD reveals variable degrees of NAA reduction and a generalized and pronounced increase in brain *myo*-Ins as conspicuous abnormalities (Kruse *et al.*, 1993). As shown in Fig. 5 for a 2-year-old patient with late infantile MLD, *myo*-Ins concentrations of gray (7.5 mM) and white matter (9.9 mM) are 2- to 3-fold above normal levels (of. Table 2). A parallel enhancement is seen for *scyllo*-Ins in white matter (0.5 mM; normal 0.2 $\pm$ 0.1 mM). Its concentration is known to be tightly coupled to that of *myo*-Ins via *myo*-inosose-2 as a single intermediate (Sherman *et al.*, 1968). The observation of a specific metabolic disturbance in glial cells is paralleled by significant increases of Cho (2.3 mM, + 65%) and Cr (7.3 mM, + 45%) in white matter.

As noted previously (Kruse *et al.*, 1993), the MRS findings are in line with a demyelination of white matter and (subsequent) degeneration of neuroaxonal tissue. Although enhanced levels of Ins and Cho may reflect accumulation of

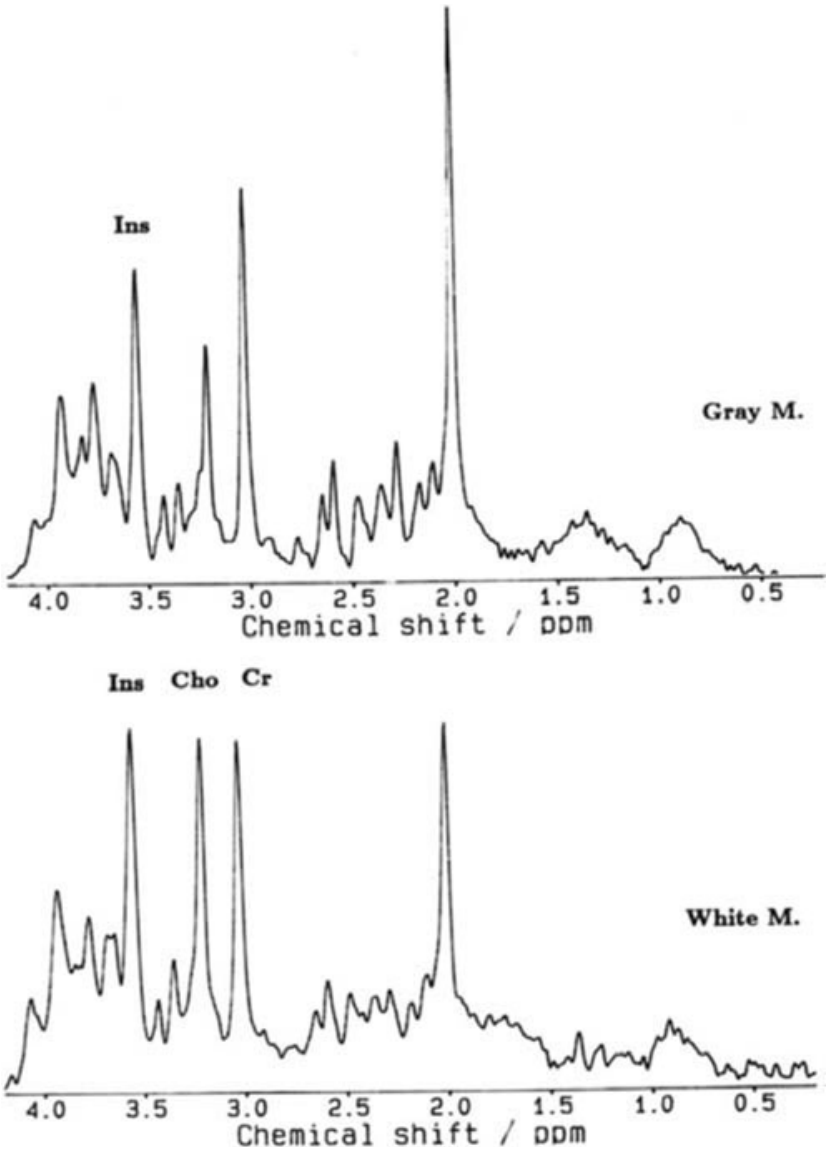

FIGURE 5. Metabolic alternations in a 2-year-old patient with metachromatic leukodystrophy as detected by ^{1}H MRS (STEAM, TR/TE/TM = 6000/20/30 msec, 64 accumulations) of gray (18 ml) and white matter (12 ml). Most prominent findings are a generalized elevation of *myo*- and *scyllo*-Ins as well as increased levels of Cho and Cr in white matter.

myelin breakdown products, they are more likely accounted for by changes in glial membrane composition that involve free *myo*-Ins and PCh contributions to the Cho level as major constituents for a synthesis of phospholipid membranes in general and the formation of myelin in particular. In fact, since other explanations such as dietary considerations or renal dysfunction could be excluded in our patients and since autopsy studies revealed a strong elevation of phosphatidylinositol relative to other phospholipids in isolated myelin from a patient with MLD (Norton and Poduslo, 1982), it may be hypothesized that ^{1}H MRS primarily reflects lipid alterations in demyelinating areas of MLD patients. Thus, elevation of *myo*-Ins (as well as of Cho and Cr) may be of more fundamental

importance for the pathogenesis of demyelination as well as for related neurodegenerative processes and neurological symptoms than the accumulation of sulfatides in MLD and, as such, clearly deserves further consideration. Related observations have been made in other leukodystrophies.

3.2. Globoid Cell Leukodystrophy (Krabbe's Disease)

Globoid cell leukodystrophy (GLD) was first described by Krabbe (1916) and is now recognized as an inherited autosomal recessive disorder. Patients develop symptoms from the age of 2 to 6 months onward and die within one or two years mostly in a decerebral state. The clinical stages of Krabbe's disease have been delineated by Hagberg *et al.* (1970). A late-onset form was found by Crome *et al.* (1973). The brain shows extensive lack of myelin as well as proliferation of glial cells in affected areas with mononuclear epitheloid cells and clusters of large multinucleated globoid cells. Involvement of the peripheral nervous system is much less pronounced than in MLD. The biochemical defect is a deficiency of galactocerebroside β-galactosidase (Suzuki *et al.*, 1971) and mapped on chromosome 14. Many symptoms are related to the increase of psychosin in brain tissue as the result of the enzyme deficiency. GLD is a rare disease; its exact incidence is unknown.

MRI reveals a diffuse demyelination of the cerebral hemispheres, brain stem, and cerebellum, while arcuate fibers are often spared (Baram *et al.*, 1986; Sasaki *et al.*, 1991; Percy *et al.*, 1994). The T_1-weighted image of an 8-month-old patient in Fig. 6 shows pronounced hypodensities indicating structural disintegration in periventricular white matter. Analysis of a spectrum from left parietal white matter depicts elevated concentrations of *myo*-Ins (8.7 mM), Cho (2.6 mM), and Cr (6.5 mM) that resemble the findings in MLD. However, reduction of NAA (3.5 mM) in affected white matter is even more pronounced than in MLD as is the occurrence of elevated Lac (3.2 mM). These MRS findings suggest that there is a similar disturbance of myelination in MLD and GLD but that the latter produces a more severe neuroaxonal degeneration and/or an even more rapid disease progression.

3.3. Pelizaeus–Merzbacher Disease

The classical X-linked type of Pelizaeus–Merzbacher disease (PMD) was described by Pelizaeus (1885) and Merzbacher (1910). Seitelberger (1970) added the congenital variant in his description of three affected brothers. Hypotonus, ataxia, spasticity, and nystagmus are early symptoms. Classical PMD does not belong to the lysosomal disorders. It is caused by a genetic defect of one of the major myelin proteins, proteolipidprotein (PLP), which results in a disturbance of myelin formation and maintenance. PLP has also a role in the differentiation of

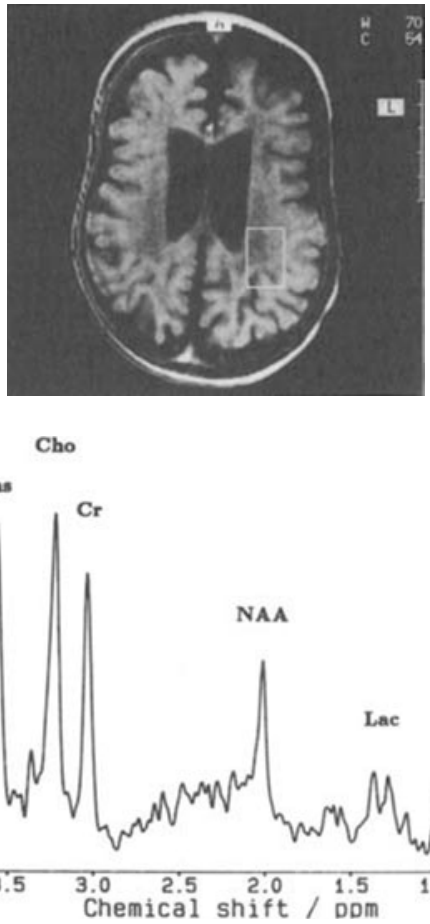

FIGURE 6. Morphological and metabolic alterations in an 8-month-old patient with Krabbe's disease as detected by T_1-weighted MRI (RF spoiled 3-D FLASH, TR/TE = 15/6 msec, 20° flip angle, 4-mm partitions) and ^{1}H MRS (STEAM, TR/TE/TM = 6000/20/30 msec, 64 accumulations). Affected white matter (6.4 ml) shows reduced NAA as well as elevated *myo*-Ins, Cho, Cr, and Lac.

oligodendrocytes. Various point mutations in its gene have been detected in many but not all patients (Doll *et al.*, 1992; Boespflug-Tanguy *et al.*, 1994). The neuropathology in classical PMD is described as patchy dys- or hypomyelination, whereas the Seitelberg type exhibits almost total absence of myelin. The peripheral nervous system is spared.

MRI of PMD shows diffuse white-matter abnormalities. The degree of signal intensity reversal in gray and white matter reflects the stage of the disease. Figure 7 shows residual myelination in basal ganglia in a 12-year-old patient. ^{1}H MRS of white matter revealed increased *myo*-Ins (5.0 mM) and Cr (6.6 mM) but mildly *decreased* Cho (1.2 mM). NAA levels were normal in both gray and white matter. In general, the altered white-matter spectra closely resembled that of normal gray matter (not shown). In comparison to MLD and GLD, the neuro-

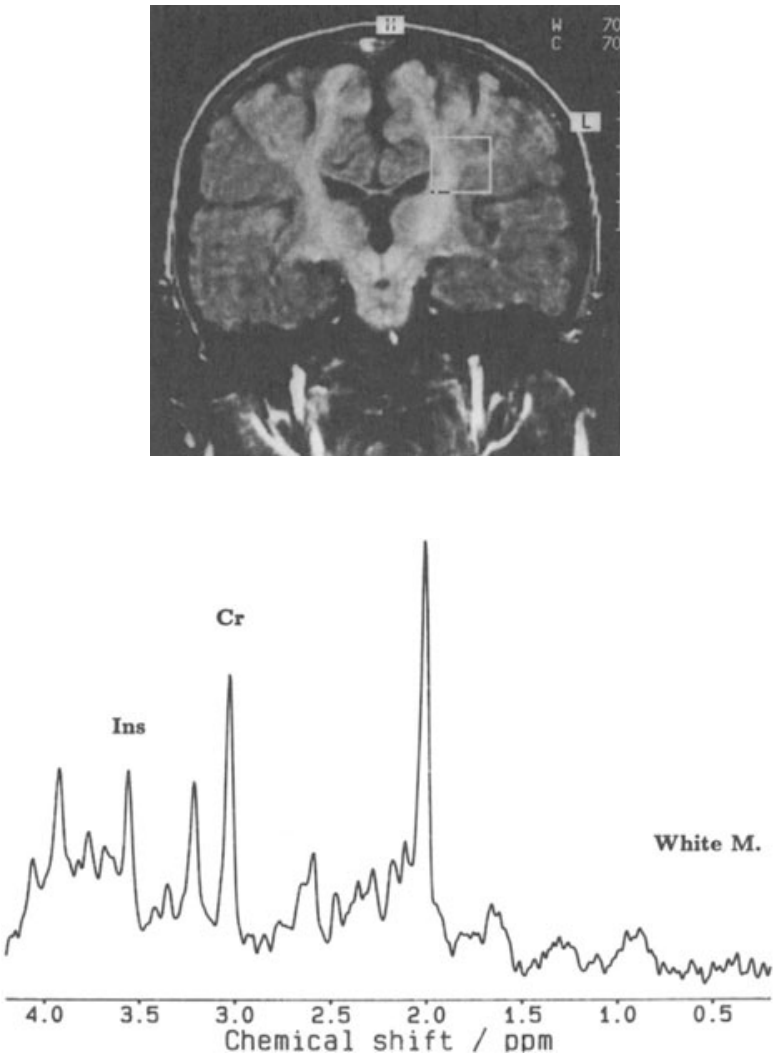

FIGURE 7. Morphological and metabolic alterations in a 12-year-old patient with Pelizaeus–Merzbacher disease as detected by T_1-weighted MRI (RF spoiled 3-D FLASH, TR/TE = 15/6 msec, 20° flip angle, 4-mm partitions) and ^{1}H MRS (STEAM, TR/TE/TM = 6000/20/30 msec, 64 accumulations) of white matter (8 ml). Mild reduction of Cho is accompanied by elevated *myo*-Ins and Cr.

chemical alterations associated with classical PMD yield an independent and characteristic pattern of abnormal myelination that differs by the absence of Cho elevation and a lack of neuroaxonal degeneration.

3.4. Canavan's Disease

Spongiform encephalopathy was first described in a case report by Canavan (1931) and later extensively studied by van Bogaert and Bertrand (1967). Among the three clinical variants of this autosomal recessive disorder, the infantile type of Canavan's disease (CD) is most frequently seen. Its clinical characteristics are macrocephaly associated with progressive spasticity, blindness, and motor and mental retardation. The metabolic defect is a deficiency of aspartoacylase, the enzyme responsible for NAA breakdown (Matalon *et al.*, 1988). Cloning of the

human aspartoacylase cDNA was accomplished and a common missense mutation in CD was reported by Kaul *et al.* (1993).

Neuropathology of CD is characterized by rarefication, vacuolation, and ultimately breakdown of neural tissue. Cavitations occur at the junction of white matter and cortex. Vacuoles are caused by the separation of the lamellae of myelin. Astrocytic cell membranes are also affected, and large pale astrocytic nuclei devoid of visible cytoplasm represent a characteristic feature of the cerebral cortex (so-called Alzheimer-II cells). MRI of the brain reveals diffuse white-matter degeneration with partial sparing of the corpus callosum. This is well appreciated in the coronal image of a 4-year-old patient with CD shown in Fig. 8.

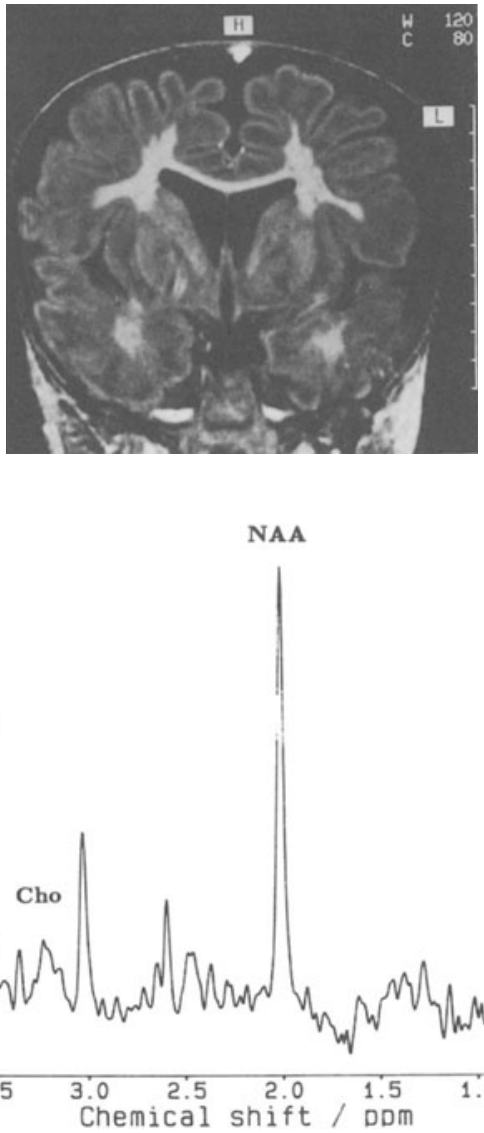

FIGURE 8. Morphological and metabolic alterations in a 4-year-old patient with Canavan's disease as detected by T_1-weighted MRI (RF spoiled 3-D FLASH, TR/TE = 15/6 msec, 20° flip angle, 4-mm partitions) and ^{1}H MRS (STEAM, TR/TE/TM = 6000/20/30 msec, 64 accumulations) of white matter (4.1 ml), gray matter (18 ml), and basal ganglia (4.1 ml). The disorder is characterized by generalized increases of NAA and *myo*-Ins as well as marked reductions of Cho.

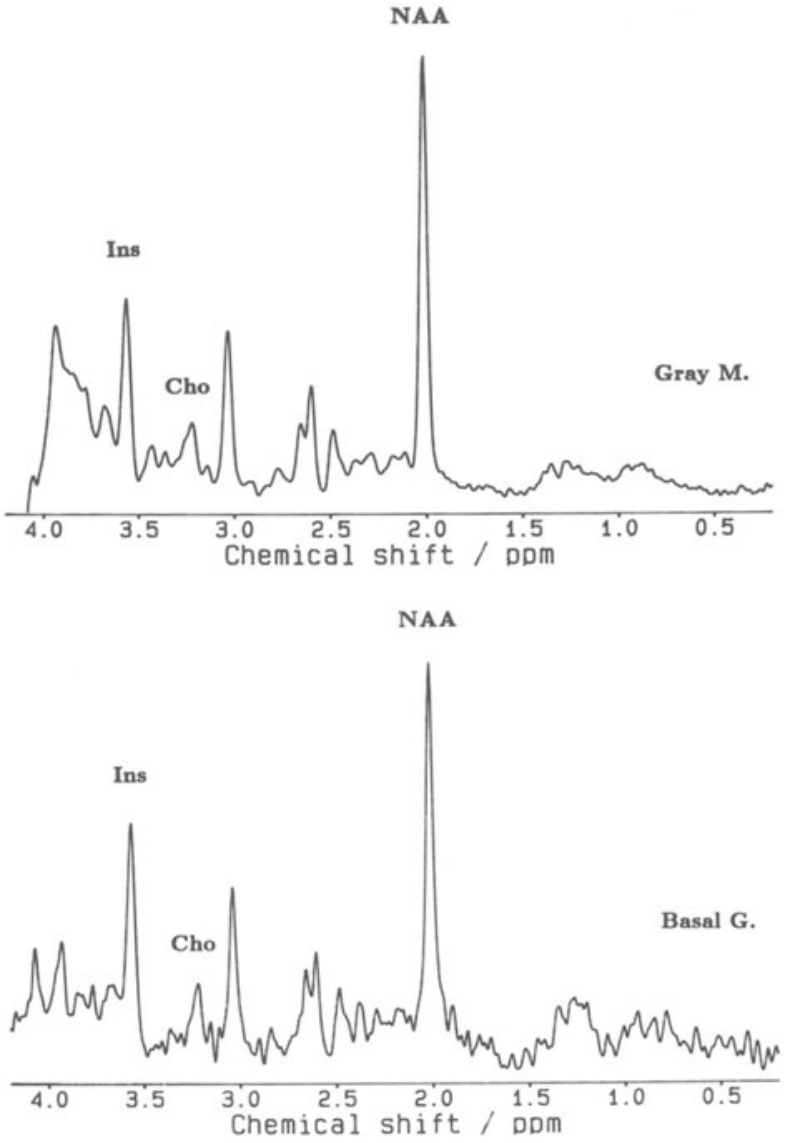

FIGURE 8. Continued

So far, several MRS case reports of CD have appeared (Grodd *et al.,* 1990; Austin *et al.,* 1991; Barker *et al.,* 1991). Experimental limitations in these studies were mainly associated with the range of identifiable metabolites (e.g., due to long-TE rather than short-TE conditions) and neurochemical data evaluation (e.g., use of short TR values and peak ratios rather than absolute metabolite concentrations). As demonstrated in Fig. 8, quantitative ^1H MRS resulted in a pattern of findings common to all areas investigated. Elevation of NAA was mild in white matter and marked in gray matter (11.5 mM, +50%), consistent with aspartoacylase deficiency and different from the findings in all other brain disorders investigated so far. With Cr levels within normal ranges, the concentrations of Cho and *myo*-Ins were markedly decreased and increased, respectively. For example, in white matter Cho (0.6 mM) was reduced by 60% while *myo*-Ins (9.7 mM) was enhanced 3-fold.

Similar to MRS findings in other forms of leukodystrophy, the strong enhancement of free *myo*-Ins in white (and gray) matter seems to indicate alterations of glial metabolism that are closely associated with disturbances of myelination. Because oligodendrocytes are involved in the formation of myelin, it may be hypothezised that they represent the primary location of *myo*-Ins. Accordingly, the observation of low Cho levels may be due to degeneration of astrocytes in this disease. High Cho concentrations have been found in astrocytomas and related to cell proliferation. An alternative explanation of the "decoupling" of Cho and *myo*-Ins changes in white matter involves a specific disease-related change in myelin composition. Further open questions are the link between elevated NAA and demyelination in CD and the discrepancy between the only mild to moderate NAA increases in brain and the strongly increased levels in plasma (and urine).

3.5. Alexander's Disease

The other macrocephalic encephalopathy identified as a clinical and probably also genetic entity (Ochi *et al.*, 1991) is Alexander's disease (AD). The description of brain pathology by Alexander (1949) referred to a "hydrocephalic infant" with progressive fibrinoid degeneration of fibrillary astrocytes and the presence of so-called Rosenthal fibers. Head enlargement occurs gradually during the first years of life. Etiology is unknown. Although the disease is rare and usually sporadic, familial cases as well as late-onset types have been reported.

In general, MRI findings are in line with a progressive white-matter disease affecting frontal lobes primarily (Arend *et al.*, 1991; Schuster *et al.*, 1991). Brain stem involvement is common, but the peripheral nervous system is spared. Ataxia, spasticity, swallowing difficulties, blindness, and severe psychomotor retardation develop early during AD. Seizures are rare and typically occur during unspecific viral infections or following mild head trauma.

Figure 9 shows the case of a 2-year-old patient with AD and severe disturbances of cortical white matter detected by MRI. ^{1}H MRS revealed a marked decrease of NAA (2.1 mM) and Cr (3.4 mM) but elevated Cho (1.8 mM) and Lac (3.8 mM). Interestingly, these abnormalities clearly resemble the metabolite pattern of astrocytomas. The white-matter findings in AD are therefore compatible with astrocytic degeneration severely affecting the viability of neuroaxonal tissue compartments.

The neurochemical behavior seen in cortical and subcortical gray matter clearly differs from that in white matter. While 30–50% reductions of NAA most likely indicate neuronal damage, the concentrations of *myo*-Ins (7.4 mM), Cho (1.7 mM), and Cr (6.8 mM) are enhanced in gray matter and even further in basal ganglia (8.6 mM, 2.7 mM, and 8.5 mM, respectively). This pattern parallels metabolic abnormalities previously found in affected white matter of patients

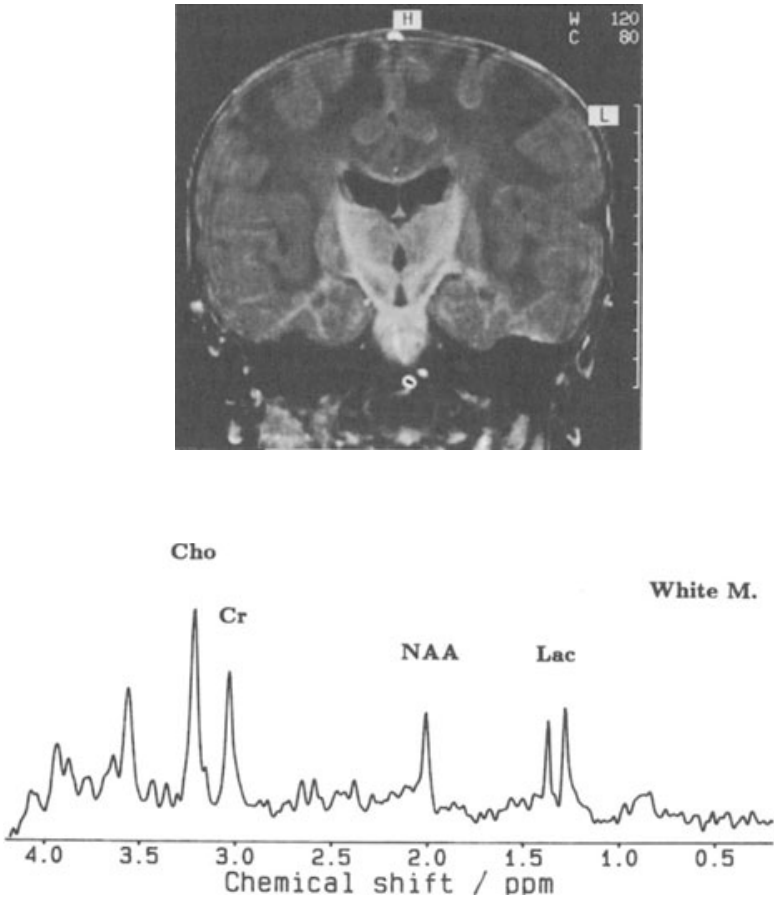

FIGURE 9. Morphological and metabolic alterations in a 2-year-old patient with Alexander's disease as detected by T_1-weighted MRI (RF spoiled 3-D FLASH, TR/TE = 15/6 msec, 20° flip angle, 4-mm partitions) and ^1H MRS (STEAM, TR/TE/TM = 6000/20/30 msec, 64 accumulations) of white matter (12 ml), gray matter (18 ml), and basal ganglia (6.4 ml). While white-matter disturbances include reduced NAA and Cr as well as elevated Cho and Lac, cortical and subcortical gray matter shows decreased NAA and elevated *myo*-Ins, Cho, and Cr.

with MLD and GLD and therefore suggests alterations in glial phospholipid metabolism rather than structural disintegration of glial cells.

3.6. Adrenoleukodystrophy

Adrenoleukodystrophy (ALD) is an X-linked disorder occurring at an incidence of 1:15,000 in males. Different clinical phenotypes are known. The cerebral form (40%) manifests itself between 5 and 12 years of age. Clinical symptoms are similar to those seen in other white-matter diseases and are dominated by ataxia, spasticity, deafness, visual problems, personality changes, and mental deterioration. In most cases, associated adrenal insufficiency (Addison's disease) emerges as the first—and in rare cases as the only—clinical expression of ALD.

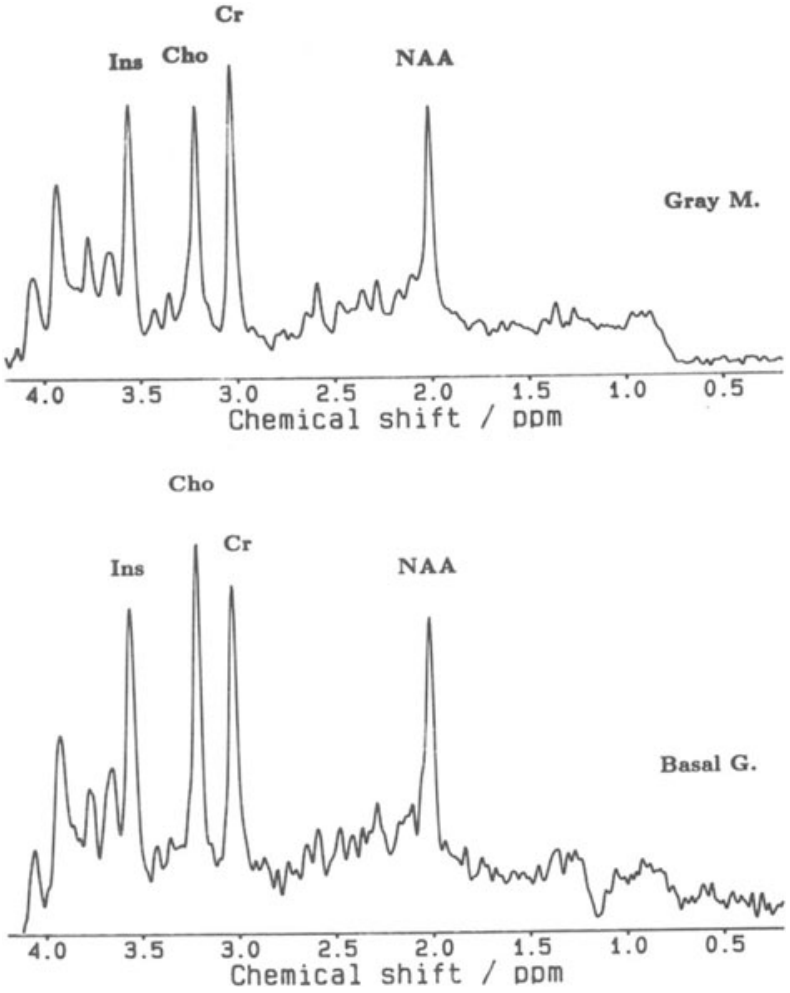

FIGURE 9. Continued

Adrenomyeloneuropathy (AMN) represents the adult phenotype. Both forms may occur in the same family. The biochemical defect is a deficiency of VLCFA synthetase in peroxisomes, which leads to an increase of very-long-chain fatty acids (VLCFA) in fibroblasts and plasma. The ALD gene on the X chromosome (Xq28) encodes a peroxisomal membrane protein (ALDP) of the "ATP binding cassette" family (Mosser *et al.*, 1993).

Typically, pathology reveals most severe demyelination in the occipital,

FIGURE 10. Morphological and metabolic alterations in an 8-year-old patient with adrenoleukodystrophy as detected by T_1-weighted MRI (RF spoiled 3-D FLASH, TR/TE = 15/6 msec, 20° flip angle, 4-mm partitions) and ^{1}H MRS (STEAM, TR/TE/TM = 6000/20/30 msec, 64 accumulations) of right frontoparietal white matter (8 ml) as well as of left and right parieto-occipital white matter (6.4 ml). While frontal white matter shows reduced NAA and enhanced levels of *myo*-Ins and Cho, left parieto-occipital white-matter disturbances include a complete loss of NAA as well as elevated *myo*-Ins and Cho. The most affected white matter in right parieto-occipital brain shows a complete loss of NAA as well as reduced Cho and Cr but still elevated *myo*-Ins.

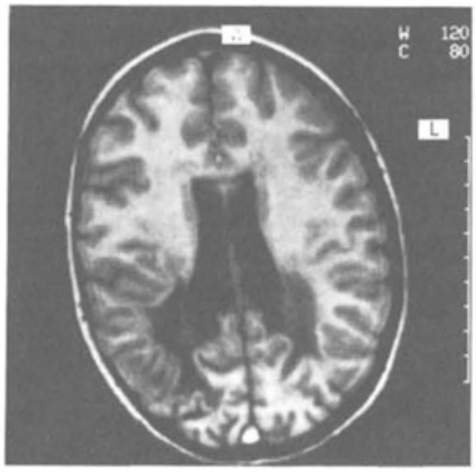
W 120
C 80
L

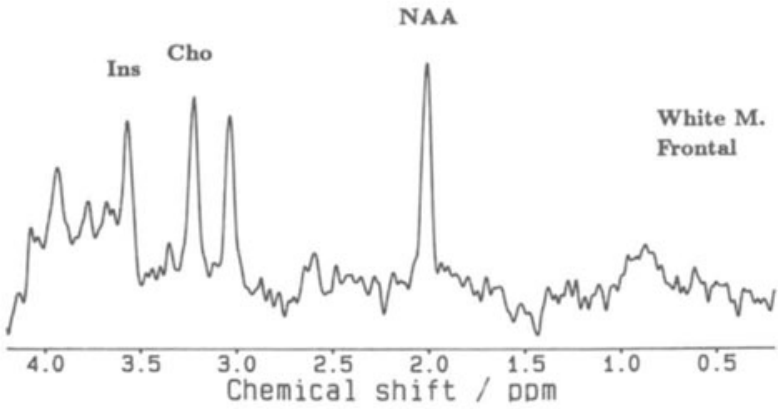
NAA
Cho
Ins
White M.
Frontal
4.0 3.5 3.0 2.5 2.0 1.5 1.0 0.5
Chemical shift / ppm

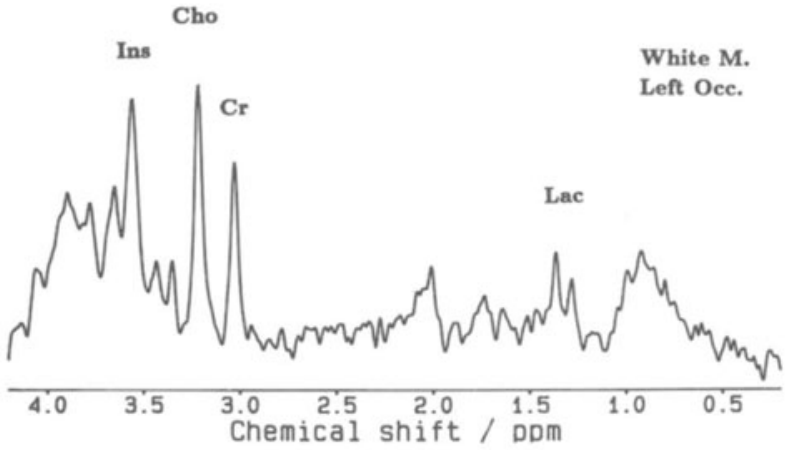
Cho
Ins
Cr
White M.
Left Occ.
Lac
4.0 3.5 3.0 2.5 2.0 1.5 1.0 0.5
Chemical shift / ppm

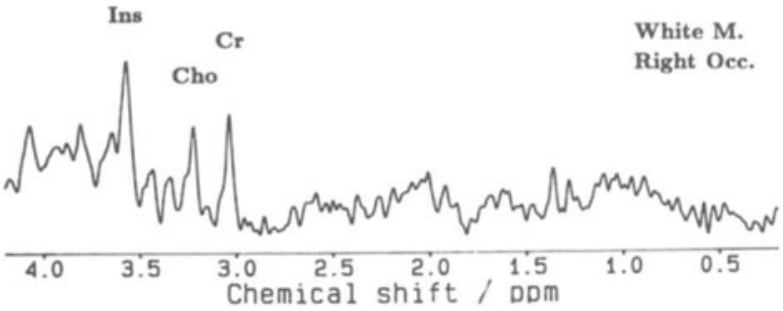
Ins
Cr
Cho
White M.
Right Occ.
4.0 3.5 3.0 2.5 2.0 1.5 1.0 0.5
Chemical shift / ppm

parietal, and temporal lobes, although some of our patients presented with an initial affection of frontal lobes. The lesions are histologically characterized by three zones, respectively showing (i) destruction of myelin and proliferation of sudanophilic macrophages, (ii) myelinated and demyelinated axons with an associated inflammatory response, and (iii) dense gliosis with loss of oligodendrocytes, myelin, and axons.

Inflammatory responses with proliferation of macrophages are particularly prominent at the edges of the lesions, and perivascular lymphocytic cuffing is marked. MRI shows related signal alterations that form a characteristic pattern of periventricular dysmyelination. This is demonstrated in Fig. 10 for the case of an 8-year-old patient. While ^{1}H MRS revealed no changes in parietal gray matter (not shown), disease progression in white matter is evidenced by metabolic alterations of increasing severity in the three regions investigated. Despite the fact that frontal white matter appears unsuspicious on MRI, it shows reduced NAA (6.2 mM) and elevated *myo*-Ins (5.6 mM) and Cho (1.7 mM). These trends are accentuated in affected left parieto-occipital white matter, yielding a severe reduction of NAA (2.0 mM) as well as strongly elevated *myo*-Ins (6.4 mM) and Cho (2.2 mM). Increase of brain Lac (3.6 mM) in such regions is a frequent finding in ALD. Finally, the lesion in right parieto-occipital white matter exhibits a generalized reduction of metabolites with residual concentrations of Cho (0.6 mM) and Cr (2.3 mM) but still elevated *myo*-Ins (5.5 mM).

The metabolic findings in white matter of ALD parallel observations in other leukodystrophies, e.g., MLD and GLD. In this case, the simultaneous occurrence of glial and neuroaxonal changes of different severity suggests a characterization of disease progression according to the following stages:

- Normal-appearing white matter (on MRI) may be affected by moderate neuroaxonal damage (or loss) as well as signs of demyelination that are in line with myelin phospholipid changes in glia.
- Affected white matter (on MRI) shows severe neuroaxonal loss and elevation of Lac as well as signs of severe demyelination (glial changes).
- Most severely affected white matter (lesions on MRI) shows a complete neuroaxonal loss as well as structural disintegration of glial cells.

A previous study using proton chemical shift imaging indicated a correlation of the Cho/NAA resonance ratio with clinical course (Kruse *et al.*, 1994a). Our data not only confirm this suggestion, with use of the Cho/NAA *concentration* ratio, but extend the correlation to the *myo*-Ins/NAA concentration ratio. The latter parameter allows a more specific assessment of the degree of neuroaxonal damage and of activity of the demyelinating process in respective neuronal and glial compartments (Pouwels *et al.*, unpublished results). For the case shown in Fig. 10, the *myo*-Ins/NAA concentration ratio increases from 0.9 (normal-appearing white matter) to 3.2 (affected) and 5.6 (severely affected) as compared

to 0.36 for normal controls. The hypothesis that the *myo*-Ins/NAA ratio is sensitive to true disease progression is further substantiated by follow-up studies in selected patients over several years (Pouwels *et al.*, unpublished results). In particular, continuous examinations of asymptomatic ALD patients at early stages prove useful, because an increase in *myo*-Ins/NAA clearly precedes a subsequent clinical deterioration. Tight patient monitoring by ^1H MRS may thus guide the selection of candidates for bone marrow transplantation (Aubourg *et al.*, 1990).

3.7. Unclassified Leukodystrophies

Among 35 children with unclassified white-matter disease, two subgroups with identical clinical characteristics and MRS abnormalities could be identified. A first disease entity has been described by Hanefeld *et al.* (1993) and termed myelinopathia centralis diffusa (MCD). Subsequent to a normal development in early infancy up to the age of 2 to 3 years, children with MCD develop ataxia and spasticity. They become wheelchair-bound between 4 and 6 years of age. Optic atrophy and dementia are late features. Six children, including one pair of siblings (brother and sister), have been studied so far. Head circumference was within normal limits. MRI revealed diffuse homogeneous hypointensity of white matter (T_1-weighting) identical to the signal from CSF in the ventricles. U-fibers were also affected. Figure 11 gives two examples, showing an early phase (top) with residual preserved white matter and a late phase (middle) characterized by cellular disintegration of white matter and a complete loss of neuroaxonal and glial tissue. This is also evidenced by ^1H MRS, showing a significant reduction (top) and final loss (middle) of all cellular metabolites except those found in CSF (Glc at 3.1 mM, Lac at 1.7 mM).

A second disease entity among patients with diffuse white-matter demyelination was first described by van der Knaap *et al.* (1995) and may be characterized as spongy or cystic leukoencephalopathy. In this group, all children are macrocephalic from birth. After normal development, focal seizures start around 3 years of age. Ataxia and spasticity develop later than in the normocephalic patients with MCD. In addition to diffuse white-matter changes, MRI is characterized by cystic lesions in the temporal and high parietal regions. As demonstrated for a 6-year-old patient in Fig. 11 (bottom), these findings are clearly distinct from the pattern seen in other macrocephalic white-matter diseases (e.g., Alexander's disease). ^1H MRS shows a severe reduction of all metabolites but no elevation of Lac. Major differences with respect to MCD patients are the macrocephaly, a slower disease progression, and the cystic white-matter abnormalities. Whether final stages entail a complete replacement of white matter by CSF and a metabolic profile equivalent to that of late MCD remains to be seen.

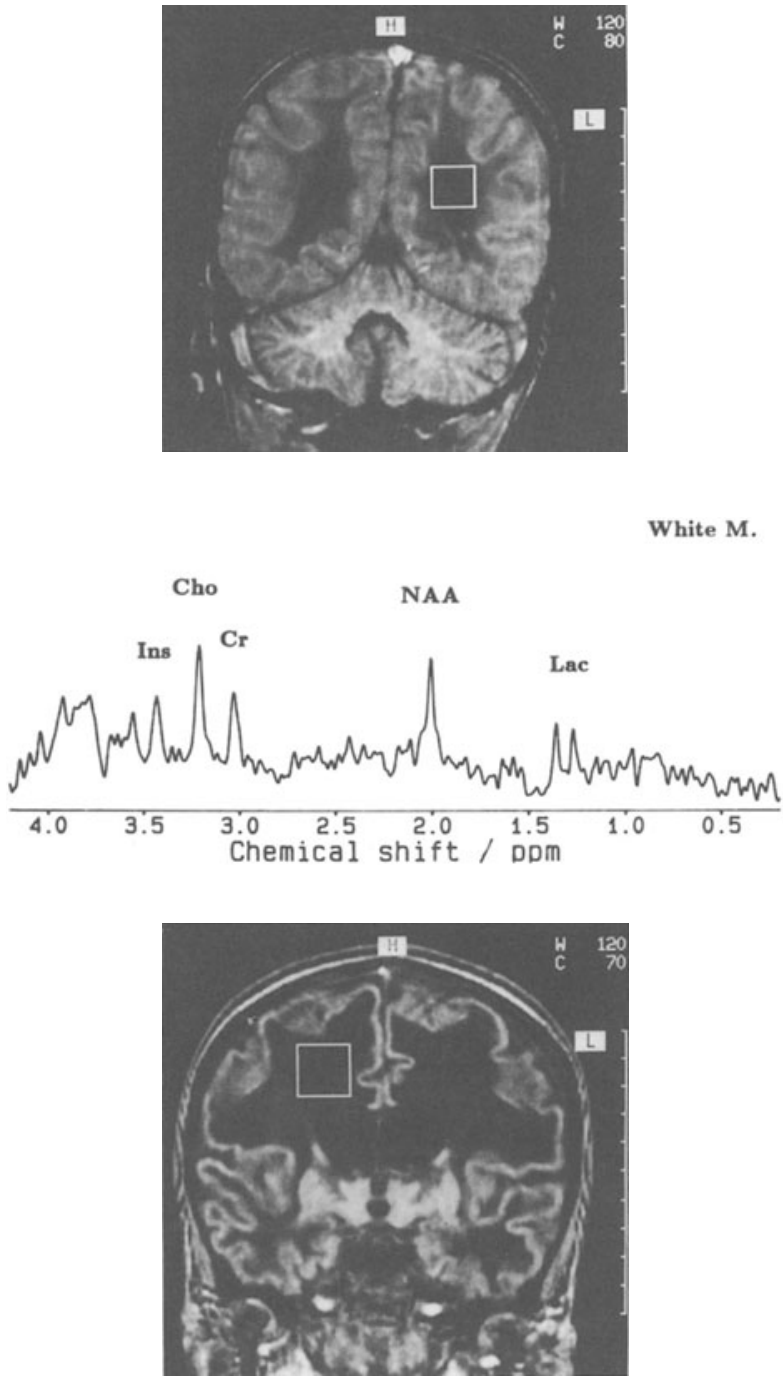

FIGURE 11. Morphological and metabolic alterations in three patients with unclassified leukodystrophy as detected by T_1-weighted MRI (RF spoiled 3-D FLASH, TR/TE = 15/6 msec, 20° flip angle, 4-mm partitions) and ^{1}H MRS (STEAM, TR/TE/TM = 6000/20/30 msec, 64 accumulations) of white matter (5.1–12 ml). *First part:* 3-year-old patient with myelinopathia centralis diffusa (MCD) as described by Hanefeld *et al.* (1993). (early phase). *Second part:* 12-year-old patient with MCD (late phase). *Third part:* 6-year-old patient with spongy or cystic leukoencephalopathy as described by van der Knaap *et al.* (1995). Both disorders are characterized by a loss of white matter and pertinent metabolites.

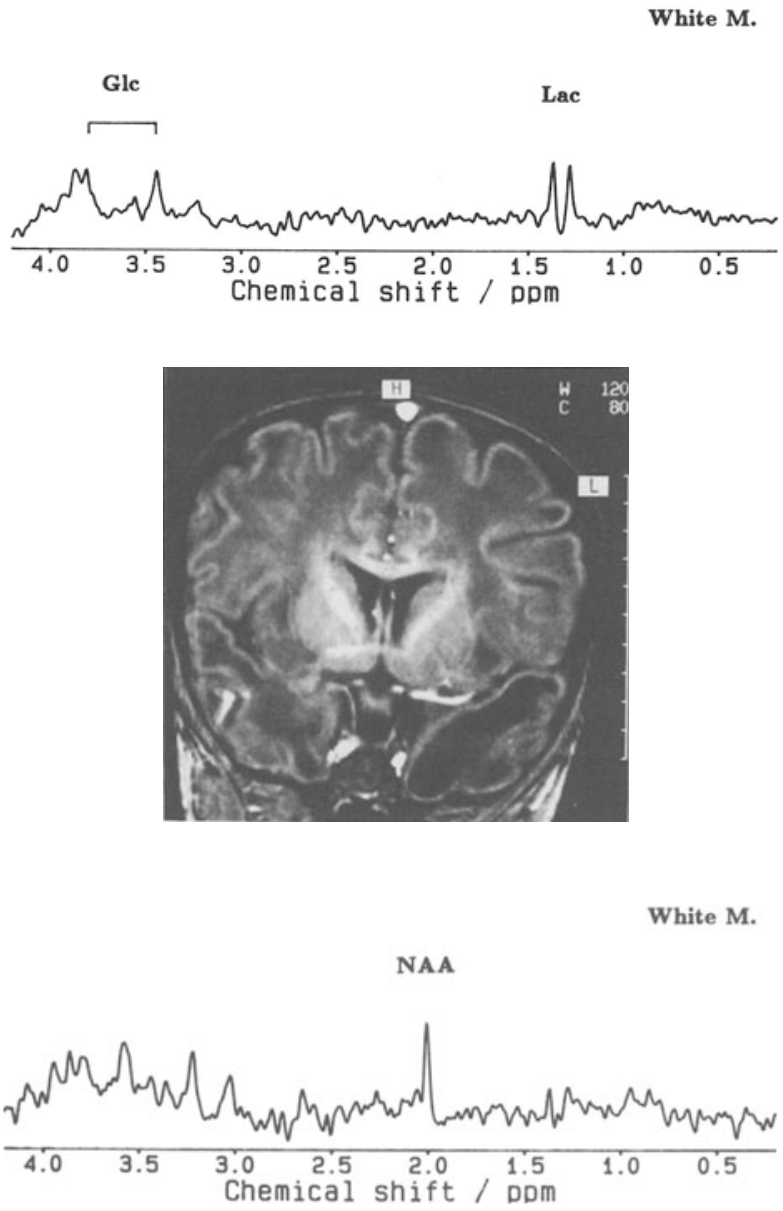

Figure 11. Continued

4. OTHER WHITE-MATTER DISEASES

In recent years the more widespread availability of MRI has led to the recognition of an increasing number of disorders with white-matter abnormalities. It would be wrong to classify these disorders among the leukodystrophies, although the clinical manifestations and the predominance of white-matter changes often suggest such a diagnosis. The following examples should illustrate this problem.

4.1. L-2-Hydroxyglutaric Aciduria

L-2-Hydroxyglutaric (L2OHglu) aciduria is a rare inherited neurometabolic disease that has only recently been described. (Barth *et al.*, 1992). Cerebellar ataxia, mental retardation, and seizures in combination with extrapyramidal and pyramidal symptoms are the main clinical characteristics. Biochemical findings include increased levels of L-2-hydroxyglutaric acid in urine, plasma, and CSF.

MRI reveals enlargement of internal and external CSF spaces as well as patchy white-matter lesions in subcortical regions and adjacent to the frontal and occipital horn. A typical example is shown in Fig. 12 for a 16-year-old patient. ^{1}H MRS of the periventricular white matter lesion revealed reduced levels of NAA (3.9 mM, −40%), Cr (3.5 mM, −20%), and Cho (0.9 mM, −25%), as well as elevation of *myo*-Ins (5.9 mM) by a factor of 2. Because these concentrations are not corrected for the use of a TR of 3000 msec, the relative deviations are given

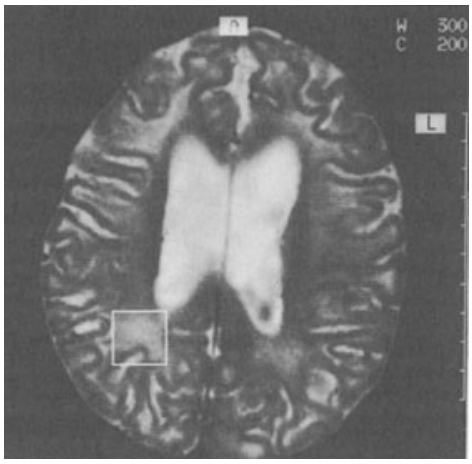

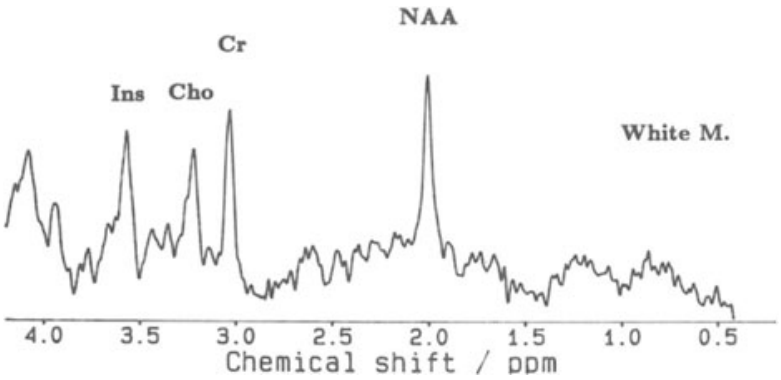

FIGURE 12. Morphological and metabolic alterations in a 16-year-old patient with L-2-hydroxyglutaric aciduria as detected by T_2-weighted MRI (CE-FAST, TR/TE = 14/−6 msec, 40° flip angle, 4-mm thickness) and ^{1}H MRS (STEAM, TR/TE/TM = 3000/20/30 msec, 128 accumulations) of white matter (8 ml). The periventricular lesion in right parietal white matter shows a decrease of NAA, Cr, and Cho as well as elevated *myo*-Ins.

with respect to corresponding control values. A reduced concentration of NAA (4.2 mM, −25%) was also found in gray matter. The observations are consistent with a generalized neurodegenerative process in L20Hglu aciduria but also suggest a defect in inositolphospholipid metabolism of glial cells (Hanefeld *et al.*, 1994). A follow-up examination of the same patient at the age of 18 years showed a slight progress of cerebral atrophy, an even more dramatic decrease of NAA (−70%), and a further increase of *myo*-Ins, in close correlation to a further clinical deterioration.

4.2. Succinate Dehydrogenase Deficiency

Figure 13 depicts metabolic alterations in a patient with succinate dehydrogenase (SDH) deficiency as detected by ^1H MRS of gray and white matter. The child presented with severe progressive spasticity at the end of the first year of life. MRI revealed marked periventricular white-matter abnormalities that suggested a leukodystrophy. However, all known peroxisomal and lysosomal disorders as well as amino and organic acidopathias and congenital infections could be excluded.

Diagnosis of the biochemical defect was made at the age of 17 months by MRS. While the spectrum of gray matter yielded normal metabolite concentrations except for a comparatively high level of Tau (4.7 mM), white matter was characterized by an extremely high concentration (8.7 mM) of an unknown compound whose MR signal was subsequently identified as originating from the four protons of the two equivalent methylene groups of succinate (Suc) resonating at 2.40 ppm. In addition, white-matter alterations included marked reductions of NAA (2.2 mM), Cr (2.2 mM), Glu, and Gln as well as strongly elevated Lac (7.6 mM). Since *myo*-Ins and Cho levels were within normal ranges, the Suc and Lac findings are consistent with a specific neuroaxonal degeneration, most likely caused by mitochondrial enzyme deficiencies.

The assumption that Suc accumulation is caused by a deficiency of SDH was confirmed biochemically. Muscle tissue showed a partial deficiency of SDH as well as a deficiency of complex II of the respiratory chain. While Suc was found to be 10-fold increased in CSF, the discrepancy between gray and white matter remains unresolved. The child died at the age of 20 months. Neuropathological observations are consistent with the diagnosis of a Leigh syndrome, suggesting a classification as a mitochondrial disease. In fact, similar findings were reported for two sisters with Leigh syndrome that presented as a leukodystrophy (Bourgeois *et al.*, 1992).

4.3. Multiple Sclerosis

The characteristics of multiple sclerosis (MS) in childhood have recently been elaborated as a result of a prospective study in Göttingen (Hanefeld *et al.*,

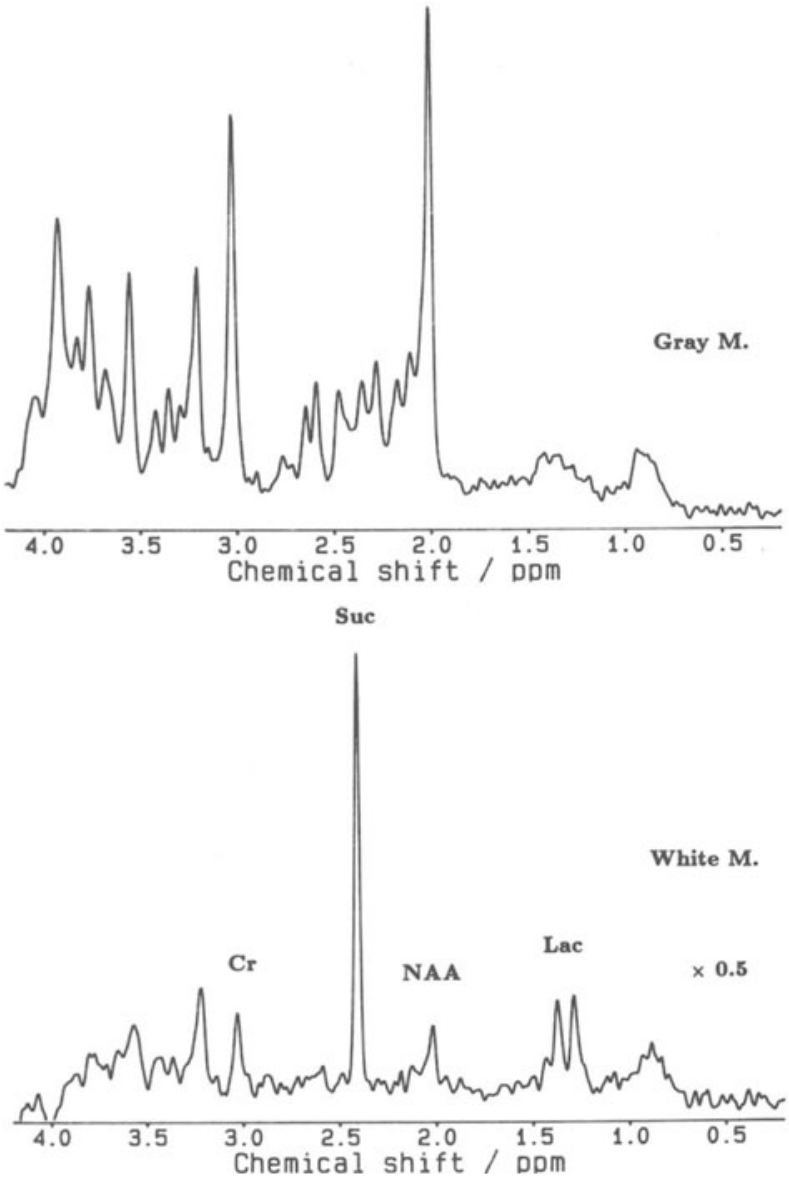

FIGURE 13. Metabolic alterations in a 17-month-old patient with succinate dehydrogenase deficiency as detected by ^{1}H MRS (STEAM, TR/TE/TM = 6000/20/30 msec, 64 accumulations) of gray (18 ml) and white matter (4.1 ml). Note the difference in scale due to the high concentration of succinate (Suc) in white matter.

1991, 1995). Early symptoms include optic neuritis, cranial nerve palsy, bulbar symptoms, ataxia, and seizures in some cases. MRI shows widespread periventricular, cerebellar, and brain stem lesions.

An example of the type of metabolic alterations found in nonenhancing (contrast agent) chronic lesions is shown in Fig. 14. In agreement with a previous report of moderate to severe decreases of NAA and Cr as well as increases of Cho in childhood MS (Bruhn *et al.,* 1992b), the spectrum (TR = 3000 msec) yields reduced NAA (4.7 mM, −30%) and elevated Cho (1.7 mM, +45%).

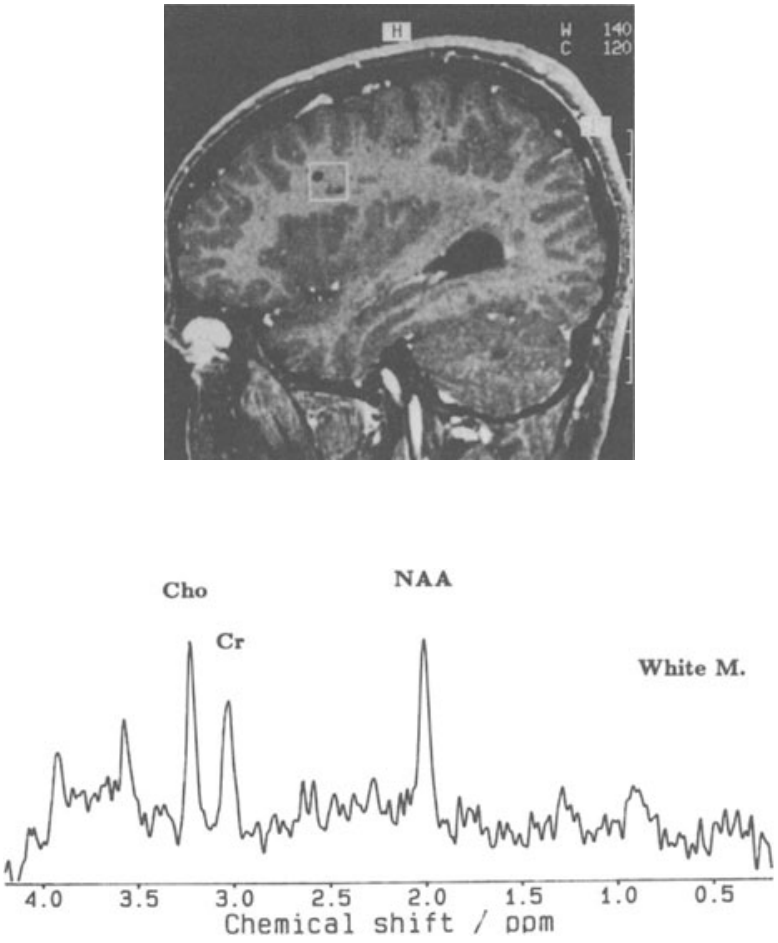

FIGURE 14. Morphological and metabolic alterations in a 13-year-old patient with multiple sclerosis as detected by T_1-weighted MRI (RF spoiled 3-D FLASH, TR/TE = 15/6 msec, 20° flip angle, 1-mm partitions, post Gd-DTPA) and ^1H MRS (STEAM, TR/TE/TM = 3000/20/30 msec, 128 accumulations) of a plaque in white matter (4.1 ml). The nonenhancing chronic lesion shows reduced NAA and elevated Cho.

Increases of *myo*-Ins were less pronounced than in MLD or GLD. No elevations of Lac, lipid, or protein resonances were observed in the children investigated. An interesting observation was a notable reduction of NAA in cortical gray matter receiving projections from neighboring MS lesions.

These findings reflect neuroaxonal degeneration and tissue replacement by glial cells with altered phospholipid composition. Probably, elevated Cho is due to enhanced concentrations of GPC as a myelin and/or membrane breakdown product. This interpretation is supported by a reduction of the broad phospholipid component in ^{31}P MRS of both lesions and normal-appearing white matter in MS subjects (Husted *et al.*, 1994). Focal demyelination may further be associated with secondary neuronal shrinkage or loss, perhaps extending into functionally related cortical gray matter.

5. GRAY-MATTER DISEASES

The term "gray matter disease" mainly applies to a group of storage disorders that affect the nervous system. The storage material—in most cases gangliosides or ceroid lipofuscin—accumulates in neurons, which ultimately cease to function and die. The vague and inaccurate expressions "amaurotic familial idiocy" and "cerebromacular degeneration" were used to designate these disorders before biochemical classification became possible. The typical clinical symptomatology of gray-matter disorders results from disturbed neuronal function: seizures, dementia, blindness, and ataxia. Ocular symptoms are the cherry-red spot of the macula, retinitis pigmentosa, and optic atrophy. Storage may also occur in other organs and in neurons of the autonomous nervous system, e.g., Auerbach's plexus. These phenomena can be detected in a rectal biopsy or as vacuoles in peripheral lymphocytes. Both tests are used for diagnosis of ceroid lipofuscinosis. Different clinical forms have been identified according to age of onset or specific enzyme deficiencies in sphingolipid degradation and resulting storage material, e.g., gangliosidoses G_{M1} and G_{M2}. An overview has been given by Herschkowitz and Schulte (1984).

5.1. Gangliosidoses

The fact that storage of gangliosides in neurons leads to cell death has been known for almost a century. Deficiency of hexosaminidase A (α–β) and B (β–β) are the biochemical characteristics of a variant described by Sandhoff *et al.* (1989). The region for the α unit has been mapped on chromosome 15 and for the β unit on chromosome 5. As typical signs of a gray-matter disorder, children with Sandhoff's disease develop seizures early in life as well as blindness and severe mental defects. Fundoscopy reveals a characteristic cherry-red spot and later optic atrophy.

MRI of a 13-month-old patient (Fig. 15) showed marked disturbances that are characterized by almost identical signal intensities from gray and white matter, cortical atrophy, and enlargement of ventricular spaces (Uyama *et al.*, 1992). ^{1}H MRS not only demonstrated a reduction of NAA in gray matter (4.1 mM), white matter (5.0 mM), and basal ganglia (6.3 mM) but also revealed the generalized occurrence of an additional *N*-acetyl compound (NA) at 2.04 ppm (left shoulder of NAA at 2.01 ppm). Although the resonance of NAAG has been found in the spectrum of normal adult white matter at this position, the presence of other *N*-acetylated compounds is much more likely in this disorder. In fact, deficiency of β-hexosaminidase A blocks the degradation of sphingolipids at a stage that results in the accumulation of gangliosides comprising *N*-acetylgalactosamine (NAcgal) and *N*-acetylneuraminic acid (NANA). The *N*-acetyl groups of both compounds yield proton spectra with a strong singlet resonance at 2.04

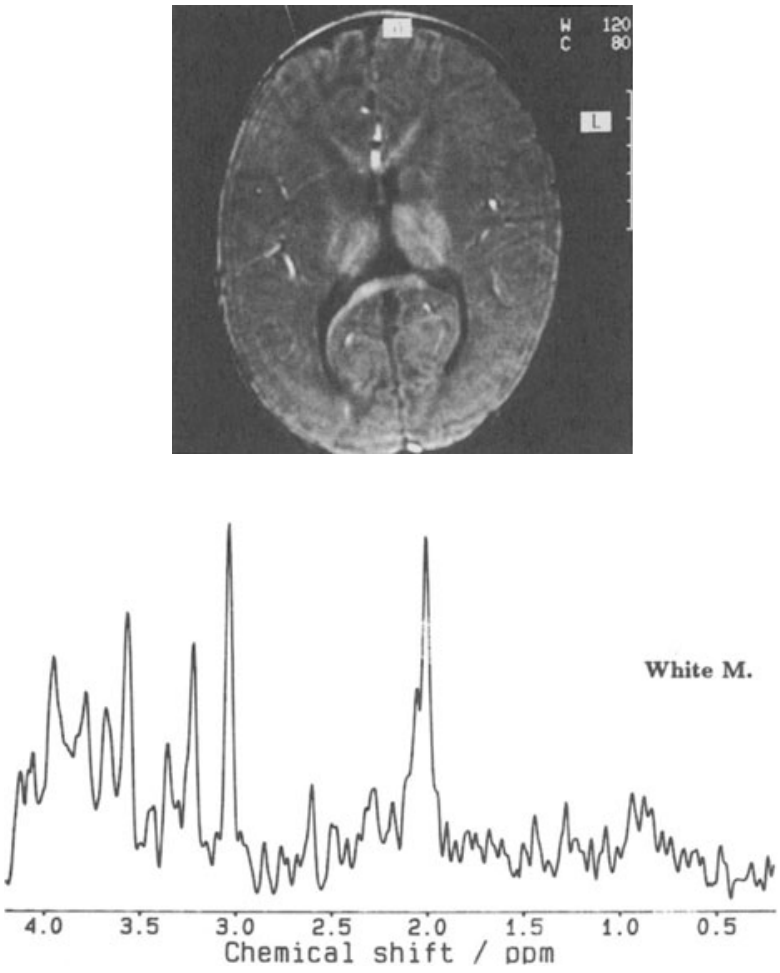

FIGURE 15. Morphological and metabolic alterations in a 13-month-old patient with Sandhoff's disease as detected by T_1-weighted MRI (RF spoiled 3-D FLASH, TR/TE = 15/6 msec, 20° flip angle, 4-mm partitions) and ^{1}H MRS (STEAM, TR/TE/TM = 6000/20/30 msec, 64 accumulations) of white matter (4.1 ml), gray matter (12 ml), and basal ganglia (4.1 ml). Most prominent findings are a generalized decrease of NAA and elevation of *myo*-Ins, *scyllo*-Ins, Cr, and *N*-acetyl compounds (NA) at 2.04 ppm, most likely *N*-acetylgalactosamine (NAcgal) and *N*-acetylneuraminic acid (NANA).

ppm (T. Michaelis, unpublished results). Here, the concentrations derived from this resonance were 1.7 mM in gray matter, 2.5 mM in white matter, and 2.0 mM in basal ganglia. Since no related *N*-acetyl disturbances have been seen with any other brain disorder investigated so far, the observation seems to be specific for Sandhoff's disease. Pertinent brain levels may be expected to directly reflect the amount of *N*-acetylated gangliosides stored in this G_{M2} disorder.

The observed regional uniformity of neuroaxonal changes also holds true for glial compartments. Prominent metabolic alterations common to gray and white matter and basal ganglia were increases of *myo*- and *scyllo*-Ins, Cho, and Cr. For example, gray-matter levels were 7.2 mM (+85%) for *myo*-Ins, 1.7 mM (+70%) for Cho, and 7.9 mM (+36%) for Cr. These abnormalities resemble

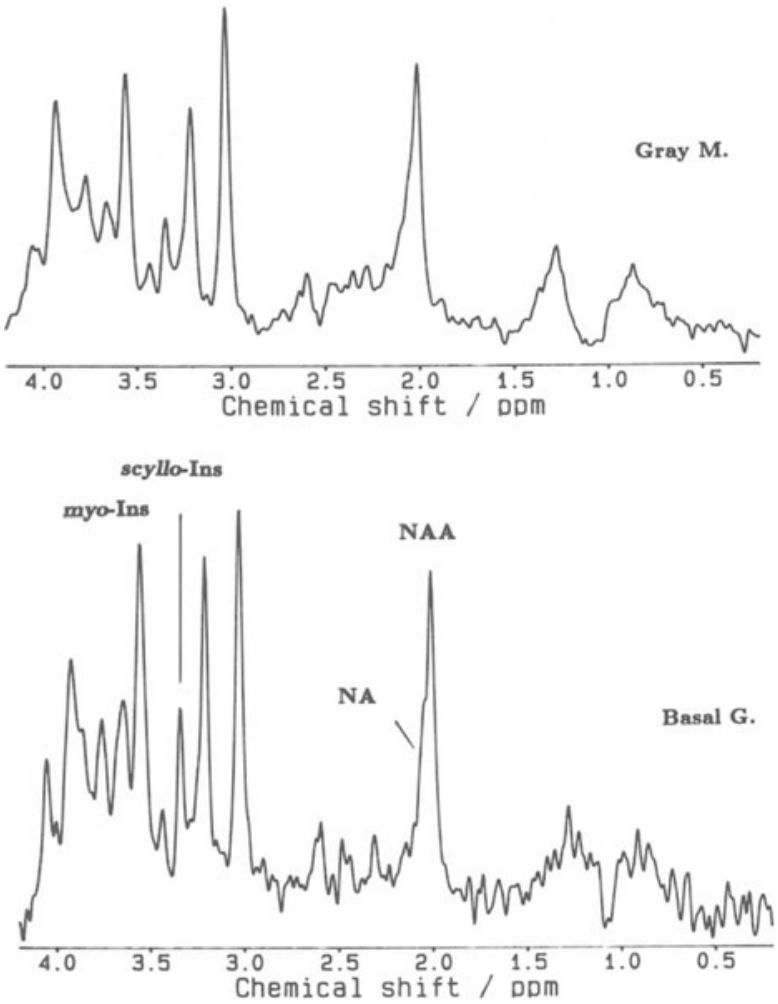

FIGURE 15. Continued

neurochemical disturbances in glial membrane metabolism usually seen in affected white matter in MLD and GLD. The results suggest a severe and generalized alteration of glial membrane composition in the brain of patients with Sandhoff's disease and, more generally, shed new light on the pathogenesis of symptoms and course of the gangliosidoses.

5.2. Neuronal Ceroid Lipofuscinosis

Neuronal ceroid lipofuscinosis (NCL) is the most frequently occurring inherited disorder affecting neurons in childhood (Claussen *et al.,* 1992). Early and late infantile, juvenile, and adult types have been identified. NCL is characterized by massive intralysosomal accumulation of storage materials due to abnormal protein processing, disturbances in protein and glycoconjugate metabolism, and impaired lysosomal function (Santavuori *et al.,* 1991; Autti *et al.,* 1992). Al-

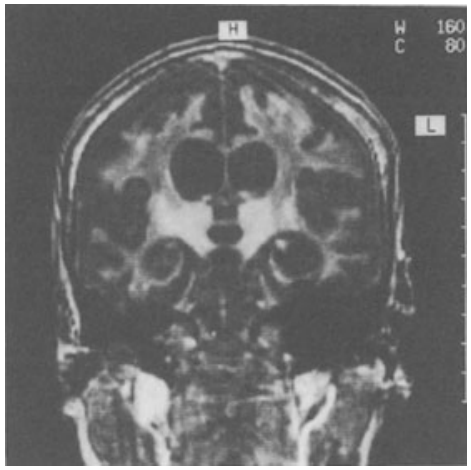

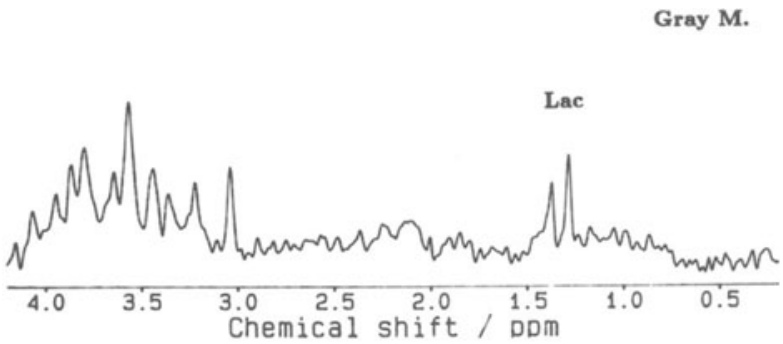

FIGURE 16. Morphological and metabolic alterations in two patients with neuronal ceroid lipofuscinosis (NCL) as detected by T_1-weighted MRI (RF spoiled 3-D FLASH, TR/TE = 15/6 msec, 20° flip angle, 4-mm partitions) and ^{1}H MRS (STEAM, TR/TE/TM = 3000/20/30 msec, 128 accumulations) of gray matter. *First part:* 5-year-old patient with infantile NCL, showing depleted NAA, Glu, Gln, marked reduction of Cr and Cho, and elevated Lac and Glc (8 ml). *Second part:* Disease progression in a patient with juvenile NCL from the age of 9 to 13 years as indicated by a reduction of NAA, Cr, and *myo*-Ins.

though the basic biochemical defect is still unknown, the gene for the early infantile type (Haltia–Santavuori) has been mapped on chromosome 1, and that for the juvenile type (Spielmeyer–Vogt) on chromosome 16 (Järvelä *et al.*, 1992). Myoclonic epilepsy, amaurosis due to retinitis pigmentosa, and progressive mental deterioration are leading symptoms. Neuropathology reveals varying degrees of cerebral and cerebellar atrophy. Neurons are distended by the storage of ceroid lipofuscin and are reduced in number. Cerebellar atrophy is most pronounced in the infantile type, combined with an almost isoelectrical electroencephalogram (EEG).

Depending on the stage and type of the disease, MRI shows severe internal and external cerebral and cerebellar atrophy. Corresponding morphological distortions and metabolic abnormalities in gray matter were readily detected in a 5-year-old patient with infantile NCL (Fig. 16, first part). In this case, ^{1}H MRS

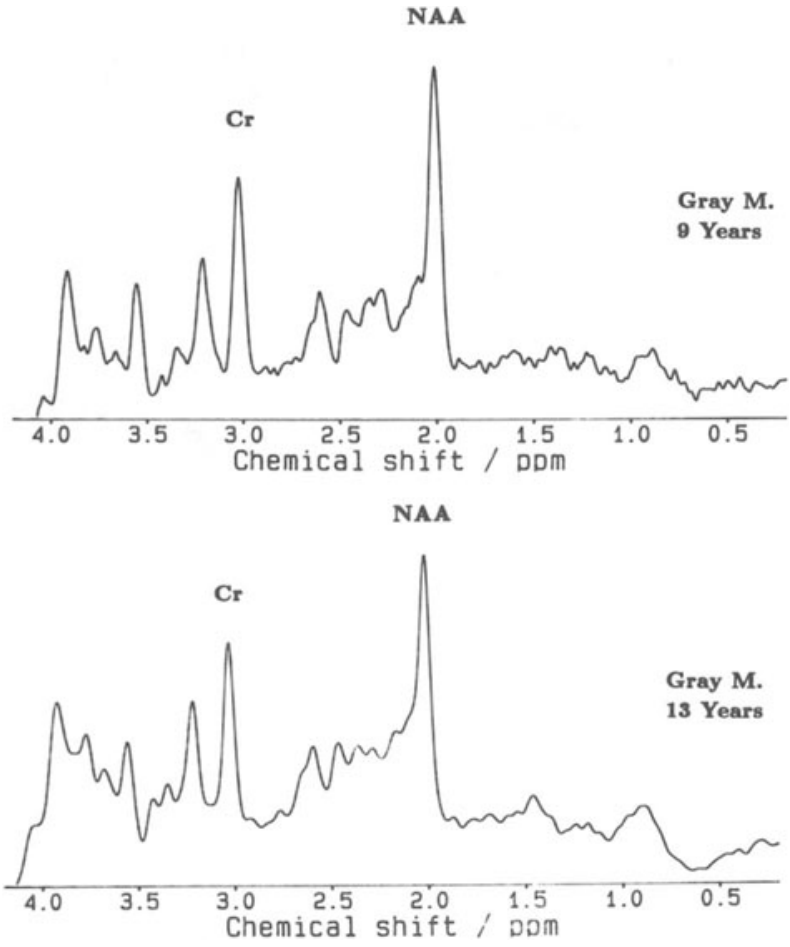

Figure 16 Continued

(TR = 3000 msec) revealed depleted NAA, Glu, and Gln, markedly reduced Cho (0.2 mM, −70%) and Cr (1.0 mM, −80%), and elevated Lac (1.9 mM) and Glc (3.5 mM). An almost identical metabolite pattern was found in white matter (not shown). These results are consistent with complete structural disintegration of gray and white matter, with a loss of viable neuroaxonal tissue being followed by a disruption of glial cells. In comparison to only moderate reductions of NAA in Sandhoff's disease, loss of neurons in infantile NCL turns out to be much more marked than in gangliosidoses. As in other diseases that lead to a loss of brain tissue, MRS findings of elevated Lac may be due to anaerobic metabolism of infiltrating macrophages or may simply reflect CSF contributions rather than indicating a mitochondrial enzyme deficiency. In fact, once cellular disintegration is completed, the resulting Lac and Glc concentrations may entirely originate from CSF in pertinent spaces.

The second part of Fig. 16 indicates disease progression in NCL by comparing follow-up studies of gray matter in a patient at the age of 9 and 13 years. In this juvenile form, the metabolite pattern was normal at the age of 9 years, but a

decrease of NAA (5.7 mM, −25%), Cr (4.2 mM, −15%), and *myo*-Ins (2.5 mM, −30%) was observed at the time of the second examination (TR = 3000 msec), indicating slow progression of neuronal and glial damage. It should be noted that the ^1H MRS results of both patients shown in Fig. 16 are not entirely in agreement with a case report by Confort-Gouny *et al.* (1993) on early infantile NCL. In particular, the reported increase of Ins and Tau may be due to age-related adjustments in early infancy and requires further clarification. In addition, the discussion of a 2.04-ppm resonance from *N*-acetylglucosamine is not substantiated here.

6. MITOCHONDRIAL DISEASES

Mitochondrial disorders comprise a group of diseases with structurally and functionally abnormal mitochondria in muscle tissue and other organs (Sengers *et al.*, 1984; Barkovich *et al.*, 1993; Cassedy and Edwards, 1993). Accordingly, mitochondrial myopathies may occur as separate disorders or as multisystem diseases (mitochondrial cytopathies, encephalomyopathies). A large number of mitochondrial myopathies with or without abnormalities in the mitochondrial DNA have been described that refer to disturbances of oxidative energy metabolism at different stages of the Krebs cycle or respiratory chain. Examples of these disorders are Leigh syndrome and the encephalomyopathies described in the following sections.

6.1. Leigh Syndrome

Leigh (1951) described an autosomal recessive disorder which he called subacute necrotizing encephalomyelopathy. Symptoms usually commence in infancy as hypotonia or acute life-threatening encephalopathy or later in life as intermittent ataxia or dystonia. An increase of Lac in urine, blood, and CSF points toward a disturbed oxidative energy metabolism. The biochemical basis of Leigh syndrome (LS) has been the subject of many studies. Defects associated with this disorder include deficiencies of pyruvate dehydrogenase (PDH) and carboxylase, cytochrome *c* oxidase (complex IV), NADH-coenzyme-Q reductase (complex I), and biotinidase. Recently, a complex II deficiency has also been noted (Bourgeois *et al.*, 1992). Mutation of mitochondrial DNA at the ATPase gene (NARP mutation) was demonstrated in LS.

Brain pathology reveals bilateral symmetrical areas of rarefication and proliferation with relatively good preservation of neurons. The optic nerves, chiasma, and tracts, basal ganglia, brain stem, corpora quadrigemina, tegmentum, and inferior olives are mainly involved, but cerebellar dentate nuclei and cerebral cortex may also be affected. MRI frequently shows abnormalities in these areas,

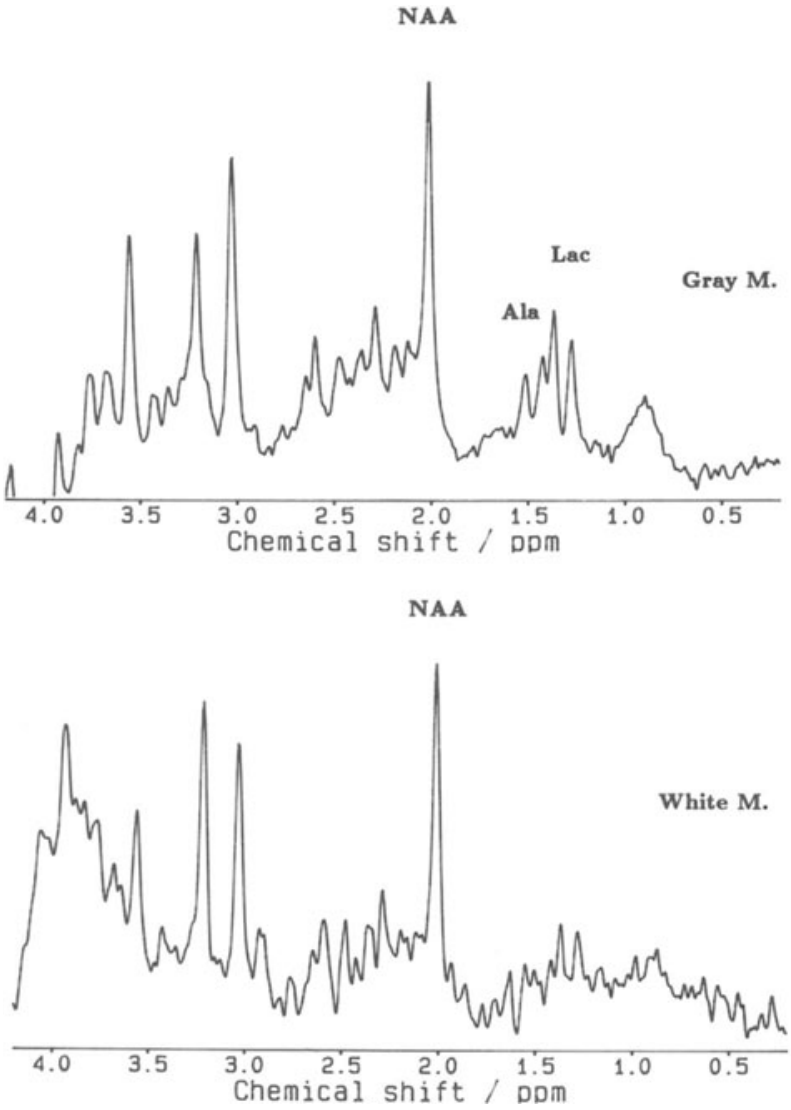

FIGURE 17. Metabolic alterations in three patients with Leigh syndrome as detected by ^{1}H MRS (STEAM, TR/TE/TM = 3000/20/30 msec, 128 accumulations) of gray and white matter. *First part:* Gray- (12 ml) and white-matter (4.1 ml) spectra of a 5-year-old patient with Leigh syndrome and elevated Lac and alanine (Ala) in gray matter. *Second part:* Basal ganglia (4.1 ml) and white-matter (4.1 ml) spectra of a patient with Leigh syndrome at the age of 12 months and 17 months, respectively, showing reduced NAA and elevated *myo*-Ins (white matter) but no elevated Lac. *Third part:* Gray-matter (9.2 ml) spectra of a patient with Leigh syndrome and high levels of Lac at the age of 4 months (*top*) and 18 months (*bottom*) after dichloroacetate therapy.

particularly in basal ganglia and brain stem, although such findings may vary in intensity in the same patient at different times. Rare cases present with a significant demyelination.

The heterogeneity of enzyme deficiencies in LS is also reflected in the variability of cerebral metabolite alterations detected by ^{1}H MRS. An example of diverse observations is shown in Fig. 17, comprising data from three different

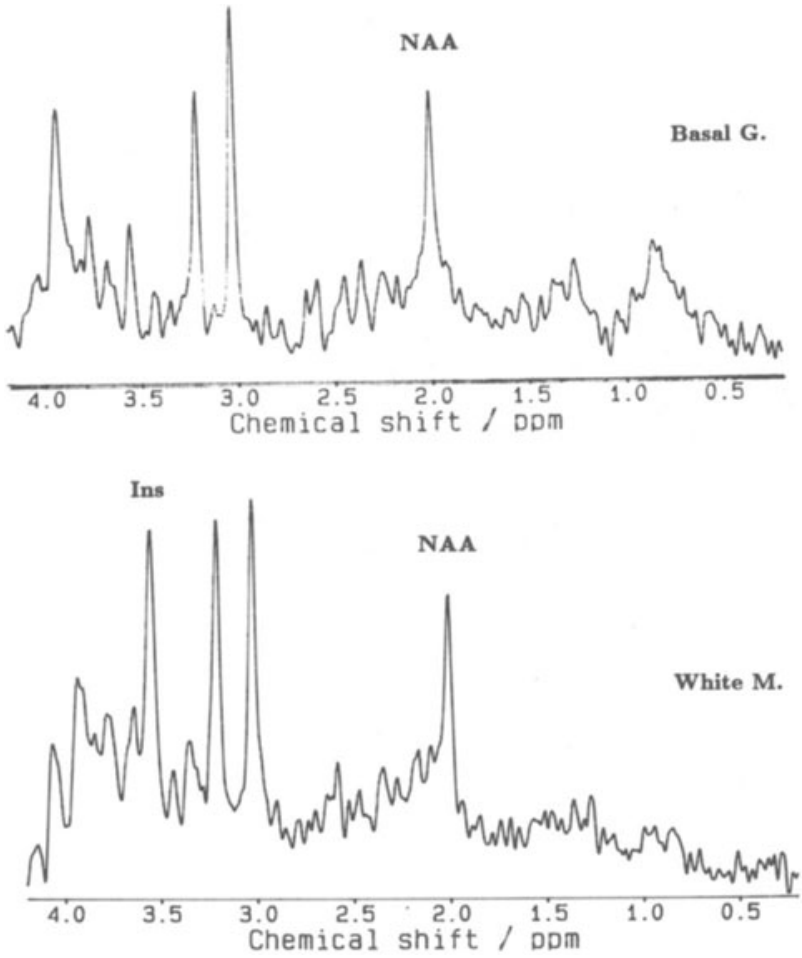

FIGURE 17. Continued

subjects (TR = 3000 msec). The gray- and white-matter spectra from a 5-year-old patient are characterized by elevated concentrations of Lac (3.3 mM) and Ala (1.6 mM) in gray matter. NAA was reduced in both gray (4.2 mM, −25%) and white matter (4.2 mM, −40%), while no glial changes were noted. These findings are consistent with a classical PDH deficiency blocking the pathway from cytosolic pyruvate (produced by glycolysis) to mitochondrial acetyl coenzyme A. It is not surprising that the consequences of a restricted capacity for oxidative metabolism are more pronounced in well-perfused cortical gray matter than in white matter.

The second part of Fig. 17 shows basal ganglia and white-matter spectra of another patient at the age of 12 and 17 months. This case clearly differs from the previous case. While reduced levels of NAA in basal ganglia (3.3 mM) and frontal white matter (3.3 mM, −50%) also suggest neuroaxonal degeneration, a 2.5-fold increase of *myo*-Ins (6.4 mM) in white matter in conjunction with Cho and Cr levels at the upper end of the normal range suggest a disturbance of

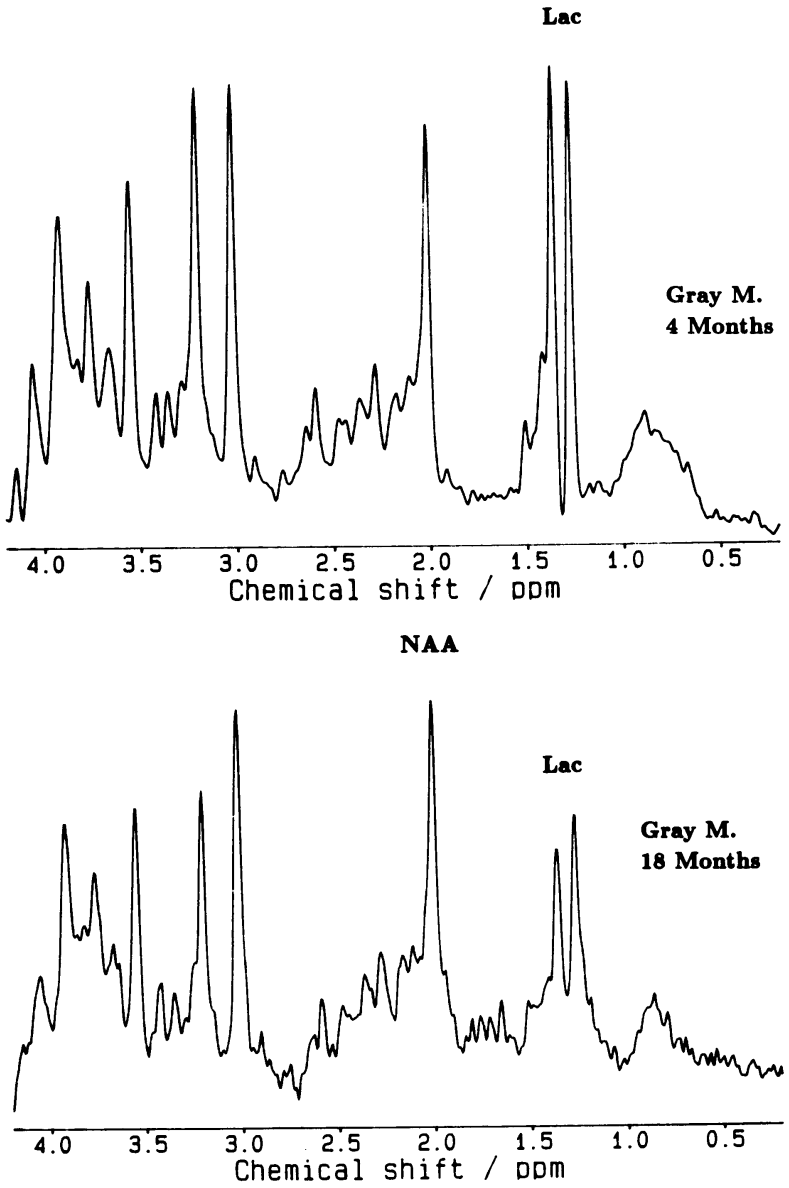

FIGURE 17. Continued

myelination similar to that seen in many leukodystrophies. Most remarkably, however, no elevation of brain Lac was detected despite a Lac concentration of 6.7 mM found in CSF.

The third part of Fig. 17 compares gray-matter spectra of a patient with LS and extremely high levels of Lac at the age of 4 months and during treatment with dichloroacetate at 18 months. Analysis of these data indicated a reduction of Lac from 8.1 to 5.1 mM and of Ala from 1.0 to 0.5 mM. While the concurrent decrease of Cho from 1.2 to 0.9 mM and of Tau from 4.5 to 2.3 mM may be considered as an age-related normalization, the NAA concentration (3.1 mM) remained low during this period instead of exhibiting the expected increase during brain maturation.

Summarizing our experience with a total of 15 patients, the only uniform and consistent finding in patients with LS is a generalized reduction of NAA by about 50%. The concentration of Lac, however, shows marked regional variability (Detre *et al.*, 1991). Moreover, since some patients show normal brain Lac levels even when CSF Lac is elevated (cf. Fig. 17, second part), the utility of brain Lac levels as a diagnostic marker for LS, as hypothesized on the basis of 5 patients with elevated Lac in basal ganglia (Krägeloh-Mann *et al.*, 1993), may be questioned (Kruse *et al.*, 1994b). While ^1H MRS determinations of brain Lac and other cerebral metabolites in the individual patient provide additional diagnostic hints, the possibility of "negative" Lac findings, even when serum and/or CSF levels are high, must be emphasized. In other words, elevated brain Lac is not a necessary finding in LS, while normal brain Lac does not exclude its diagnosis.

6.2. Encephalomyopathies

The encephalomyopathies belong to the continuously increasing number of known mitochondrial diseases. From the original description of progressive external ophthalmoplegia (von Graefe, 1866), the concept of encephalomyopathies has evolved as a representation of multiorgan diseases that are caused by a mutation or deletion of mitochondrial DNA. At least four different disorders can be distinguished according to their clinical characteristics and mitochondrial defect:

- Mitochondrial encephalopathy, lactic acidosis, and stroke-like episodes (MELAS)
- Myoclonic epilepsy with ragged red fibers (MERRF)
- Kearns–Sayre syndrome (KSS)
- Chronic progressive external ophthalmoplegia (CPEO)

These myopathies present with a wide range of additional organ involvement, e.g., of the endocrine and hematopoietic system. Diagnosis is based on clinical, morphological, biochemical, and genetic abnormalities. Muscle biopsy shows ragged red fibers as an accumulation of abnormally structured and malfunctioning mitochondria, which can also be observed by electron microscopy. Deficiencies of respiratory chain complexes are infrequently found in muscle tissue, but biochemical determinations often demonstrate lactic acidosis and increase of Lac in plasma and CSF. Mitochondrial DNA deletions have been reported in KSS and CPEO, and point mutations in MELAS and MERRF.

MRI of mitochondrial disorders frequently shows involvement of basal ganglia as well as white-matter abnormalities. The stroke-like lesions in MELAS (Gropen *et al.*, 1994; Lee *et al.*, 1994) resemble infarcts of the cortex and adjacent white matter (Matthews *et al.*, 1991a), as shown in Fig. 18, but are not restricted to a specific vascular territory. Postmortem investigation of the 18-

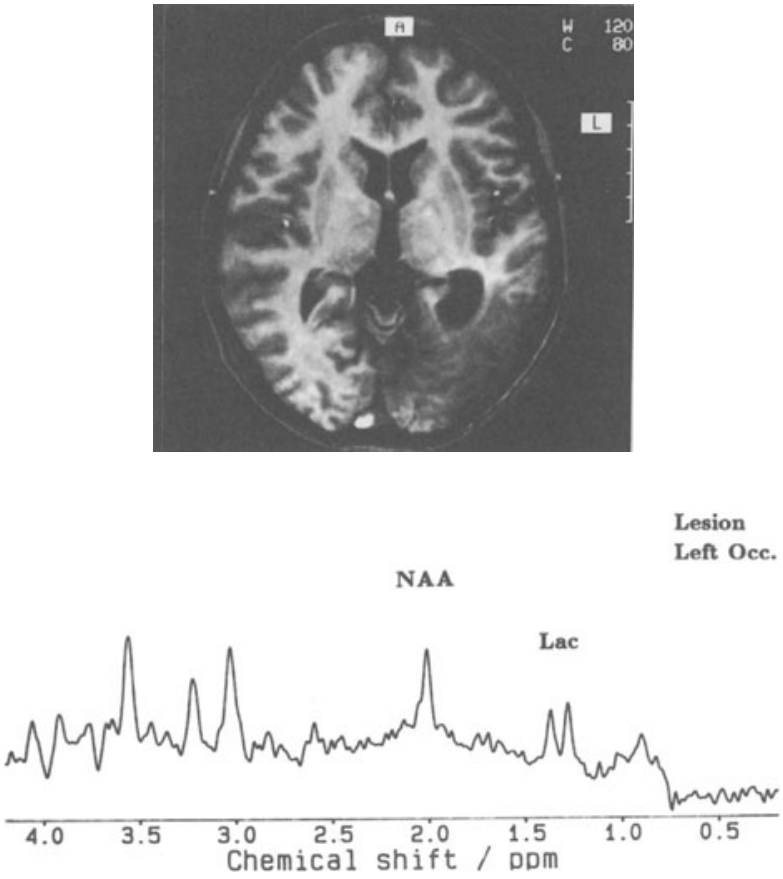

FIGURE 18. Morphological and metabolic alterations in an 18-year-old patient with mitochondrial encephalopathy, lactic acidosis, and stroke-like episodes (MELAS) as detected by T_1-weighted MRI (RF spoiled 3-D FLASH, TR/TE = 15/6 msec, 20° flip angle, 4-mm partitions) and ^{1}H MRS (STEAM, TR/TE/TM = 6000/20/30 msec, 64 accumulations) of a lesion (8 ml) and gray (18 ml) and white matter (6.4 ml). The lesion is characterized by decreased levels of NAA, Cr, and Cho as well as elevated Lac.

year-old subject of this MRI investigation revealed distortions in endothelial and smooth muscle cells of small cerebral arteries. Proton MRS of the left occipital lesion showed reduced NAA, Cr, and Cho but elevated *myo*-Ins (4.9 mM) and Lac (3.5 mM). This pattern of metabolite alterations is consistent with findings in affected brain areas of patients after acute stroke (Bruhn *et al.*, 1989a). While contralateral white matter was normal with regard to morphological and metabolic criteria, neighboring midsagittal parietal gray matter revealed a mild reduction of NAA (6.2 mM) and Cho (0.8 mM) but also high Lac (3.4 mM).

Figure 19 shows metabolic alterations in gray and white matter of a 6-year-old patient with MERRF (TR = 3000 msec). The general pattern is similar to that found for MELAS and consistent with neuroaxonal degeneration, possibly leading to complete cellular disruption. Changes of NAA (3.8 mM, −45%) and Lac 3.7 mM) are observed in white matter but become much more pronounced in gray matter, where function is tightly linked to oxidative energy metabolism (Glc

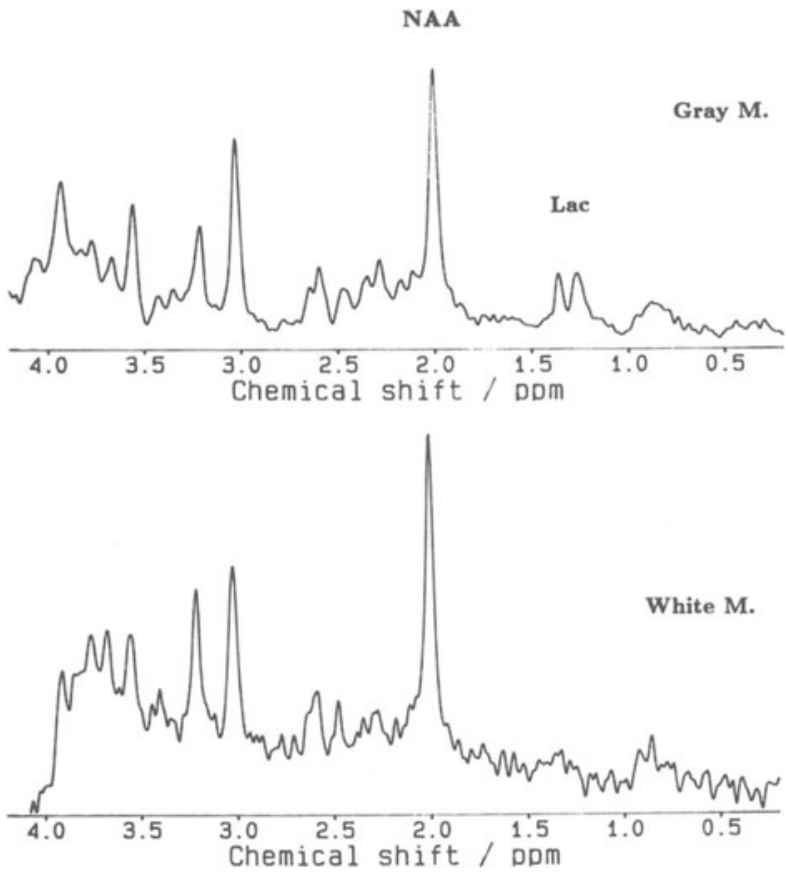

Figure 18. Continued

consumption). Corresponding concentrations of NAA (1.5 mM, −75%), Cr (2.0 mM, −55%), and Cho (0.5 mM, −40%) are markedly reduced, while Lac is considerably enhanced (5.5 mM). A ^{31}P MRS study of 8 patients with MERRF revealed increased intracellular inorganic phosphate (P_i) and decreased PCr/P_i ratios in resting muscle but no alterations of phosphate metabolites and intracellular pH in the brain (Matthews *et al.*, 1991b).

Gray- and white-matter spectra of a 23-year-old patient with KSS are shown in Fig. 20. Partial malfunction of mitochondrial respiration is indicated by a generalized though mild elevation of Lac in gray (2.4 mM) and white matter (2.9 mM). An unexpected finding is a concomitant reduction of *myo*-Ins (2.7 and 2.1 mM, respectively). In addition, gray matter showed reduced NAA (6.5 mM) and Cho (0.7 mM), while Cho (1.6 mM) and Cr (6.5 mM) were elevated in white matter. The significance of these observations is not yet clear.

7. RETT SYNDROME

The syndrome described by Rett (1966) is now defined by criteria for diagnosis first formulated at a conference in 1985 in Vienna (Hagberg, 1993).

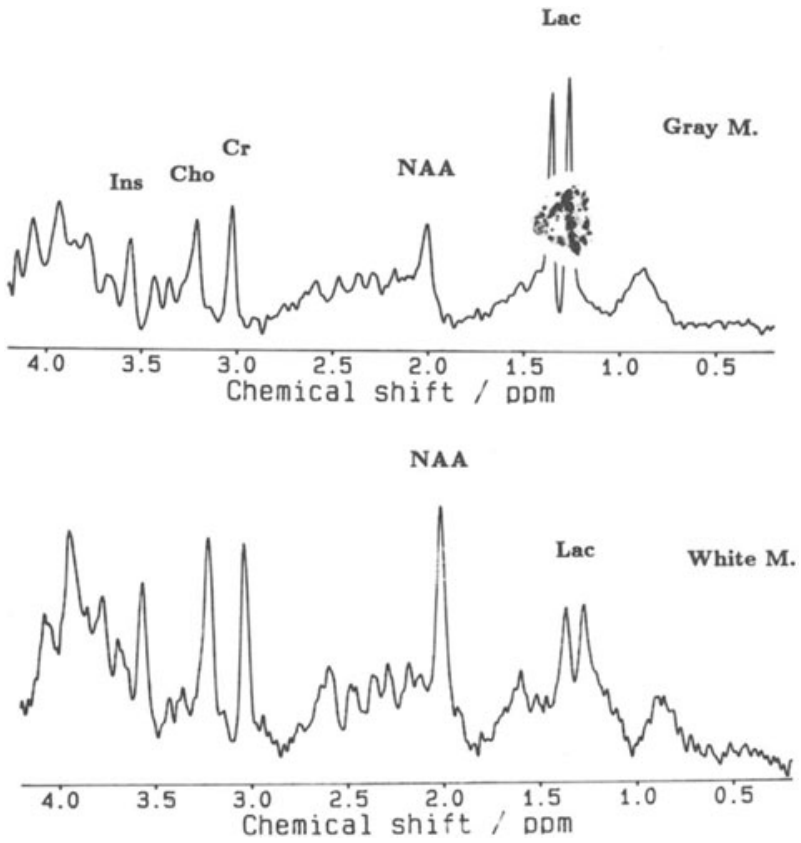

FIGURE 19. Metabolic alterations in a 6-year-old patient with myoclonal epilepsy with ragged red fibers (MERRF) as detected by ^{1}H MRS (STEAM, TR/TE/TM = 3000/20/30 msec, 128 accumulations) of gray (18 ml) and white matter (8 ml). The reduction of NAA and elevation of Lac is most pronounced in gray matter.

Only girls are affected. They are born into normal families after uneventful pregnancy. Usually between 6 and 8 months of age, movement disorders (ataxia, apraxia), behavioral changes (autistic features), and alterations of head growth (deceleration leading to microcephaly) develop as characteristic symptoms. Psychomotor regression is associated with loss of purposeful use of hands, acquired words, and ambulatory capacity in many children. No biochemical, metabolic, neurophysiological, or morphological marker for the disease is known at present. Neuropathology shows small brains packed with small neurons in normal numbers. Dendritic branching has been found to be decreased or deranged in combination with other synaptic abnormalities. The absence of typical degenerative changes, signs of gliosis, or mitochondrial dysfunction (Nielsen *et al.,* 1993) suggests a developmental disorder.

In a preliminary ^{1}H MRS study, we hypothesized that slow disease progression with no or only mild metabolic alterations in early infancy might become more pronounced in older children and young adult patients (Hanefeld *et al.,* 1995a). As demonstrated in Table 3, more recent examinations of two larger

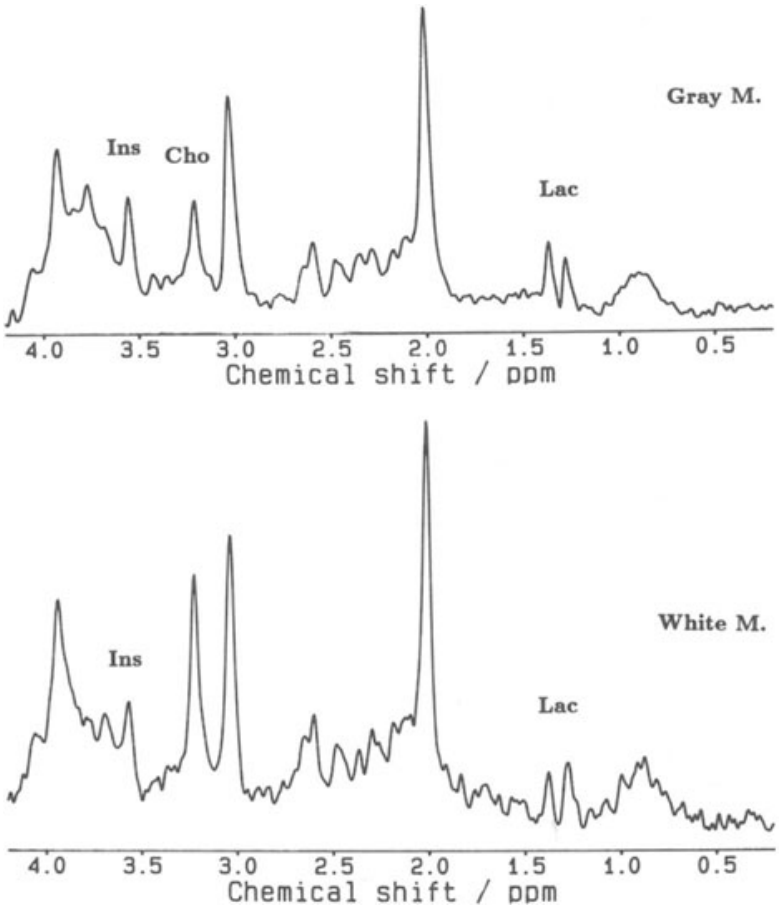

FIGURE 20. Metabolic alterations in a 23-year-old patient with Kearns–Sayre syndrome (KSS) as detected by ^1H MRS (STEAM, TR/TE/TM = 6000/20/30 msec, 64 accumulations) of gray (18 ml) and white matter (8 ml). Generalized findings are a mild increase of Lac and a decrease of *myo*-Ins.

TABLE 3. Absolute Tissue Concentrations (Mean ± SD) of Major Cerebral Metabolites in Parietal Gray and White Matter of Patients with Rett Syndrome below and above 10 Years of Age

	Concentration (mM) in gray matter at age (years):		Concentration (mM) in white matter at age (years):	
Metabolite[a]	4.3 ± 2.0 (n = 9)	18 ± 7 (n = 7)	4.1 ± 1.8 (n = 12)	18 ± 7 (n = 10)
NAA+NAAG	6.8 ± 0.8	6.8 ± 1.0	7.8 ± 0.8	8.1 ± 0.6
PCr+Cr	5.7 ± 0.8	5.7 ± 0.7	5.1 ± 0.3	5.3 ± 0.3
Cholines	1.0 ± 0.2	1.1 ± 0.1	1.5 ± 0.2	1.5 ± 0.2
myo-Inositol	3.9 ± 0.6	3.4 ± 0.4	2.5 ± 0.3	2.5 ± 0.6
Glutamate	7.5 ± 1.1	6.7 ± 1.4	6.3 ± 1.1	6.0 ± 1.4
Glutamine	4.1 ± 0.9	4.4 ± 1.1	2.6 ± 0.9	3.4 ± 2.4

[a]Abbreviations as in Table 2.

patient populations below and above 10 years of age resulted in rather stable values for the mean concentrations of most metabolites. Whether disease progression in individual patients may be monitored, for example, by following decreasing NAA concentrations, remains to be elucidated in a longer follow-up study. A comparison with adult controls yields only mild (10%) reductions of NAA in both groups of patients and a slight trend for the elevation of Gln at the expense of Glu with increasing age. Accordingly, the Glu/Gln ratio decreases from 2.2 (control) to 1.8 (Rett, <10 years) and 1.5 (Rett, >10 years) in gray matter and from 2.9 to 2.4 and 1.8 in white matter, respectively.

8. CREATINE DEFICIENCY

Creatine (α-methylguanidinoacetate) and creatine phosphate play essential roles in the storage and transmission of phosphate-bound energy. In humans, Cr is synthesized in liver and pancreas using Arg, Gly, and *S*-adenosylmethionine as substrates and arginine:glycine amidinotransferase and guanidinoacetate methyltransferase as enzymes. Blood transport ensures delivery to muscle and brain, which contain high activities of creatine kinase. This enzyme catalyzes phosphorylation and dephosphorylation of Cr/PCr and thus provides a high-energy phosphate buffering system during states of ATP synthesis and utilization.

Using combined ^{1}H and ^{31}P MRS, we were able to

- diagnose the first known case of a generalized and selective Cr deficiency in a 22-month-old boy,
- propose adequate treatment and monitor its efficacy over more than two years, and
- identify the biochemical defect of the disease as a lack of guanidinoacetate methyltransferase activity (Stöckler *et al.*, 1994).

The patient with this new treatable inborn error of metabolism first developed abnormalities at the age of 5 months. They consisted of muscular hypotonia and severe extrapyramidal symptoms of a hemiballistic-dystonic type. Owing to uncoordinated swallowing and frequent vomiting, he required nasogastric tube feeding. Particular metabolic findings included hyperammonemia, orotic aciduria, hyperornithinemia, and extremely low concentrations of creatinine in serum and urine. Oral substitution of creatine monohydrate (400 mg kg^{-1} day^{-1}) but not of Arg (300 mg kg^{-1} day^{-1}) improved his clinical state considerably including recovery from his extrapyramidal movement disorder and epileptic seizures. His previously pathological EEG normalized, and bilateral hypointensities in globus pallidus (T_1-weighted MRI) vanished during treatment.

Figure 21 a–c shows ^{1}H MR spectra of gray matter at diagnosis, after 1 month of Arg supplementation, and after 18 months of oral Cr treatment, respectively. During Arg treatment as the initial therapeutic trial, the depletion of Cr in

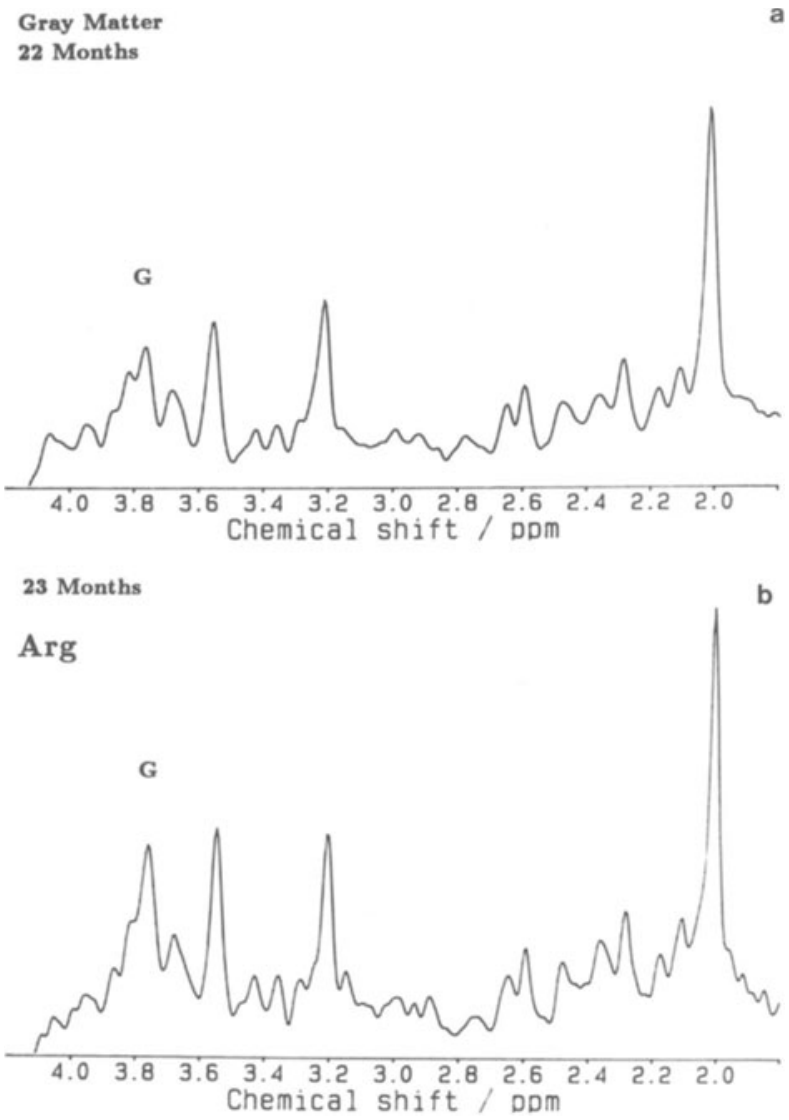

FIGURE 21. Metabolic alterations in a 2-year-old patient with Cr deficiency as detected by ^{1}H and ^{31}P MRS. (a)–(c) Localized proton MRS (STEAM, TR/TE/TM = 6000/20/30 msec, 64 accumulations) of gray matter (8 ml) at diagnosis (22 months), during oral Arg substitution (23 months), and after 18 months of oral Cr substitution (41 months) reveals a partial restoration of brain Cr and a reduction of initially elevated guanidinoacetate (G), the immediate precursor of Cr. (d)–(f) Non-localized ^{31}P MRS (FID, TR = 22,000 msec, 16 accumulations) of the head during oral Arg substitution (23 months), after 3 months of Arg and 2 months of Cr substitution (25 months), and after 18 months of oral Cr substitution (41 months) shows an almost complete restoration of brain PCr and normalization of phosphorylated guanidinoacetate (GP). Other ^{31}P resonances are due to adenosine triphosphate (ATP), inorganic orthophosphate (P_i), phosphomonoesters (PME), and phosphodiesters (PDE).

all brain areas investigated was not reversed but was complemented by a substantial increase of guanidinoacetate (resonance G in Fig. 21a,b) as the immediate precursor of Cr. Since this finding indicated that Cr synthesis was blocked at the final step, direct substitution of Cr led to remarkable spectroscopic and clinical improvements. During the course of more than 18 months of Cr treatment, brain

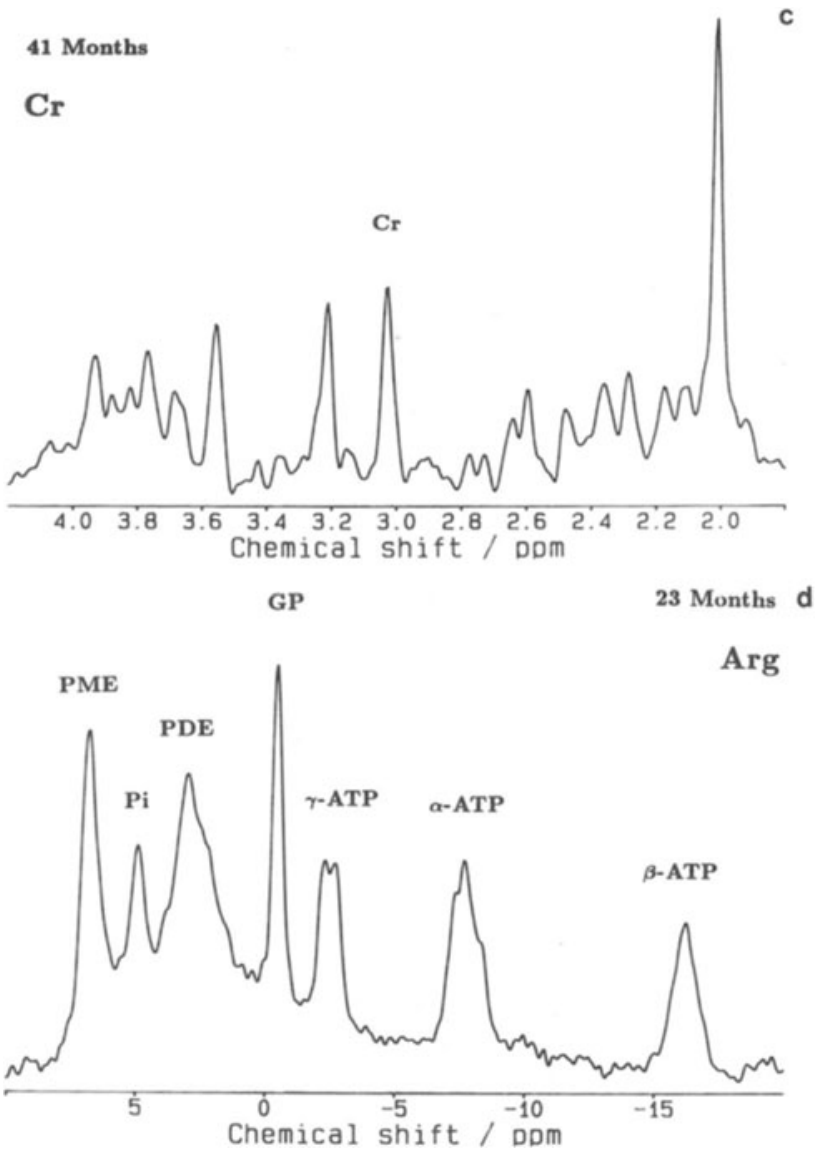

FIGURE 21. Continued

Cr concentrations steadily increased to 65% of adult control levels, while guanidinoacetate levels returned to very low values. Time courses of NAA and Cr concentrations in gray and white matter are summarized in Table 4. The increase of NAA over this period represents normal brain maturation.

The deficiency of guanidinoacetate methyltransferase suggested by ^{1}H MRS was confirmed biochemically by demonstrating lack of pertinent enzyme activity in liver tissue. To evaluate whether the newly formed pool of brain Cr was metabolically active, ^{31}P MRS (homogeneous phosphorus head coil) was performed subsequent to ^{1}H MRS but during the same examination (Requardt, 1995). Figure 21d demonstrates that no PCr was detectable during oral Arg substitution. Instead, ^{31}P MRS revealed a strong resonance that could be assigned to guanidinoacetate phosphate (GP). Its distinction from PCr becomes evident in

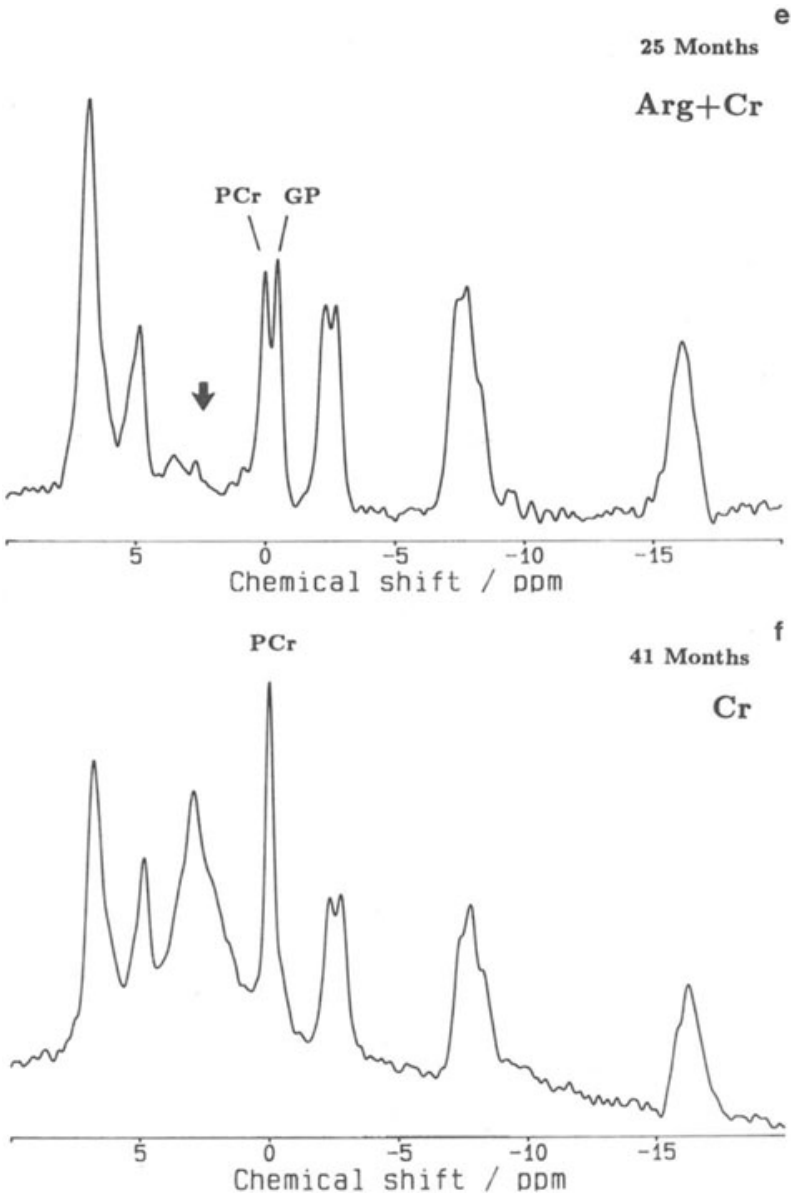

FIGURE 21. Continued

spectra obtained after oral Cr substitution and concomitant PCr increase (Fig. 21e, f). GP nearly vanished over the course of treatment.

Quantitative assessments of high-energy phosphate concentrations were accomplished with use of localized STEAM spectra (TR/TE/TM = 9000/4/5 msec) from a 96-ml VOI ($4 \times 4 \times 6$ cm^3) in parietal cortex (Merboldt *et al.*, 1990; Requardt, 1995). The time course of PCr concentrations in Table 4 demonstrates a proportional increase to total Cr during therapy. In all stages, PCr was about 50% of the mean ^{1}H-MRS-detected concentration of total Cr in gray and white matter. These findings indicate normal Cr phosphorylation, i.e., creatine kinase activity, which is further supported by the fact that control measurements in young adults ($n = 21$) resulted in a PCr level of 2.5 ± 0.4 mM, or about 50%

TABLE 4. Absolute Tissue Concentrations (Mean ± SD) of Major Cerebral Metabolites in Parietal Gray and White Matter of a Patient with Creatine Deficiency as Detected by ^{1}H and ^{31}P MRS at Diagnosis and during Treatment[a]

	Concentration (mM)					
	Gray matter		White matter			
Age (months)	NAA	Cr	NAA	Cr	Whole brain PCr	Therapy
22	5.7	0.0	6.1	0.1	—	—
23	6.0	0.0	6.3	0.0	0.0	Arg
25	6.2	2.0	6.9	1.2	0.7	Arg + Cr
26	5.8	2.5	6.9	1.8	—	Cr
33	7.3	3.0	8.1	2.6	1.5	Cr
38	8.1	4.1	7.9	3.1	2.1	Cr
41	7.4	3.8	8.7	3.7	2.0	Cr

[a]Abbreviations: NAA, *N*-acetylaspartate; Cr, creatine; PCr, phosphocreatine; Arg, arginine.

of total Cr (Requardt, 1995). In addition, direct measurements of the kinetics of phosphate exchange between PCr and ATP using a pulsed saturation transfer technique failed to demonstrate any transfer from γ-ATP to the metabolically inactive GP. On the other hand, Cr substitution led to a significant phosphate transfer from γ-ATP to the newly formed PCr at a rate similar to that found in controls.

Thus, dynamic MRS studies in this patient not only demonstrated the cerebral uptake of oral Cr by ^{1}H MRS but further proved its phosphorylation and normal metabolic function, i.e., phosphate exchange with ATP on the proper time scale, by ^{31}P MRS. In addition to providing information for the clinical management of the patient, these results may further help to elucidate the questions of Cr "visibility," its compartmentalization into different (neuronal and glial) pools, and the phosphorylation of the respective concentrations. Whether a full restoration of brain Cr (and PCr) levels will be possible still remains to be seen, as time constants of cerebral uptake are surprisingly small. Correspondingly, the delayed onset of clinical symptoms several months after birth may also have been due to a slow depletion of a normal Cr pool supplied by maternal Cr during pregnancy and/or postnatal feeding.

9. MISCELLANEOUS DISORDERS

9.1. Carbohydrate-Deficient Glycoprotein Syndrome

The carbohydrate-deficient glycoprotein (CDG) syndromes are genetic multisystemic disorders characterized by glycosylation defects in certain glycopro-

teins, most likely at the level of protein synthesis and processing in endoplasmatic reticulum (Jaeken *et al.*, 1991). The gene for type I has recently been mapped on chromosome 16 (Martinsson *et al.*, 1994). The demonstration of abnormal transferrins is used for diagnosis. Multiorgan involvement includes cerebral and peripheral nervous system, subcutaneous fat, eyes, liver function, coagulation, and the endocrine system depending on the stage of the disease.

Three types of CDG syndrome have been described by Hagberg *et al.* (1993), Ramaeckers *et al.* (1991), and Stibler *et al.* (1993), respectively. Type I represents the most frequent form and typically leads to severe cerebellar atrophy. Type III shows the most severe clinical course with infantile spasms, cerebral atrophy, and severe mental and motor retardation. The skin of these patients exhibits characteristic areas of depigmentation.

Metabolic alterations detected by ^1H MRS of patients with CDG syndromes reflect the above clinical classification (Holzbach *et al.*, 1995). Figure 22 shows gray- and white-matter changes in two different patients with type I and III CDG syndrome, respectively. In type I CDG syndrome (Fig. 22, first part), gray-matter metabolite concentrations were all within normal ranges, in line with only mild cortical atrophy. White matter showed mild reductions of NAA (6.6 mM), Cr (4.2 mM), and Cho (1.2 mM) but no signs of disturbed myelination. In a 2-year-old girl with type III CDG syndrome (Fig. 22, second part), ^1H MRS revealed more severe metabolic alterations in both gray and white matter. Gray-matter spectra yielded reduced NAA (6.0 mM) as well as elevated *myo*-Ins (5.1 mM), Cho (1.15 mM), and Cr (6.6 mM). Similar though more pronounced alterations were seen in white matter, representing a marked reduction of NAA (4.7 mM) and increases in *myo*-Ins (4.1 mM), Cho (1.8 mM), and Cr (6.2 mM). These findings indicate that neuroaxonal degeneration, as evidenced by a 50% loss of NAA, is accompanied by a demyelinating process similar to that in certain leukodystrophies. Histological observations and ^1H MRS suggest that both peripheral and central axons are affected in CDG syndrome.

9.2. Cerebro-Hepato-Renal Syndrome of Zellweger

The cerebro-hepato-renal syndrome of Zellweger is the prototype of peroxisomal disorders (Barth *et al.*, 1988). It presents in the newborn with typical facial dysmorphism, high forehead, low and broad nasal bridge, epicanthus, and dysplastic external ears. Dominating neurological symptoms are severe hypotonia, nystagmus, and poor sucking and swallowing as well as generalized seizures often starting during the first days of life, retinal degeneration, and optic atrophy. Hepatomegaly, polycystic kidneys, and skeletal deformities are constant findings. MRI shows gyral abnormalities, polymicroglia, and pachygyria. White-matter abnormalities have been described as sudanophilic leukodystrophy. Absence of demonstrable peroxisomes in liver tissue and loss of peroxisomal en-

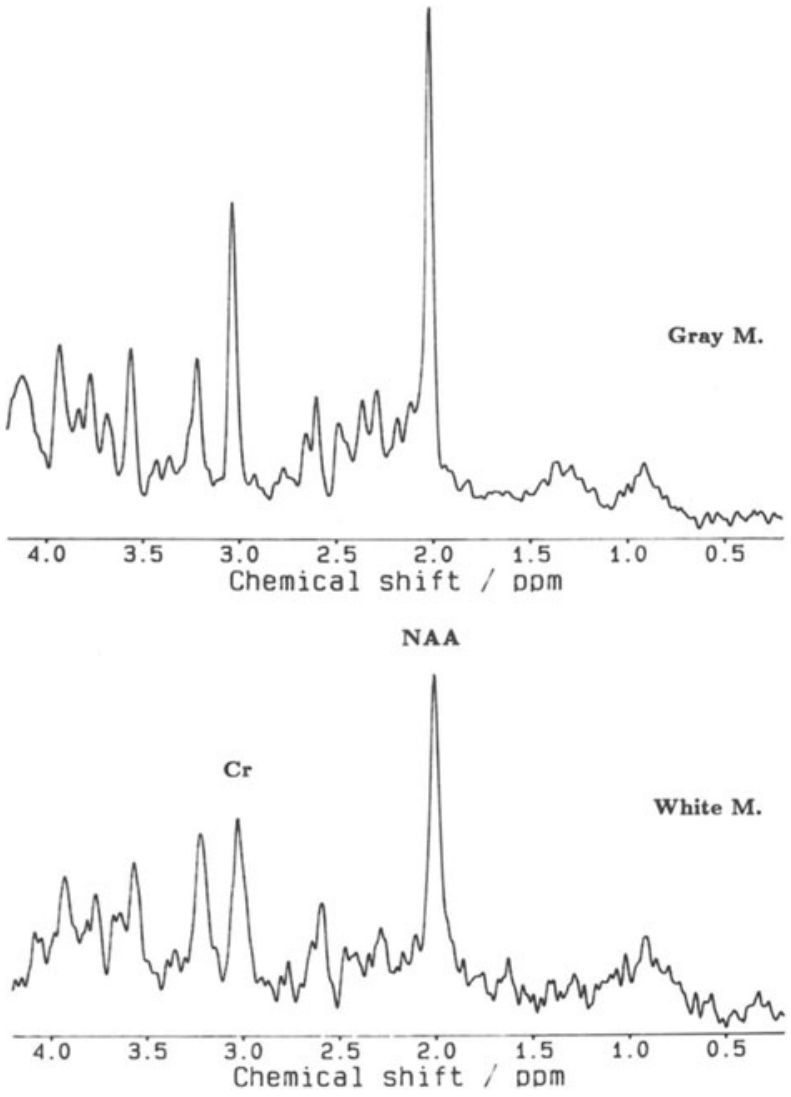

FIGURE 22. Metabolic alterations in two patients with carbohydrate-deficient glycoprotein (CDG) syndrome as detected by ^{1}H MRS (STEAM, TR/TE/TM = 6000/20/30 msec, 64 accumulations) of gray (8–12 ml) and white matter (5.1 ml). *First part:* 8-year-old patient with CDG syndrome type I and mildly decreased NAA and Cr in white matter. *Second part:* 2-year-old patient with CDG syndrome type III, showing elevated *myo*-Ins and Cr in gray matter as well as elevated *myo*-Ins, Cho, and Cr and decreased NAA in white matter.

zyme function lead to an increase of VLCFA and later also of phytanic acid. Most children succumb during the first year of life.

Figure 23 shows ^{1}H MR spectra (TR = 3000 msec) of gray and white matter of two patients with Zellweger syndrome, aged 3 months (first part) and 12 months (second part). In the younger patient, the most characteristic abnormality is a drastic increase of aliphatic hydrocarbon resonances (0.5–1.5 ppm range) from cytosolic proteins, cholesterol, or—less likely—mobile lipids. The effect is most notable in white matter and probably reflects the accumulation of break-

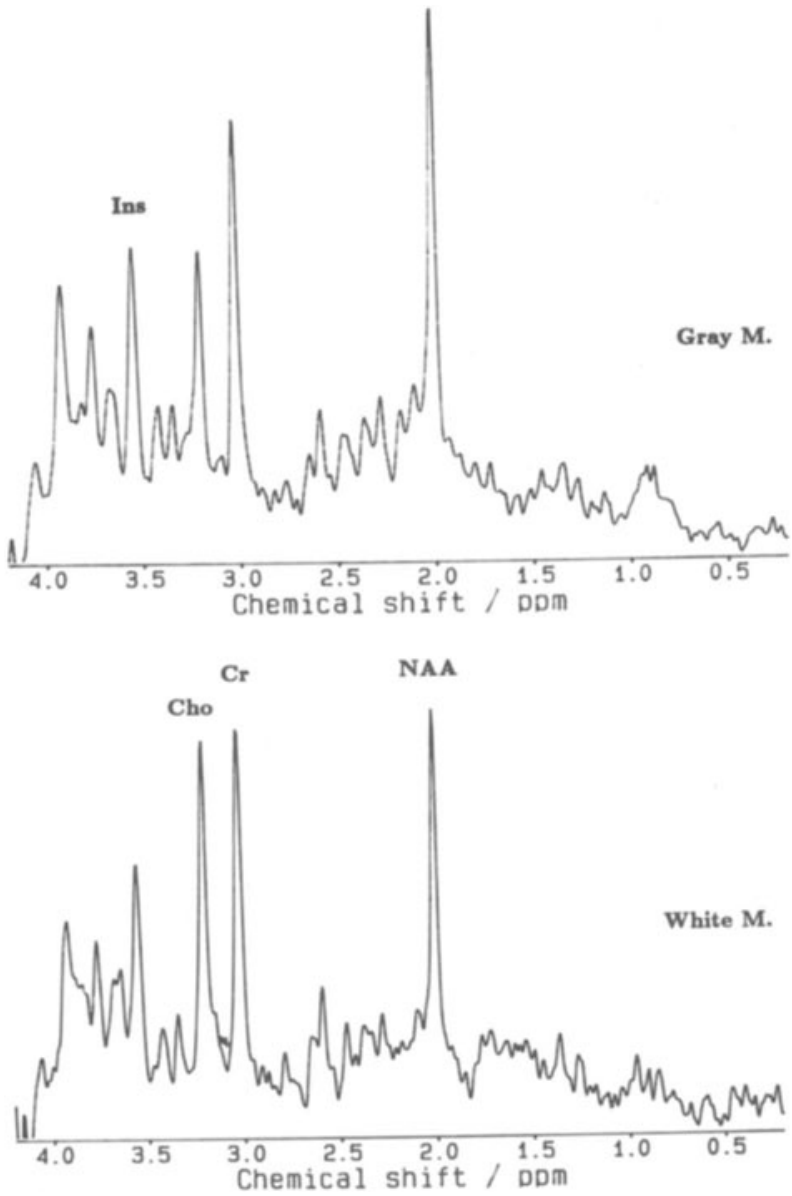

Figure 22 Continued

down products due to disturbed developmental processes such as impaired formation of myelin. A correlation between the extent to which these resonances are increased and the severity of the clinical status has been suggested (Bruhn *et al.*, 1992c). Although the detailed origin of the hydrocarbon resonances has not yet been identified, they may be due to mobile residues from thymosin β4 that have been reported to contribute to ^1H spectra of brain tissue (Kauppinen *et al.*, 1992).

Because only a limited number of controls are yet available at this age, reliable assessments of other disturbances remain difficult. However, apart from rather low NAA levels in gray (2.9 mM) and white matter (2.3 mM), strong elevation of Gln (8.2 and 9.8 mM, respectively) clearly manifests a major abnor-

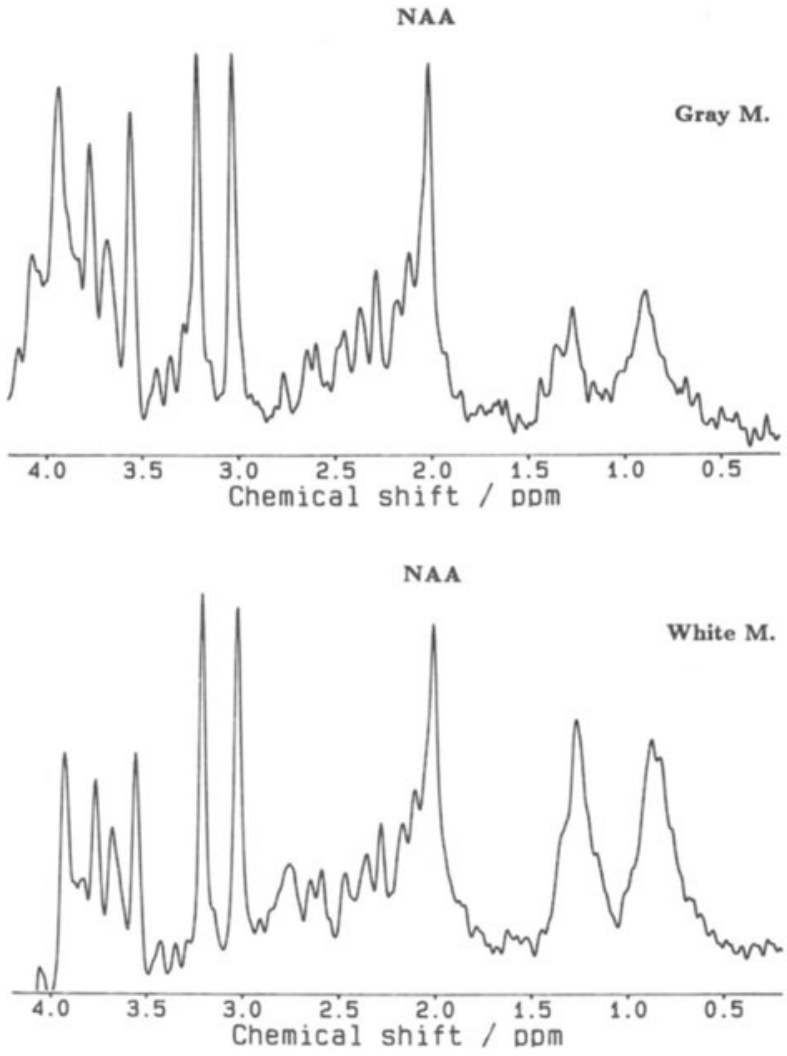

FIGURE 23. Metabolic alterations in two patients with cerebro-hepato-renal syndrome (Zellweger) as detected by ^{1}H MRS (STEAM, TR/TE/TM = 3000/20/30 msec, 128 accumulations) of gray (8 ml) and white matter (8 ml). *First part:* 3-month-old patient showing reduced NAA and elevation of aliphatic hydrocarbon resonances (0.5–1.5 ppm), most likely from mobile residues of cytosolic proteins. *Second part:* 12-month-old patient with strongly elevated Gln in gray matter, indicating impaired liver function.

mality that may be ascribed to impaired liver function as a characteristic feature of this disease with peroxisomal enzyme deficiencies. The resulting cerebral metabolic disturbance is even more pronounced in the 1-year-old patient; Fig. 23 (second part) shows extremely elevated Gln in gray matter (18.1 mM) and high values in white matter (9.1 mM). Enhanced synthesis of brain Gln from Glu and elevated blood ammonia has also been reported in hepatic encephalopathy (Kreis *et al.,* 1990, 1992). It particularly occurs in gray matter as a result of glutamine synthetase activity in astrocytes. The absence of protein resonances may be related to the later age of onset (Bruhn *et al.,* 1992c).

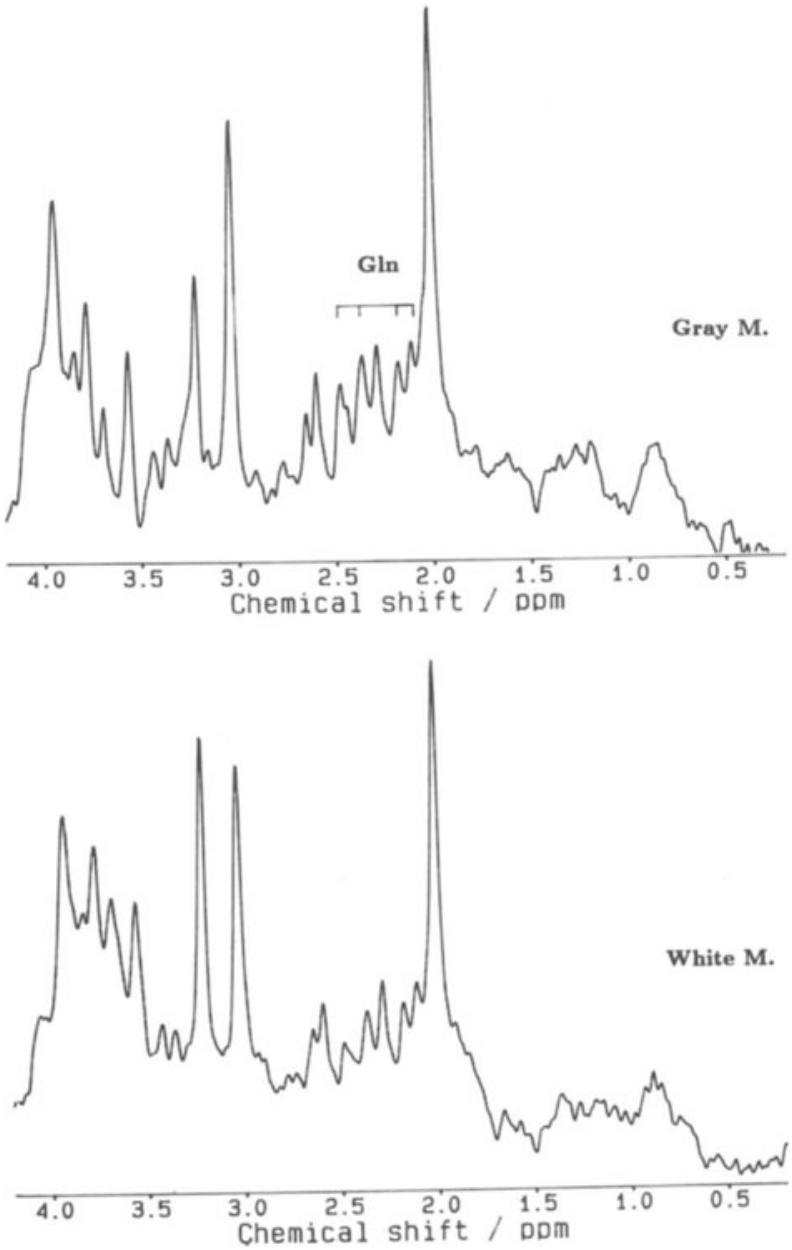

Figure 23. Continued

9.3. Hemimegalencephaly

Hemimegalencephaly (HME) is now frequently diagnosed during life. It may be idiopathic but is more often associated with vascular malformations and neurocutaneous syndromes (Hallervorden, 1923; Barkovich and Chuang, 1990). Clinical symptoms include mental retardation, hemiparesis, and intractable epileptic seizures. The enlarged cerebral hemisphere usually shows additional anatomical anomalies such as pachygyria, polymicrogyria, and gliosis. MRI may demonstrate the thickened pachygyric cortex and white-matter gliosis.

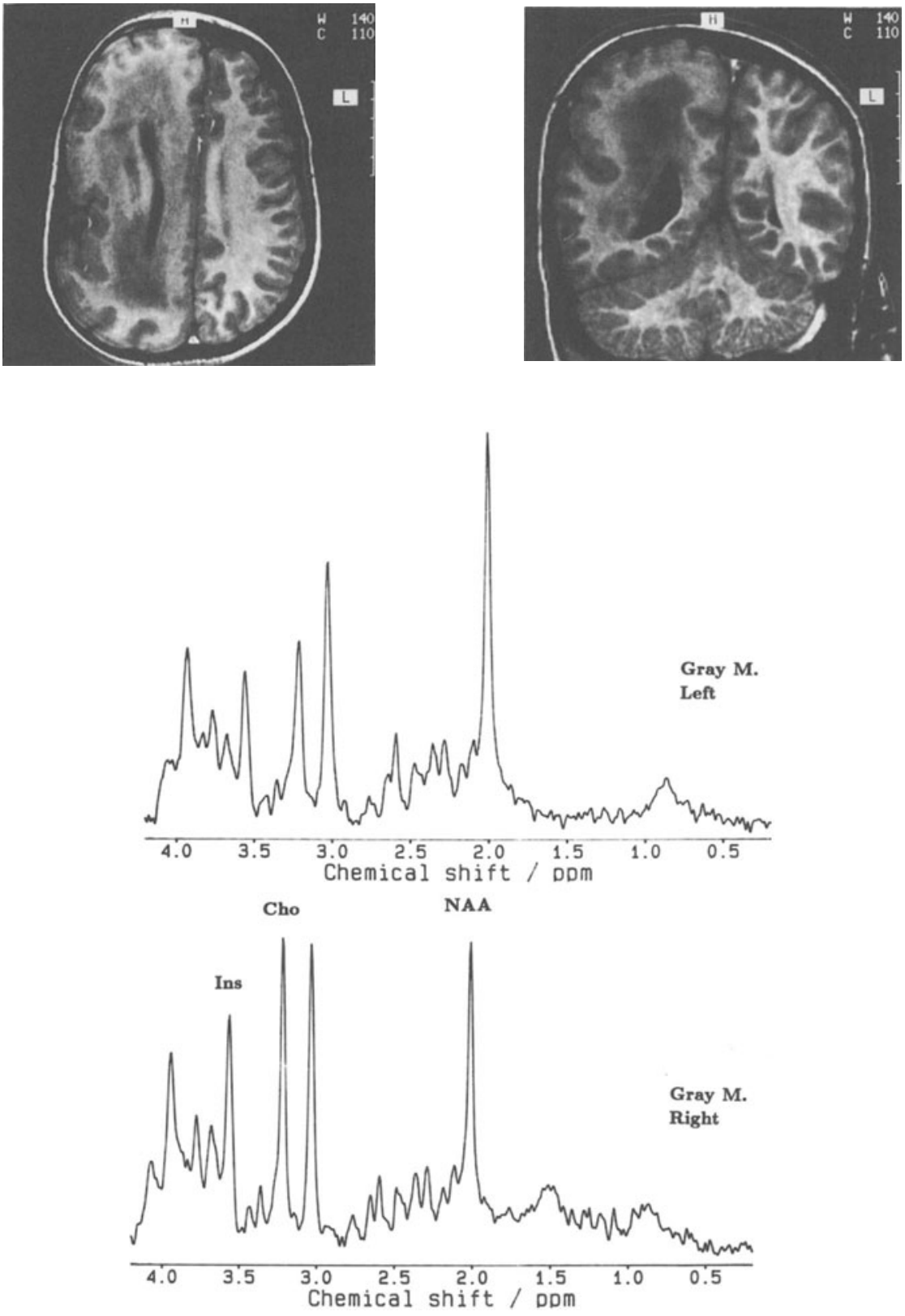

FIGURE 24. Morphological and metabolic alterations in a 13-year-old patient with hemimegalencephaly as detected by T_1-weighted MRI (RF spoiled 3-D FLASH, TR/TE = 15/6 msec, 20° flip angle, 4-mm partitions) and ^{1}H MRS (STEAM, TR/TE/TM = 6000/20/30 msec, 64 accumulations) of gray matter in the insular area (14.4 ml) and parietal white matter (12 ml) in the left and the right hemisphere. The affected hemisphere shows decreased NAA and increased *myo*-Ins and Cho in gray matter as well as markedly reduced NAA, Glu, and Cr and increased *myo*-Ins in white matter.

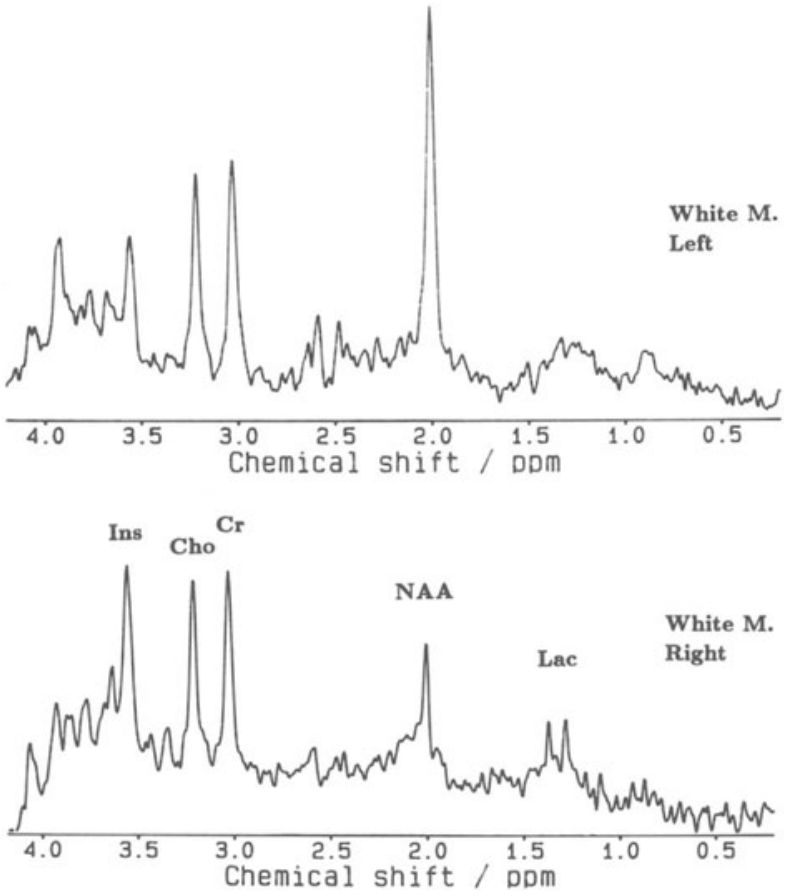

Figure 24. Continued

A ^1H MRS study of HME was undertaken to characterize the abnormal half of the brain and to identify neurochemical abnormalities in the apparently healthy hemisphere. Morphological and metabolic alterations in a 13-year-old patient are shown in Fig. 24 (Hanefeld *et al.*, 1995b). Metabolic disturbances in white matter of the enlarged hemisphere include a marked reduction of NAA (2.1 mM), Glu- (1.5 mM), Cr (3.3 mM), and Cho (1.0 mM) as well as elevation of *myo*-Ins (5.0 mM). Affected gray matter in the right insular area showed reduced NAA (4.9 mM) as well as increased *myo*-Ins (5.9 mM), Cho (1.8 mM), and Cr (6.3 mM). These findings may result from neuroaxonal degeneration and further reflect a pattern of disturbed glial metabolism such as found in leukodystrophies. The reduction of all metabolites in white matter except *myo*-Ins suggests a process that leads to complete cellular disintegration starting with neuroaxonal tissue components.

The normal-appearing hemisphere showed mildly decreased NAA (7.1 mM) in contralateral white matter as well as increased Cho (1.5 mM) and mild elevation of *myo*-Ins (4.4 mM) and Cr (6.8 mM) in gray matter. Cerebral Gln was strongly enhanced in all areas investigated, e.g., in affected (10.8 mM) and normal (12.8 mM) gray matter, indicating impaired liver function. Partial in-

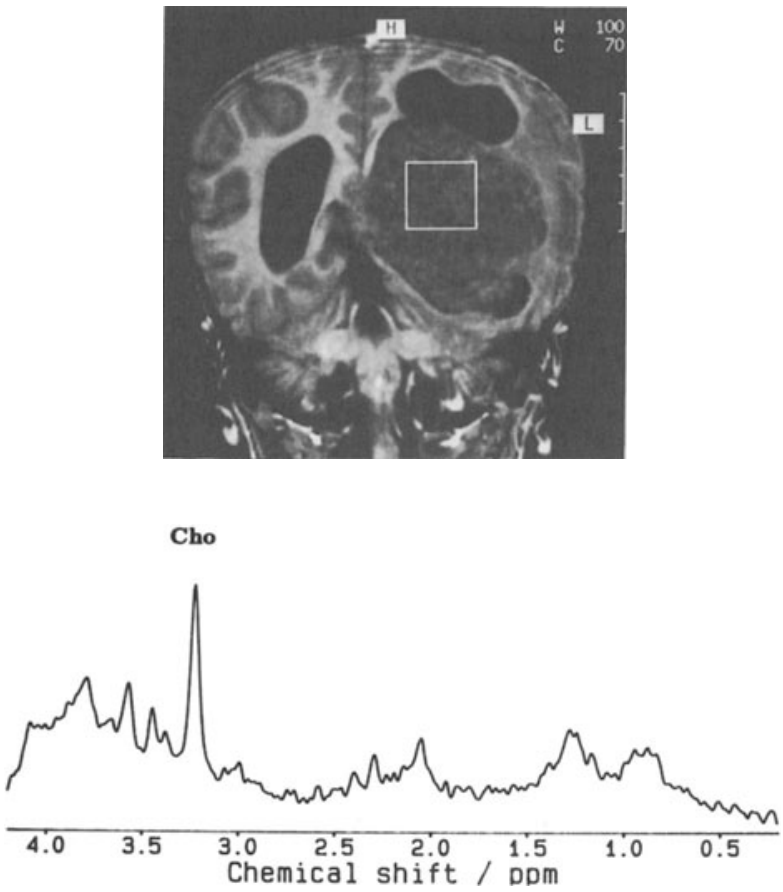

FIGURE 25. Morphological and metabolic alterations in two patients with intracranial tumors as detected by T_1-weighted MRI (RF spoiled 3-D FLASH, TR/TE/ = 15/6 msec, 20° flip angle, 4-mm partitions) and ^{1}H MRS (STEAM, TR/TE/TM = 6000/20/30 msec, 64 accumulations) of the neoplasm. *First part:* 20-month-old patient with a plexus papilloma (15.6 ml), showing strongly reduced metabolite levels except for Cho. *Second part:* 2-year-old patient with a cerebellar astrocytoma (4.1 ml), showing marked increases of *myo*-Ins and Cho as well as decreased NAA.

volvement of the contralateral hemisphere was in line with the presence of additional epileptic activity in this patient. The ability to detect metabolic abnormalities in the normal-appearing hemisphere is expected to significantly improve the diagnostic evaluation of HME patients, in particular when hemispherectomy is considered as a therapeutic option due to intractable seizures.

9.4. Brain Tumors

Brain tumors are the second most frequent malignancy in childhood. Medulloblastomas, ependymomas, and brain stem gliomas dominate, and infratentorial locations occur in more than 50% (Kucharczyk *et al.*, 1985; Cohen and Duffner, 1994). However, despite methodological progress in CT, MRI, and angiography, accurate diagnosis often poses problems. For example, in a child with cerebellar symptoms differential diagnosis between a neoplasm and gliosis

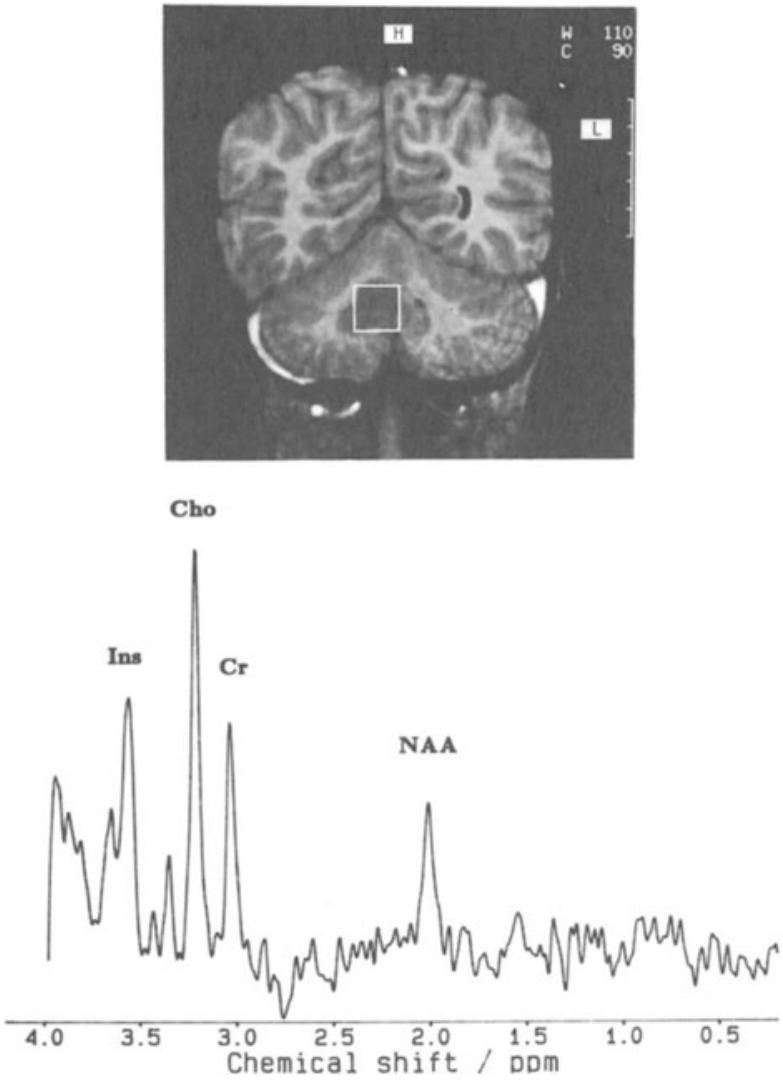

Figure 25 Continued

may be difficult. Similar arguments hold true for the distinction between a brain tumor and perinatally acquired gliotic scars, chronic inflammation, or hamartomas in supratentorial lesions. The putative role of MRS aims at enhanced specificity in tissue characterization as it provides metabolic profiles that may be linked to the proliferation (or degeneration) of certain cells types.

Two cases in which ^1H MRS has been successfully employed for differential diagnosis are shown in Fig. 25. In both the 20-month-old patient with a plexus papilloma (first part) and the 2-year-old patient with a cerebellar astrocytoma (second part), suggestion of a tumor by MRS, as opposed to, for example, a vascular malformation, was confirmed histologically after surgery. The following combination of findings may be considered diagnostic for a brain tumor:

- A focal lesion on MRI
- Moderate to strong elevation of Cho (1.7 and 3.0 mM in the papilloma and astrocytoma, respectively)
- A partial or complete loss of NAA and Cr

Here, the observed metabolic profiles are clearly in line with previous findings in primary brain tumors both *in vitro* (Kinoshita *et al.*, 1994) and *in vivo* [e.g., see Bruhn *et al.* (1989b), Frahm *et al.* (1991b), and Fulham *et al.* (1992)].

ACKNOWLEDGEMENTS

We gratefully acknowledge the help of Petra Pouwels, Ph.D., Wolfgang Hänicke, Dipl. Math., and Knut Brockmann, M.D., in the preparation of this chapter. Many thanks go to our colleagues in the Biomedizinische NMR Forschungs GmbH am Max-Planck-Institut für biophysikalische Chemie and the Abteilung Neuropädiatrie des Klinikums der Universität Göttingen. We also thank the many colleagues from external hospitals for allowing us to study their patients. Last but not least, our warm thanks go to the parents and their children. Without their cooperation and understanding, the present study would not have been possible.

REFERENCES

Aicardi, J., 1992, "Diseases of the Nervous System in Childhood," Mac Keith Press, London.

Aicardi, J., 1993, The inherited leukodystrophies: A clinical overview, *J. Inherited Metab. Dis.* **16:**733–743.

Alexander, W. S., 1949, Progressive fibrinoid degeneration of fibrillary astrocytes associated with mental retardation in a hydrocephalic infant, *Brain* **72:**373–381.

Arend, A. O., Leary, P. M., and Rutherfoord, G. S., 1991, Alexander's disease: A case report with brain biopsy, ultrasound, CT scan and MRI findings, *Clin. Neuropathol.* **10:**122–126.

Arus, C., Chang, Y., and Barany, M., 1985, Proton nuclear magnetic resonance spectra of excised rat brain. Assignment of resonances, *Physiol. Chem. Phys. Med. NMR* **17:**23–33.

Aubourg, P., Balancne, S., Jambaque, I., Rocchiccioli, R., Kalifa, G., Naud-Saudreau, C., Rolland, M. O., Debre, M., Chaussain, J. L., Greiscelli, C., Fische, A., and Baugneres P.-F., 1990, Reversal of early neurologic and neuroradiologic manifestations of X-linked adrenoleukodystrophy by bone marrow transplantation, *N. Engl. J. Med.* **322:**1860–1866.

Austin, J. H., Balasubramanian, A. S., Pattabiraman, T. N., Saraswathi, S., Basu, D. K., and Bachhawat, B. K., 1963, A controlled study of enzymatic activities in three human disorders of glycolipid metabolism, *J. Neurochem.* **10:**805–816.

Austin, S. J., Connelly, A., Gadian, D. G., Benton, J. S., and Brett, E. M., 1991, Localized proton NMR spectroscopy in Canavan's disease: A report of two cases, *Magn. Reson. Med.* **19:**439–445.

Autti, T., Raininko, R., Jaunes, J., Nuutila, A., and Santavuori, P., 1992, Jansky–Bielschowsky variant disease: CT, MRI, and SPECT findings, *Pediatr. Neurol.* **8:**121–126.

Baram, T. Z., Goldman, A. M., and Percy, A. K., 1986, Krabbe disease: Specific MRI and CT findings, *Neurology* **36:**111–115.

Barker, P. B., Kumar, A. J., and Naidu, S., 1991, ^{1}H NMR spectroscopy of Canavan's disease, *in* "Book of Abstracts," 10th Annual Meeting, p. 381, Society of Magnetic Resonance in Medicine, Berkeley, California.

Barkovich, A. J., 1995, "Pediatric Neuroimaging," Raven Press, New York.

Barkovich, A. J., and Chuang, S. H., 1990, Unilateral megalencephaly: Correlation of MR imaging and pathologic characteristics, *Am. J. Neuroradiol.* **11:**523–531.

Barkovich, A. J., Good, W. V., Koch, T. K., and Berg, B. O., 1993, Mitochondrial disorders: Analysis of their clinical and imaging characteristics, *Am. J. Neuroradiol.* **14:**1119–1137.

Barth, P. G., Schüttgens, R. B. H., Wanders, R. J., and Heymans, H. S. A., 1988, The spectrum of peroxisomal disorders, *in* "Child Neurology and Developmental Disabilities. Selected Proceedings of the Forth International Child Neurology Congress" (J. H. French, ed.), Paul H. Brookes, Baltimore, pp. 67–82.

Barth, P. G., Hoffmann, G. F., Jaeken, J., Lehnert, W., Hanefeld, F., van Gennip, A. H., Duran, M., Valk, J., Schutgens, R. B. H., Trefz, F. K., Reimann, G., and Hartung, H. P., 1992, L-2-Hydroxyglutaric acidemia: A novel inherited neurometabolic disease, *Ann. Neurol.* **32:**66–71.

Behar, K. L., den Hollander, J. A., Stromski, M. E., Ogino, T., Shulman, R. G., Petroff, O. A. C., and Prichard, J. W., 1983, High-resolution ^{1}H nuclear magnetic resonance study of cerebral hypoxia *in vivo*, *Proc. Natl. Acad. Sci. USA* **80:**4945–4948.

Birken, D. L., and Oldendorf, W. H., 1989, *N*-Acetyl-L-aspartic acid: A literature review of a compound prominent in ^{1}H-NMR spectroscopic studies of brain, *Neurosci. Biobehav. Rev.* **13:**23–31.

Boespflug-Tanguy, O., Mimault, C., Melki, J., Cavagna, A., Giraud, G., Dinh, D. P., Dastugue, B., and Dautigny, A., 1994, Genetic homogeneity of Pelizaeus–Merzbacher disease: Tight linkage to the proteolipoprotein locus in 16 affected families, *Am. J. Hum. Genet.* **55:**461–467.

Bottomley, P. A., 1984, U.S. Patent 44 80 228.

Bottomley, P. A., 1987, Spatial localization in NMR-spectroscopy *in vivo*, *Ann. N. Y. Acad. Sci.* **508:**333–348.

Bottomley, P. A., 1991, The trouble with spectroscopy papers, *Radiology* **181:**344–350.

Bottomley, P. A., Edelstein, W. A., Foster, T. H., and Adams, W. A., 1985, *In vivo* solvent-suppressed localized hydrogen nuclear magnetic resonance spectroscopy: A window to metabolism?, *Proc. Natl. Acad. Sci. USA* **82:**2148–2152.

Bourgeois, M., Goutieres, F., Chretien, D., Rustin, P., Munnich, A., and Aicardi, J., 1992, Deficiency in complex II of the respiratory chain, presenting as a leukodystrophy in two sisters with Leigh syndrome, *Brain Dev.* **14:**404–408.

Brand, A., Richter-Landsberg, C., and Leibfritz, D., 1993, Multinuclear NMR studies on the energy metabolism of glial and neuronal cells, *Dev. Neurosci.* **15:**289–298.

Bruhn, H., Frahm, J., Gyngell, M. L., Merboldt, K. D., Hänicke, W., and Sauter, R., 1989a, Cerebral metabolism in man after acute stroke: New observations using localized proton NMR spectroscopy, *Magn. Reson. Med.* **9:**126–131.

Bruhn, H., Frahm, J., Gyngell, M. L., Merboldt, K. D., Hänicke, W., Sauter, R., and Hamburger, C., 1989b, Noninvasive differentiation of tumors using localized H-1 MR spectroscopy *in vivo*: Initial experience in patients with cerebral tumors, *Radiology* **172:**541–548.

Bruhn, H., Michaelis, T., Merboldt, K. D., Hänicke, W., Gyngell, M. L., and Frahm, J., 1991, Monitoring cerebral glucose in diabetics by proton MRS, *Lancet* **337:**745–746.

Bruhn, H., Michaelis, T., Merboldt, K. D., Hänicke, W., Gyngell, M. L., Hamburger, C., and Frahm, J., 1992a, On the interpretation of proton NMR spectra from brain tumours *in vivo* and *in vitro*, *NMR Biomed.* **5:**253–258.

Bruhn, H., Frahm, J., Merboldt, K. D., Hänicke, W., Christen, H. J., Kruse, B., Hanefeld, F., and

Bauer, H. J., 1992b, Multiple sclerosis in children. Cerebral metabolic alterations monitored by localized proton magnetic resonance spectroscopy *in vivo, Ann. Neurol.* **32:**140–150.

Bruhn, H., Kruse, B., Korenke, G. C., Hanefeld, F., Hänicke, W., Merboldt, K. D., and Frahm, J., 1992c Proton NMR spectroscopy of cerebral metabolic alterations in infantile peroxisomal disorders, *J. Comput. Assist. Tomogr.* **16:**335–344.

Canavan, M. M., 1931, Schilder's encephalitis periaxialis diffusa. Report of a case in a child aged sixteen and one-half months, *Arch. Neurol. Psychiatry* **25:**299–308.

Cassedy, K. J., and Edwards, M. K., 1993, Metabolic and degenerative diseases of childhood, *Top. Magn. Reson. Imaging* **5:**73–95.

Claussen, M., Heim, P., Knispel, J., Goebel, H. H., and Kohlschütter, A., 1992, Incidence of neuronal ceroid-lipofuscinoses in West Germany: Variation of a method for studying autosomal recessive disorders, *Am. J. Med. Genet.* **42:**536–538.

Cohen, M. E., and Duffner, P. K., 1994, "Brain Tumors in Children. Principles of Diagnosis and Treatment," Raven Press, New York.

Confort-Gouny, S., Chabrol, B., Vion-Dury, J., Mancini, J., and Cozzone, P. J., 1993, MRI and localized proton MRS in early infantile form of neuronal ceroid-lipofuscinosis, *Pediatr. Neurol.* **9:**57–60.

Crome, L., Hanefeld, F., Patrick, D., and Wilson, J., 1973, Late onset globoid cell leukodystrophy, *Brain* **96:**841–848.

Detre, J. A., Wang, Z. Y., Bogdan, A. R., Gusnard, D. A., Bay, C. A., Bingham, P. M., and Zimmerman, R. A., 1991, Regional variation in brain lactate in Leigh syndrome by localized ^{1}H magnetic resonance spectroscopy, *Ann. Neurol.* **29:**218–221.

Doll, R., Natowicz, M. R., Schiffman, R., and Smith, F. I., 1992, Molecular diagnostics for myelin proteolipid protein gene mutations in Pelizaeus–Merzbacher disease, *Am. J. Hum. Genet.* **51:**161–169.

Ernst T., and Hennig, J., 1991, Coupling effects in volume-selective ^{1}H spectroscopy of major brain metabolites, *Magn. Reson. Med.* **21:**82–96.

Frahm, J., 1993, Nuclear magnetic resonance studies of human brain *in vivo:* Anatomy, function, and metabolism, *Adv. Exp. Med. Biol.* **333:**257–271.

Frahm, J., and Hänicke, W., 1994, Single voxel localized spectroscopy, *in* "Advanced Magnetic Resonance Spectroscopy," Syllabus, 2nd Annual Meeting, pp. 206–213, Society of Magnetic Resonance, Berkeley, California.

Frahm, J., and Hänicke, W., 1996, Single voxel proton NMR. Methods and applications to human subjects, *in* "Encyclopedia of Nuclear Magnetic Resonance" (D. M. Grant and R. K. Harris, eds.), Wiley, Chichester.

Frahm, J., Haase, A., Hänicke, W., Merboldt, K. D., and Matthaei, D., 1984, Verfahren und Einrichtung zur ortsaufgelösten Untersuchung einer Probe mittels magnetischer Resonanz von Spinmomenten, German Patent DE 3445689.

Frahm, J., Merboldt, K. D., and Hänicke, W., 1987, Localized proton spectroscopy using stimulated echoes, *J. Magn. Reson.* **72:**502–508.

Frahm, J., Michaelis, T., Merboldt, K. D., Hänicke, W., Gyngell, M. L., Chien, D., and Bruhn, H., 1989, Localized NMR spectroscopy *in vivo.* Progress and problems, *NMR Biomed.* **2:**188–195.

Frahm, J., Michaelis, T., Merboldt, K. D., Bruhn, H., Gyngell, M. L., and Hänicke, W., 1990, Improvements in localized ^{1}H-NMR spectroscopy of human brain. Water suppression, short echo times, and 1 mL resolution, *J. Magn. Reson.* **90:**464–473.

Frahm, J., Michaelis, T., Merboldt, K. D., Hänicke, W., Gyngell, M. L., and Bruhn, H., 1991a, On the *N*-acetyl methyl resonance in localized ^{1}H-NMR spectra of human brain *in vivo, NMR Biomed.* **4:**201–204.

Frahm, J., Bruhn, H., Merboldt, K. D., Hänicke, W., Mursch, K., and Markakis, E., 1991b, Localized

proton NMR spectroscopy of brain tumors. Methodologic improvements using short-echo time STEAM sequences, *J. Comput. Assist. Tomogr.* **15:**915–922.

Frahm, J., Gyngell, M. L., and Hänicke, W., 1991c, Rapid scan techniques, *in* "Magnetic Resonance Imaging" (D. D. Stark and W. G. Bradley, eds.), pp. 165–203, CV Mosby, St. Louis.

Frahm, J., Bruhn, H., and Hanefeld, F., 1995, Proton NMR studies of human brain metabolism, *in* "Proceedings of the 2nd International Conference on Applications of Magnetic Resonance in Food Science, University of Aveiro, Portugal, 19–21 September 1994" (P. S. Belton, I. Delgadillo, A. M. Gil, and G. A. Webb, eds.), pp. 191–205, Royal Society of Chemistry, Cambridge.

Frahm, J., Krüger, G., Merboldt, K. D., and Kleinschmidt, A., 1996, Dynamic uncoupling and recoupling of perfusion and oxidative metabolism during focal brain activation in man, *Magn. Reson. Med.* **35:**143–148.

Fulham, M. J., Bizzi, A., Dietz, M. J., Shih, H. H., Raman, R., Sobering, G. S., Frank, J. A., Dwyer, A. J., Alger, J. R., and Di Chiro, G., 1992, Mapping of brain tumor metabolites with proton MR spectroscopic imaging: Clinical relevance, *Radiology* **185:**675–686.

Grodd, W., Krägeloh-Mann, I., Petersen, D., Trefz, F. K., and Harzer, K., 1990, *In vivo* assessment of *N*-acetylaspartate in brain in spongy degeneration (Canavan's disease) by proton spectroscopy, *Lancet* **336:**437–438.

Grodd, W., Krägeloh-Mann, I., Klose, U., and Sauter, R., 1991, Metabolic and destructive brain disorders in children: Findings with localized proton MR spectroscopy, *Radiology* **181:**173–181.

Gropen, T. I., Prohovnik, I., Tatemichi, T. K., and Hirano, M., 1994, Cerebral hyperemia in MELAS, *Stroke* **25:**1873–1876.

Gyngell, M. L., Michaelis, T., Bruhn, H., Hänicke, W., Merboldt, K. D., and Frahm, J., 1991, Cerebral glucose is detectable by localized proton NMR spectroscopy in normal rat brain *in vivo*, *Magn. Reson. Med.* **19:**489–495.

Haase, A., Frahm, J., Hänicke, W., and Matthaei, D., 1985, ^1H NMR chemical shift selective (CHESS) imaging, *Phys. Med. Biol.* **30:**341–344.

Hagberg, B., 1993, "Rett Syndrome—Clinical & Biological Aspects", Mac Keith Press, London.

Hagberg, B., Kollberg, H., Sourander, P., and Akerson, H. O., 1970, Infantile globoid cell leucodystrophy (Krabbe's disease): A clinical, morphological, and genetical study of 32 Swedish cases, *Neuropädiatrie* **1:**74–88.

Hagberg, B., Blennow, G., Kristiansson, B., and Stibler, H., 1993, Carbohydrate-deficient glycoprotein syndromes: Peculiar group of new disorders, *Pediatr. Neurol.* **9:**255–262.

Hahn, E. L., 1950, Spin echoes, *Phys. Rev.* **80:**580–592.

Hallervorden, J., 1923, Angeborene Hemihypertrophie der linken Körperhälfte ein-schließlich des Gehirns, *Zentralbl. Gesamte Neurol. Psychiatr.* **33:**518–519.

Hanefeld, F., 1995, Characteristic of childhood multiple sclerosis, *Int. M. S. J.* **1:**91–97.

Hanefeld, F., Bauer, H. J., Christen, H. J., Kruse, B. Bruhn, H., and Frahm, J., 1991, Multiple sclerosis in childhood: Report of 15 cases, *Brain Dev.* **13:**410–416.

Hanefeld, F., Holzbach, U., Kruse, B., Wilichowski, E., Christen, H. J., and J. Frahm, 1993, Diffuse white matter disease in three children: An encephalopathy with unique features on magnetic resonance imaging and proton magnetic resonance spectroscopy, *Neuropediatrics* **24:**244–248.

Hanefeld, F., Kruse, K., Bruhn, H., and Frahm, J., 1994, *In vivo* proton magnetic resonance spectroscopy of the brain in a patient with L-2-hydroxyglutaric aciduria, *Pediatr. Res.* **35:**614–616.

Hanefeld, F., Christen, H. J., Holzbach, U., Kruse, B., Frahm, J., and Hänicke, W., 1995a, Cerebral proton magnetic resonance spectroscopy in Rett syndrome, *Neuropediatrics* **26:**126–127.

Hanefeld, F., Kruse, B., Holzbach, U., Christen, H. J., Merboldt, K. D., Hänicke, W., and Frahm, J., 1995b, Hemimegalencephaly. Localized proton magnetic resonance spectroscopy *in vivo*, *Epilepsia* **36:**1215–1224.

Hashimoto, T., Tayama, M., Miyazaki, M., Fuji, E., Harada, M., Miyoshi, H., Tanouchi, M., and Kuroda, Y., 1995, Developmental brain changes investigated with proton magnetic resonance spectroscopy, *Dev. Med. Child Neurol.* **37**:398–405.

Herschkowitz, N., and Schulte, F. J., 1984, Gangliosidoses and leukodystrophies: A correlative approach in pediatric neurobiology, *Neuropediatris* **15**(Suppl.):1–112.

Holzbach, U., Hanefeld, F., Helms, G., Hänicke, W., and Frahm, J., 1995, Localized proton magnetic resonance spectroscopy of cerebral abnormalities in children with carbohydrate-deficient glycoprotein syndrome, *Acta Paediatr.* **84**:781–786.

Hoult, D. I., and Richards, R. E., 1976, The signal-to-noise ratio of the nuclear magnetic resonance experiment, *J. Magn. Reson.* **24**:71–85.

Howe, F. A., Maxwell, R. J., Saunders, D. E., Brown, M. M., and Griffiths, J. R., 1993, Proton spectroscopy in vivo, *Magn. Reson. Q.* **9**:31–59.

Hüppi, P. S., Posse, S., Lazeyras, F., Burri, R., Bossi, E., and Herschkowitz, N., 1991, Magnetic resonance in preterm and term newborns: ^{1}H-spectroscopy in developing human brain, *Pediatr. Res.* **30**:574–578.

Hüppi, P. S., Fusch, C., Boesch, C., Burri, R., Bossi, E., Amato, M., and Herschkowitz, N., 1995, Regional metabolic assessment of human brain during development by proton magnetic resonance spectroscopy *in vivo* and by high-performance liquid chromatography/gas chromatography in autopsy tissue, *Pediatr. Res.* **37**:145–150.

Husted, C. A., Matson, G. B., Adams, D. A., Goodin, D. S., and Weiner, M. W., 1994, In vivo detection of myelin phospholipids in multiple sclerosis with phosphorus magnetic resonance spectroscopic imaging, *Ann. Neurol.* **36**:239–241.

Jaeken, J., Stibler, H., and Hagberg B. (eds.), 1991, The carbohydrate-deficient glycoprotein syndrome. A new inherited multisystemic disease with severe nervous system involvement, *Acta Paediatr. Scand.* **375**:1–71.

Järvelä, I., Vesa, J., Santavuori, P., Hellsten, E., and Peltonen, L., 1992, Molecular genetics of neuronal ceroid lipofuscinoses, *Pediatr. Res.* **32**:645–648.

Kaul, R., Gao, G. P., Balamurugan, K., and Matalon, R., 1993, Cloning of the human aspartoacylase cDNA and a common missense mutation in Canavan disease, *Nat. Genet.* **5**:118–123.

Kauppinen, R. A., Nissinen, T., Kärkkäinen, A. M., Pirttila, T. R. M., Palrimo, J., Kokko, H., and Williams, S. R., 1992, Detection of thymosin β4 *in situ* in a guinea pig cerebral cortex preparation using ^{1}H NMR spectroscopy, *J. Biol. Chem.* **267**:9905–9910.

Kemp, G. J., and Radda, G. K., 1994, Quantitative interpretation of bioenergetic data from ^{31}P and ^{1}H magnetic resonance spectroscopic studies of skeletal muscle: An analytical review, *Magn. Reson. Q.* **10**:43–63.

Kendall, B. E., 1993, Inborn errors and demyelination: MRI and the diagnosis of white matter disease, *J. Inherited Metab. Dis.* **16**:771–786.

Kinoshita, Y., Kajiwara, H., Yokota, A., and Koga, Y., 1994, Proton magnetic resonance spectroscopy of brain tumors: An in vitro study, *Neurosurgery* **35**:606–614.

Kolodny, E. H., 1989, Metachromatic leukodystrophy and multiple sulfatase deficiency: Sulfatide lipidosis, *in* "The Metabolic Basis of Inherited Disease" (C. R. Scriver, A. L. Beaudet, W. S. Sly, and D. Valle, eds), pp. 1721–1750, McGraw-Hill, New York.

Kolodny, E. H., 1993, Dysmeylinating and demyelinating conditions in infancy, *Curr. Opin. Neurol. Neurosurg.* **6**:379–386.

Krabbe, K., 1916, A new familial form of diffuse brain-sclerosis, *Brain* **39**:74–114.

Krägeloh-Mann, I., Grodd, W., Schöning, M., Marquard, K., Nägele, I., and Ruitenbeek, W., 1993, Proton spectroscopy in five patients with Leigh's disease and mitochondrial enzyme deficiency, *Dev. Med. Child. Neurol.* **35**:769–776.

Kreis, R., and Ross, 1992, Cerebral metabolic disturbances in patients with subacute and chronic diabetes mellitus: Detection with proton MR spectroscopy, *Radiology* **184**:123–130.

Kreis, R., Farrow, N. A., and Ross, B. D., 1990, Diagnosis of hepatic encephalopathy by proton magnetic resonance spectroscopy, *Lancet* **336:**635–636.

Kreis, R., Ross, B. D., Farrow, N. A., and Ackermann, Z., 1992, Metabolic disorders of the brain in chronic hepatic encephalopathy detected with H-1 MR spectroscopy, *Radiology* **182:**19–27.

Kreis, R., Ernst, T., and Ross, B. D., 1993, Development of the human brain: In vivo quantification of metabolite and water content with proton magnetic resonance spectroscopy, *Magn. Reson. Med.* **30:**424–437.

Kruse, B., Hanefeld, F., Christen, H. J., Bruhn, H., Michaelis, T., Hänicke, W., and Frahm, J., 1993, Alterations of brain metabolites in metachromatic leukodystrophy as detected by localized proton MR spectroscopy *in vivo*, *J. Neurol.* **241:**68–74.

Kruse, B., Barker, P. B., van Zijl, P. C., Duyn, J. H., Moonen, C. T., and Moser, H. W., 1994a, Multislice proton magnetic resonance spectroscopic imaging in X-linked adrenoleukodystrophy, *Ann. Neurol.* **36:**595–608.

Kruse, B., Hanefeld, F., Holzbach, U., Wilichowski, E., Christen, H. J., Merboldt, K. D., Hänicke, W., and Frahm, J., 1994b, *Dev. Med. Child. Neurol.* **36:**839–840. [Letter to: Krägeloh-Mann, I., Grodd, W., Schöning, M., Marquard, K., Nägele, T., and Ruitenbeek, W., Proton spectroscopy in patients with Leigh's disease and mitochondrial enzyme deficiency, *Dev. Med. Child. Neurol.* **35:**769–776].

Kucharczyk, W., Brant-Zawadzki, M., Sobel, D., Edwards, M. B., Kelly, W. M., Norman, D., and Newton, T. H., 1985, Central nervous system tumors in children: Detection by magnetic resonance imaging, *Radiology* **155:**131–136.

Lee, M. L., Chaou, W. T., Yang, A. D., Jong, Y. J., Tsai, J. L., Pang, C. Y., and Wei, Y. H., 1994, Mitochondrial myopathy, encephalopathy, lactic acidosis and stroke-like episodes (MELAS): Report of a sporadic case and review of the literature, *Acta Paediatr. Sin.* **35:**148–156.

Leigh, D., 1951, Subacute necrotizing encephalomyelopathy in an infant, *J. Neurol. Neurosurg. Psychiatry*, **14:**216–221.

Martinsson, T., Bjursell, C., Stibler, H., Kristiansson, B., Skovby, F., Jaeken, J., Blennow, G., Strömme, P., Hanefeld, F., and Wahlström, J., 1994, Linkage of a locus for carbohydrate-deficient glycoprotein syndrome type I (CDG I) to chromosome 16p and linkage dysequilibrium to microsatellite marker D16S406, *Hum. Mol. Genet.* **3:**2037–2042.

Matalon, R., Michals, K., Sebesta, D., Deanching, M., Gashkoff, P., and Casanova, J., 1988, Aspartoacylase deficiency and *N*-acetylaspartic aciduria in patients with Canavan disease, *Am. J. Med. Genet.* **29:**463–471.

Matthews, P. M., Tampieri, D., Berkovic, S. F., Andermann, F., Silver, K., Chityat, D., and Arnold, D. L., 1991a, Magnetic resonance imaging shows specific abnormalities in the MELAS syndrome, *Neurology* **41:**1043–1046.

Matthews, P. M., Berkovic, S. F., Shoubridge, E. A., Andermann, F., Karpati, G., Carpenter, S., and Arnold, D. L., 1991b, *In vivo* magnetic resonance spectroscopy of brain and muscle in a type of mitochondrial encephalopathy (MERRF), *Ann. Neurol.* **29:**435–438.

Mehl, E., and Jatzkewitz, H., 1965, Evidence for the genetic block in metachromatic leukodystrophy (ML), *Biochem. Biophys. Res. Commun.* **19:**407–411.

Merboldt, K. D., Chien, D., Hänicke, W., Gyngell, M. L., Bruhn, H., and Frahm, J., 1990, Localized ^{31}P-NMR spectroscopy of the adult human brain *in vivo* using stimulated echo (STEAM) sequences, *J. Magn. Reson.* **89:**343–361.

Merboldt, K. D., Bruhn, H., Hänicke, W., Michaelis, T., and Frahm, J., 1992, Decrease of glucose in the human visual cortex during photic stimulation, *Magn. Reson. Med.* **25:**187–194.

Merzbacher, L., 1910, Eine eigenartige familiär-hereditäre Erkrankungsform (Aplasia axialis extracorticalis congenita), *Z. Gesamte Neurol. Psychiatr.* **3:**1–138.

Michaelis, T., Merboldt, K. D., Hänicke, W., Gyngell, M. L., Bruhn, H., and Frahm, J., 1991, On the

identification of cerebral metabolites in localized ^{1}H-NMR spectra of human brain *in vivo, NMR Biomed.* **4:**90–98.

Michaelis, T., Helms, G., Merboldt, K. D., Hänicke, W., Bruhn, H., and Frahm, J., 1993a, Identification of *scyllo*-inositol in proton NMR spectra of human brain *in vivo, NMR Biomed.* **6:**105–109.

Michaelis, T., Merboldt, K. D., Bruhn, H., Hänicke, W., and Frahm, J., 1993b, Absolute concentrations of metabolites in the adult human brain *in vivo:* Quantification of localized proton MR spectra, *Radiology* **187:**219–227.

Miller, B. L., Moats, R. A., Shonk, T., Ernst, T., Woolley, S., and Ross, B. D., 1993, Alzheimer disease: Depiction of increased cerebral *myo*-inositol with proton MR spectroscopy, *Radiology* **187:**433–437.

Mosser, J., Douar, A. M., Sarde, C. O., Kioschis, P., Feil, R., Moser, R., Poustka, A. M., Mandel, J. L., and Aubourg, P., 1993, Putative X-linked adrenoleukodystrophy gene shares unexpected homology with ABC transporters, *Nature (London)* **361:**726–730.

Nielsen, J. B., Toft, P. B., Reske-Nielsen, E., Jensen, K. E., Christiansen, P., Thomsen, C., Henriksen, O., and Lou, H. C., 1993, Cerebral magnetic resonance spectroscopy in Rett syndrome. Failure to detect mitochondrial disorder, *Brain Dev.* **15:**107–112.

Norton, W. T., and Poduslo, S. E., 1982, Biochemical studies of metachromatic leukodystrophy in three siblings, *Acta Neuropathol.* **57:**188–196.

Ochi, N., Kobayashi, K., Mehara, M., Nakayama, A., Negoro, T., Shinohara, H., Watanabe, K., Nagatsu, T., and Kato, K., 1991, Increment of α B-crystallin mRNA in the brain of a patient with infantile type Alexander's disease, *Biochem. Biophys. Res. Commun.* **179:**1030–1035.

Ordidge, R. J., Bendall, M. R., Gordon, R. E., and Connelly, A., 1985, Volume selection for in-vivo biological spectroscopy, *in* "Magnetic Resonance in Biology and Medicine" (G. Govil, C. L. Khetrapal, and A. Saran, eds.), p. 387, Tata McGraw-Hill, New Delhi.

Peden, C. J., Cowan, F. M., Bryant, D. J., Sargentoni, J., Cox, I. J., Menon, D. K., Gadian, D. G., Bell, J. D., and Dubowitz, L. M., 1990, Proton MR spectroscopy of the brain in infants, *J. Comput. Assist. Tomogr.* **14:**886–894.

Peeling, J., and Sutherland, G., 1993, ^{1}H magnetic resonance spectroscopy of extracts of human epileptic neocortex and hippocampus, *Neurology* **43:**589–594.

Pelizaeus, E., 1885, Über eine eigentümliche Form spastischer Lähmungen mit Cerebralerscheinungen auf hereditärer Grundlage, *Arch. Psychiatr.* **16:**698–710.

Percy, A. K., Odrezin, G. T., Knowles, P. D., Rouah, E., and Armstrong, D. D., 1994, Globoid cell leukodystrophy: Comparison of neuropathology with magnetic resonance imaging, *Acta Neuropathol.* **88:**26–32.

Perry, T. L., Hansen, S., Berry, K., Mok, C., and Lesk, D., 1971, Free amino acids and related compounds in biopsies of human brain, *J. Neurochem.* **18:**521–528.

Perry, T. L., Hansen, S., and Gandham, S. S., 1981, Postmortem changes of amino compounds in human and rat brain, *J. Neurochem.* **36:**407–412.

Petroff, O. A. C., Spencer, D. D., Alger, J. R., and Prichard, J. W., 1989, High-field proton magnetic resonance spectroscopy of human cerebrum obtained during surgery for epilepsy, *Neurology* **39:**1197–1202.

Polten, A., Fluharty, A. L., Fluharty, C. B., Kappler, J., von Figura, K., and Gieselmann, V., 1991, Molecular basis of different forms of metachromatic leukodystrophy, *N. Engl. J. Med.* **324:**18–22.

Pouwels, P. J. W., Hänicke, W., and Frahm, J., 1995a, On a concentration gradient of cerebral metabolites in human gray matter as determined by quantitative localized proton MRS, *in* "Book of Abstracts," 3rd Annual Meeting, Society of Magnetic Resonance, Berkeley, California.

Pouwels, P. J. W., Kruse, B., Hanefeld, F., and Frahm, J., 1995b, Quantitative localized proton MRS in adrenoleukodystrophy, *Neuropediatrics,* **26:**341–341.

Prichard, J. W., and Shulman, R. G., 1986, NMR spectroscopy of brain metabolism in vivo, *Annu. Rev. Neurosci.* **9:**61–85.

Prichard, J., Rothman, D., Novotny, E., Petroff, O., Kuwabara, T., Avison, M., Howseman, A., Hanstock, C., and Shulman, R. G., 1992, Lactate rise detected by ^1H NMR in human visual cortex during physiologic stimulation, *Proc. Natl. Acad. Sci. USA* **88:**5829–5831.

Provencher, S. W., 1982, A constrained regularization method for inverting data represented by linear algebraic or integral equations, *Comput. Phys. Commun.* **27:**213–227.

Provencher, S. W., 1993, Estimation of metabolite concentrations from localized *in vivo* NMR spectra, *Magn. Reson. Med.* **30:**672–679.

Radda, G. K., 1986, The use of NMR spectroscopy for the understanding of disease, *Science* **233:**640–645.

Ramaeckers, V. T., Stibler, H., Kint, J., and Jaeken, J., 1991, A new variant of the carbohydrate-deficient glycoprotein syndrome, *J. Inherited Metab. Dis.* **14:**385–388.

Requardt, M., 1995, Dissertation, University of Göttingen, Göttingen.

Rett, A., 1966, Über ein eigenartiges hirnatrophisches Syndrom bei Hyperammonämie im Kindesalter, *Wien. Med. Wochenschr.* **116:**723–726.

Rosenberg, R. N., Prusiner, S. B., DiMauro, S., Barchi, R. L., and Kunkel, L. M. (eds), 1993, "The Molecular Biology and Genetic Basis of Neurological Disease," Butterworth-Heineman, Boston.

Ross, B. D., and Michaelis, T., 1994, Clinical applications of magnetic resonance spectroscopy, *Magn. Reson. Q.* **10:**191–248.

Sandhoff, K., Conzelmann, E., Neufeld, E. F., Kaback, M. M., and Suzuki, K., 1989, The GM2-gangliosidosis, *in* "The Metabolic Basis of Inherited Disease" (C. R. Scriver, A. L. Beaudet, W. S. Sly, and D. Valle, eds.), pp. 1807–1839, McGraw-Hill, New York.

Santavuori, P., Rapola, J., Nuutila, A., Raininko, R., Lappi, M., Launes, J., Herva, R., and Sainio, K., 1991, The spectrum of Jansky–Bielschowsky disease, *Neuropediatrics* **22:**92–96.

Sasaki, M., Sakuragawa, N., Takashima, S., Hanaoka, S., and Arima, M., 1991, MRI and CT findings in Krabbe disease, *Pediatr. Neurol.* **7:**283–288.

Scholz, W., 1925, Klinische, pathologisch-anatomische und erbbiologische Untersuchungen bei familiärer, diffuser Hirnsklerose im Kindesalter, *Z. Gesamte Neurol. Psychiatr.* **99:**651–717.

Schuster, V., Horwitz, A. E., and Kreth, H. W., 1991, Alexander's disease: Cranial MRI and ultrasound findings, *Pediatr. Radiol.* **21:**133–134.

Seitelberger, F., 1970, Pelizaeus–Merzbacher disease, *in* "Handbook of Clinical Neurology, Vol. 10, Leucodystrophies and Poliodystrophies" (P. J. Vinken and G. W. Brown, eds.), pp. 150–202, North-Holland, Amsterdam.

Sengers, R. C. A., Stadhouders, A. M., and Trijbels, J. M. F., 1984, Mitochondrial myopathies. Clinical, morphological, and biochemical aspects, *Eur. J. Pediatr.* **141:**192–207.

Sherman, W. R., Stewart, M. A., Kurien, M. M., and Goodwin, S. L., 1968, The measurement of *myo*-inositol, *myo*-inosose-2 and *scyllo*-inositol in mammalian tissues, *Biochim. Biophys. Acta* **158:**197–205.

Stibler, H., Westerberg, B., Hanefeld, F., and Hagberg, B., 1993, Carbohydrate-deficient glycoprotein (CDG) syndrome—a new variant type III, *Neuropediatrics* **24:**51–52.

Stöckler, S., Holzbach, U., Hanefeld, F., Marquardt, I., Helms, G., Requardt, M., Hänicke, W., and Frahm, J., 1994, Creatine deficiency in the brain: A new treatable inborn error of metabolism, *Pediatr. Res.* **36:**409–413.

Suzuki, K., Suzuki, Y., and Eto, Y., 1971, Deficiency of galactocerebroside β-galactosidase in Krabbe's globoid cell leukodystrophy, *in* "Lipid Storage Diseases: Enzymatic Defect and Clinical Implications" (J. Bersohn and H. J. Grossman, eds.), p. 396, Academic Press, New York.

Toft, P. B., Leth, H., Lou, H. C., Pryds, O., and Henrikson, O., 1994, Metabolite concentrations in the

developing brain estimated with water proton MR spectroscopy, *J. Magn. Reson. Imaging* **4:**674–680.

Tzika, A. A., Vigneron, D. B., Ball, W. S., Jr., Dunn, R. S., and Kirks, D. R., 1993a, Localized proton MR spectroscopy of the brain in children, *J. Magn. Reson. Imaging* **3:**719–729.

Tzika, A. A., Ball, W. S., Jr., Vigneron, D. B., Dunn, R. S., and Kirks, D. R., 1993b, Clinical proton MR spectroscopy of neurodegenerative disease in childhood, *Am. J. Neuroradiol* **14:**1267–1281.

Uyama, E., Terasaki, T., Watanabe, S., Naito, M., Owada, M., Araki, S., and Ando, M., 1992, Type 3 GM1 gangliosidosis: Characteristic MRI findings correlated with dystonia, *Acta Neurol. Scand.* **86:**609–615.

Valk, J., and van der Knaap, M. S., 1989, "Magnetic Resonance of Myelin, Myelination, and Myelin Disorders," Springer, Berlin.

van Bogaert, L., and Bertrand, I., 1967, "Spongy Degeneration of the Brain in Infancy," North-Holland, Amsterdam.

van der Knaap, M. S., van der Grond, J., van Rijen, P. C., Faber, J. A., Valk, J., and Willemse, K., 1990, Age-dependent changes in localized proton and phosphorus MR spectroscopy of the brain, *Radiology* **176:**509–515.

van der Knaap, M. S., van der Grond, J., Luyten, P. R., den Hollander, J. A., Nauta, J. P., and Valk, J., 1992, ^{1}H and ^{31}P magnetic resonance spectroscopy of the brain in degenerative cerebral disorders, *Ann. Neurol.* **31:**202–211.

van der Knaap, M. S., Barth, P. G., Stroink, H., van Nieuwenhuizen, O., Arts, W. F. M., Hoogenraad, F., and Valk, J., 1995, Leukoencephalopathy with swelling and a discrepancy mild clinical course in eight children, *Ann. Neurol.* **37:**324–334.

von Graefe, A., 1866, Bemerkungen über doppelseitige Augenmuskellähmungen basilären Ursprunges, *Albrecht von Graefes Arch. Ophthalmol.* **12:**265.